Utrecht University

Master thesis

A box model of Mediterranean deep-water formation applied to sapropels

Author:
Sebastiaan Meyer Viol, Bsc

Supervisor:
Dr. Paul Meijer

July 24, 2014

Contents

Chapter 1

Introduction

The Neogene sedimentary record of the Mediterranean basin is characterised by the regular alternation of organic-rich layers (sapropels) and normal marine marls (1.1). Formation of these sapropels coincides closely with minima in the Milankovitch precession index (Rohling & Hilgen, 1990). These precession minima occur every 21.000 years. The precession cycle causes climate variations. These climate variations can influence the circulation and depositional environment of the Mediterranean sea. There are two main theories for the formation of the organic rich sapropels. The first theory is that the climatic variations may be the cause for an increase in organic materials in the Mediterranean, resulting in an increased organic-carbon preservation (Bard et al., 2002). The second theory states that an increased river runoff, precipitation and the variance in the insolation have an effect on the thermohaline circulation in the Mediterranean. The sapropel/marl alternation is often considered to reflect changes in the thermohaline circulation of the sea. Changes in this circulation may cause the flow of oxygen rich surface water to the deep water (deep-water formation) to stop, causing an oxygen depleted deep water zone which can conserve organic materials (Pinardi & Masetti, 2000). This thesis will try to give a model-based understanding of the second theory.

The precession cycle has 2 main effects on the climate in the Mediterranean region. The first effect is that during a precession minimum on the Northern hemisphere the summers are warmer and the winters are colder (Bard et al., 2002). A second effect is that during a precession minimum various extra sources of fresh water have been identified. Minima in the precession index are characterized by intensified Indian Ocean SW monsoonal circulation, with enhanced discharge of the river Nile into the eastern Mediterranean. It is also believed that during precession minima there is an increase in precipitation in the Mediterranean (Meijer & Tuenter, 2007). These climatic changes may have caused the deep-water formation to stop (Rohling & Hilgen, 1990).

Remarkably little of the explanations as to how periodic variations in earth's climate result in changes in sedimentation is backed by physical models. 3-dimensional oceanic general circulation models (OGCM's) have been applied to specific stages in

Figure 1.1: Photograph of late Miocene (9.3-8.4 Ma) sapropel bedding cycles in south central Sicily. The dark layers are organic-rich sapropel layers, while the light layers are the marine marls. (Hilgen et al., 1995).

the precession cycle to investigate circulation in the Mediterranean (Myers et al., 1998). However these OGCM's are too time-consuming to follow the whole precession cycle. A different approach is the use of a 2-dimensional box model. These models aim to observe for longer time spans (kyr-Myr), and to gain insight into the basic physical mechanisms. Earlier attempts of box models of the Mediterranean (Tziperman & Speer, 1994; Matthiesen & Haines., 2003) were physically limited. These box models divided the Mediterranean into three layers. The lack of a fourth layer constrained deep-water formation in these models to outflow of the Mediterranean into the Atlantic. Therefore deep-water formation is not a good indicator of the circulation regime in these 3-layer box models. The objective of this research thesis is to make a computational model with four layers which can give us physical insights of deep-water formation during a precession cycle. The model will link climate variations due to the precession cycle to deep-water formation, and hereby attempt to give a model-based understanding of the sapropel-marl alternation.

It is important to have an understanding of the process of deep-water formation in the Mediterranean and the formation of the sapropel-marl alternation for two main reasons. The calibration of cyclic sapropel patterns of Neogene and Quaternary age has led to dating of the stratigraphic stages in these epochs (Hilgen, 1990). The sapropels in the Mediterranean Neogene-Quaternary are coded using the correlative peak of the precession index as numbered from recent. Sapropels can be dated with an accuracy of 1 ka, if a time lag of 3-4 ka between the precession minimum and the sapropel formation is used (Hilgen, 1990). This time lag is only observed and dated for the youngest Holocene sapropel (S1) though. While this time-lag has been observed it is not fully understood.

One of the purposes of the box model is to physically understand this time lag, and to investigate if it is justified to apply this time lag to all precession minima. The second reason why it is important to understand the process of deep- water formation in the Mediterranean is that the this helps us understand the Atlantic meridional overturning circulation (AMOC) (Rahmstorf, 2002). The AMOC is the dominant north-south ocean circulation feature in the Atlantic. About 80% of the heat from global warming over the past 50 years was absorbed by the ocean. Large variations of the AMOC impact sea ice, ecosystems, ocean temperatures, and sea level. Understanding the thermohaline circulation in the Mediterranean may also provide us with a better understanding of the more complex AMOC.

This thesis will start in Chapter 2 by explaining the configuration and theory of the 4-layer box model. Chapter 3 will look at the physical properties of the Mediterranean at present. The temperature, salinity and density in the Mediterranean will be obtained from the MEDAR database (MEDAR group, 2002). A comparison between the box model and the MEDAR data is made to validate and calibrate the model. This chapter also contains an analysis on climatological fluctuations due to both seasonal and precessional variations. These variations are incorporated into the box model. Chapter 4 will present the results of the box model. This chapter will start by performing a sensitivity analysis on the essential parameters in the model. Afterwards seasonal variations are included in the model. The output of the seasonal model is compared to Mediterranean data to check the validity of the model. The model will then be adjusted to include climatological variations due to the precessional Milankovitch cycle. With this inclusion deep- water formation on the timescale of the precessional cycle (21.000 years) can be modelled. In the final part we will model climatic conditions during the formation of the S1 sapropel. As there is more climatological information available on the last precession cycle, we can model this cycle in more detail. Chapter 5 will look at the limitations of the 4-layer box model, and the possibility of using a less complex 3-layer box model. Finally Chapter 6 concludes this research thesis.

Chapter 2

Theory box model

This chapter will start by giving a qualitative description of the box model in Section 2.1. Section 2.2 contains the equations governing the dynamics of the model. The main quantities which describe the dynamics of the model are the temperature (T)and the salinity (S). From these quantities the density can be obtained which determines the flow characteristics. The box model is programmed in Fortran. Section 2.3 contains a short description of the program, and an explanation of how the model is calibrated.

2.1 Qualitative description

2.1.1 Box model

The Mediterranean sea box model contains 4 layers and is based on the schematic representation of Figure 2.1. The proposed box model is schematically depicted in Figure 2.2. The Strait of Sicily which divides the Eastern and Western Mediterranean sea is not included in the model for simplification. Each layer has a thickness h, which does not vary over time. The Upper (U) and Lower (L) layer box are in contact with the Atlantic ocean (A). Water flows in from the Atlantic into the Upper layer (q_1), and flows back from the Lower layer into the Atlantic (q_2). The Upper layer represents the Modified Atlantic Water (MAW) of Figure 2.1. The Lower layer can be seen as the Levantine Intermediate water which has an average thickness of around 500 m (Pinardi & Masetti, 2000). The water Formation box (F) (surface layer) is in contact with the atmosphere and has a thickness of 30 m. Water inflow from the Atlantic takes place from the upper 150 m (Tsimplis & Bryden, 2000), therefore the thickness of the Upper layer is 120 m in the model. From the water Formation box surface/boundary processes with the atmosphere take place via evaporation (E), precipitation (P), river runoff (R), and heat exchange (H). The fourth box is the Deep water box (D). This box has a thickness of 850 m, bringing the total depth of the Mediterranean to 1500 m in the model, which is approximately the average depth of the sea. From the Formation box deep-water formation (q_{FD}) and intermediate water formation (q_{FL}) take place. To conserve the

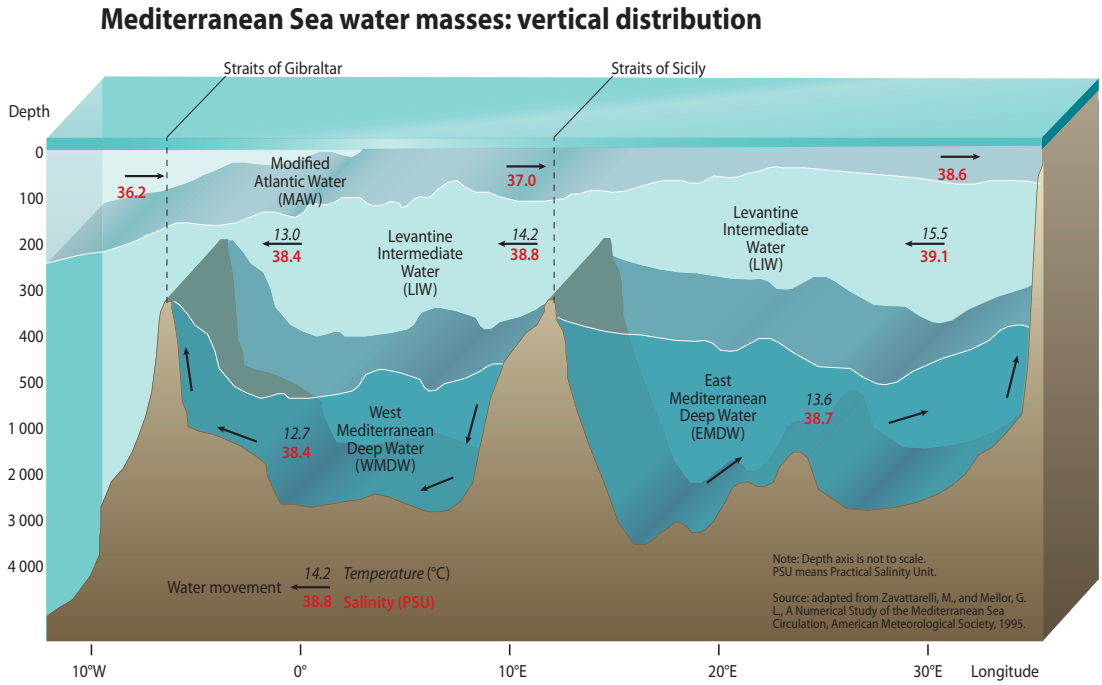

Figure 2.1: Schematically, the Mediterranean Sea comprises three main water masses, and a surface layer. The Modified Atlantic Water (MAW) has thickness between 50 and 200 m. The Levantine Intermediate Water (LIW), formed in the Levantine basin, lies in depth between 200 and 800 m (GRID Arendal, 2013)

volume of the different boxes there is flow from the Deep water box into the Lower layer (q_{DL}) and from the Upper layer into the Lower layer (q_{UL}) and the Formation layer (q_{UF}). Apart from the flow terms there is a mixing component between all layers that are in contact with each other (Millot, 1999; Jayne et al., 2004). The mixing of the Upper layer with the Formation layer is c_{FU}, and the mixing of the Upper layer with the Lower layer is c_{UL}. The mixing between the Lower layer and the Deep layer is c_{LD}.

2.1.2 Deep-water formation

Deep-water formation can be seen as a process of three phases. During the first phase, the preconditioning phase, a background of low static stability is created. The main preconditioning is provided by the presence of a cyclonic gyre (Gascard, 1978). The second mixing phase is characterized by intense and rapid cooling and/or evaporation. Surface waters then become denser than deeper waters, and as a consequence the dense surface waters descent. In the Mediterranean this phase is initiated by the surface heat loss in the winter. In the Western Mediterranean strong Mistral events, which are cold and dry winds from the North, cool the surface during winter (Lascaratos et al., 1999). In the Eastern Mediterranean the local meteorological conditions form dense surface water and cause deep-water formation. During the third phase, the sinking and

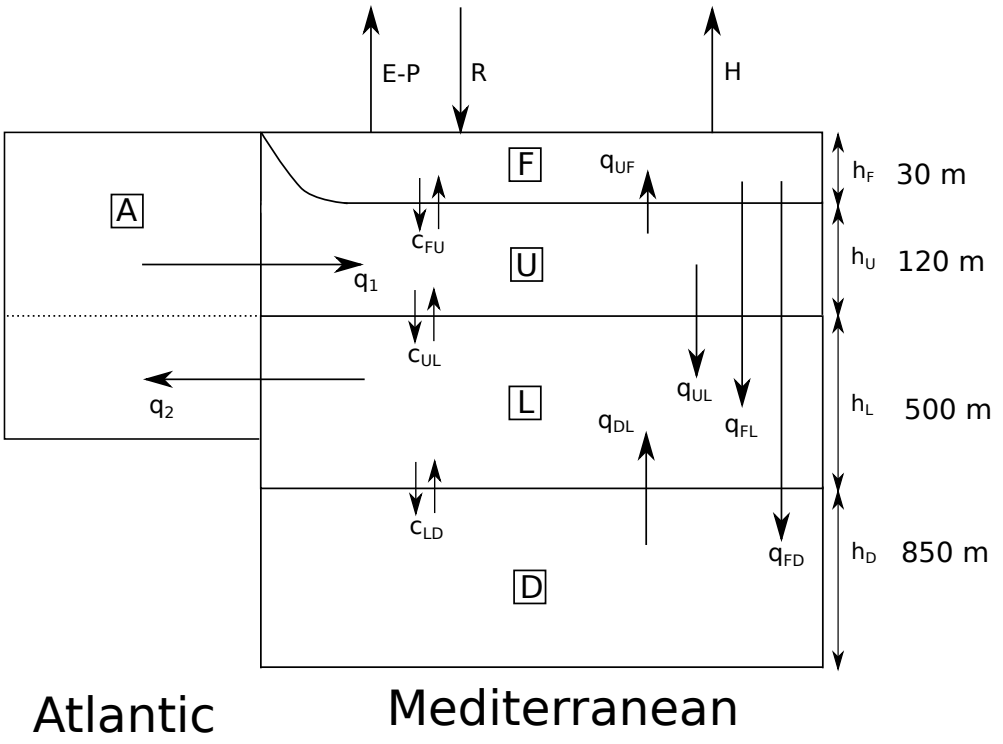

Figure 2.2: 4-layer box model of the Mediterranean sea, which consists of a water Formation box (F), an Upper layer box (U), a Lower layer box (L), and a Deep water box (D). The water Formation box interacts with the atmosphere via evaporation (E), precipitation (P), river runoff (R) and heat exchange (H). The depth (h) of the layers is constant. Furthermore there is flow (q) between the different layers and the Atlantic (A), and mixing (c) between the different layers.

spreading phase, the newly formed dense water equilibrates with the surrounding and spreads horizontally (Paluszkiewicz et al., 1994) .

Deep-water formation is a process on different scales. Among them we clearly identity three scales: the so called chimney, the mesoscale eddies, and the small-scale features (Gascard, 1991). The chimney was introduced by the Medoc group (1970) to define the area where deep water formation is active. Killworth (1976) presented the chimney as a narrow and unstable region (about 50 km in diameter) with intense vertical mixing forced by atmospheric cooling at the surface. Frequently mesoscale eddies are observed in deep convection regimes. These eddies result from a baroclinic instability of the chimney (Gascard, 1991). On a smaller scale (in the order of 1 km) convectively driven plumes play a role (Paluszkiewicz et al., 1994). In the box model we look at the process on a large scale and deep-water formation will be modelled as a convective flow from the Formation box to the Deep water box. Smaller scale features are included in the mixing terms. One could argue that mixing decreases with less deep- and intermediate water being formed. While this is not included in the model, the effect of changing the mixing will be investigated.

2.2 Model equations

We will start the description of the model equations by formulating the transport rates between the different layers. After that we will describe how the temperature and salinity of the layers are affected over time by these flows between the layers. This is done by using salt and heat conservation laws. The new temperature and salinity determine the density of the layers, which again modify the flow.

2.2.1 Transport and mixing

The outflow of the Meditteranean into the Atlantic in m^3/s (q_2) is proportional to the density difference between the lower layer of the Mediterranean and the Atlantic. It is parameterized by a pressure constant (p_c), which which can be adjusted such that q_2 represents observed present day values of 0.9 Sv (Bryden et al., 1994):

$$q_2 = p_c \cdot (\rho_L - \rho_A). \tag{2.1}$$

The density of the sea water is calculated with an equation of state (Johnson et al., 2007), and is dependent on the salinity and the temperature:

$$\rho = \rho_0(1 - \alpha(T - T_0 + \beta(S - S_0)), \tag{2.2}$$

with $\rho_0 = 1027.5$ kg/m^3, $\alpha = 2 \cdot 10^{-4}$ ^{o}C^{-1}, and $\beta = 8 \cdot 10^{-4}$ kg/g. $T_0 = 5^o$C, and $S_0 = 35$ g/kg. There are different methods to measure the salinity of water. Sea water with a salinity of 35.2 g/kg corresponds to a practical salinity unit (PSU) of 35.0, and a Knudsen salinity of 35 ppt. If the density differences in the sea water are small, as is the case in the Mediterranean sea, the different measurement methods for salinity give

approximately the same result. In the rest of this thesis we will use PSU as a unit for salinity.

At present day the Mediterranean has a net loss of water to the atmosphere. This is because the evaporation is larger than the precipitation and river runoff together. The inflow from the Atlantic into the Mediterranean Upper layer compensates for this net water loss to the atmosphere and for the outflow of the Mediterranean into the Atlantic such that

$$q_1 = q_2 + (E - P - R). \tag{2.3}$$

In this way the water balance of the Mediterranean sea is in equilibrium.

The next step is to define when deep-water formation takes place. The deep water is formed when the density of the Formation layer is higher than the density of the Deep water layer. The rate at which this deep water is formed is parameterized by the constant μ (Matthiesen & Haines, 2003):

$$q_{FD} = \begin{cases} \mu(\rho_F - \rho_D) & : \rho_F > \rho_D \\ 0 & : \rho_F < \rho_D. \end{cases} \tag{2.4}$$

The rate at which deep water forms is one of the parameters that can be varied while using the model. If the water is not dense enough to flow to the Deep water box, it can flow to the Lower layer if the density $\rho_F > \rho_L$,

$$q_{FL} = \begin{cases} \mu(\rho_F - \rho_L) & : \rho_F > \rho_L \\ 0 & : \rho_F < \rho_L. \end{cases} \tag{2.5}$$

In addition to the transport rates there is a mixing component between all the layers. This diffusive mixing (Jayne et al., 2004) can be described by the following equations (Tziperman & Speer, 1994; Matthiesen & Haines, 2003):

$$c_{FU} = \frac{\kappa}{d_{FU}}, \tag{2.6}$$

$$c_{UL} = \frac{\kappa}{d_{UL}}, \tag{2.7}$$

$$c_{LD} = \frac{\kappa}{d_{LD}}, \tag{2.8}$$

with κ the background diffusion coefficient, and d_{FU}, d_{UL} and d_{LD} the effective diffusion lengths. The effective diffusion length is taken as the distance between the middle of the two layers between which mixing takes place. The background diffusion coefficient is unknown and is varied in the model to look at different possible outcomes.

The layers have a constant layer thickness, which means the water budget of each layer over time should be exactly closed at all time. Because we need water conservation in each layer there is a flow between the different layers to obtain this:

$$q_{UF} = E - P - R + q_{FL} + q_{FD}, \tag{2.9}$$

$$q_{UL} = q_2 - q_{FL} - q_{FD}, \tag{2.10}$$

$$q_{DL} = q_{FD}. \tag{2.11}$$

The next step is defining how the temperature and salinity of the layers change over time due to this transport and mixing. For this we use salt and heat conservation in the Mediterranean.

2.2.2 Salt conservation

Transport and mixing affect the salinity and temperature of the boxes. The salinity of the inflowing water from the Atlantic is S_I. The salinity of the Formation layer is also affected by excess evaporation E-P-R. The model is simplified by assuming each box has an area $A = 2.4 \cdot 10^{12}$ m^2 (which is the area of the Mediterranean surface). Using salt conservation for each of the layers this leads to the following equations of change in salinity over time dt:

$$h_F \frac{dS_F}{dt} = (S_U - S_F) \cdot (c_{FU} + q_{UF}) + S_F(E - P - R) \tag{2.12}$$

$$h_U \frac{dS_U}{dt} = (S_I - S_U)\frac{q_1}{A} + (S_L - S_U)c_{UL} + (S_F - S_U)c_{FU} \tag{2.13}$$

$$h_L \frac{dS_L}{dt} = (S_U - S_L) \cdot (c_{UL} + q_{UL}) + (S_D - S_L) \cdot (c_{LD} + q_{DL}) \tag{2.14}$$

$$h_D \frac{dS_D}{dt} = (S_F - S_D)q_{FD} + (S_L - S_D)c_{LD} \tag{2.15}$$

2.2.3 Heat conservation

The heat conservation equations work in a similar way as the salt conservation equations only this time there is a heat loss H from the surface, and a temperature of Atlantic inflowing water of T_I. Using heat balance the temperature of the layers changes over time with the following rates:

$$h_F \frac{dT_F}{dt} = (T_U - T_F) \cdot (c_{FU} + q_{UF}) + \frac{H}{C_{\text{Water}}\rho_F} \tag{2.16}$$

$$h_U \frac{dT_U}{dt} = (T_A - T_U)\frac{q_1}{A} + (T_L - T_U)c_{UL} + (T_F - T_U)c_{FU} \tag{2.17}$$

$$h_L \frac{dT_L}{dt} = (T_D - T_L) \cdot (c_{LD} + q_{DL}) + (T_U - T_L) \cdot (c_{UL} + q_{UL}) \tag{2.18}$$

$$h_D \frac{dT_D}{dt} = (T_F - T_D)q_{FD} + (T_L - T_D)c_{LD} \tag{2.19}$$

$C_{\text{Water}} = 3993$ J/(kg·K) is the heat capacity of water.

2.2.4 Strait of Gibraltar

So far this model has worked with a simplified version of the Strait of Gibraltar. The model can be extended to include a more detailed strait by using hydraulic control theory. There are two advantages of the addition of hydraulic control theory. The first advantage is that hydraulic control theory gives more accurate equations for the in- and outflow in the Strait of Gibraltar (Meijer, 2012). A second advantage is that with hydraulic control theory sea level variations can be included, as the in- and outflow become dependent upon the water depth of the Strait. As we will investigate what the influence of sea level variations during the last precession cycle was on the circulation in the Mediterranean we will include hydraulic control theory in the model for this purpose. With hydraulic control theory the inflow q_1 and outflow q_2 in the strait can be calculated by using (Meijer, 2012):

$$\frac{q_1^2}{h_1^3 W^2} + \frac{q_2^2}{h_2^3 W^2} = g\frac{\rho_L - \rho_I}{\rho_L}. \tag{2.20}$$

In this equation W is the width of the strait, h_1 and h_2 are the layer thicknesses of the inflowing and outflowing water at the strait, and g is the gravitational constant. $H_{Strait} = h_1 + h_2$ is the total depth of the strait. It is assumed in this equation that the Strait of Gibraltar has a rectangular shaped cross-section. The real cross-section of the Strait of Gibraltar however captures a much smaller area. For this smaller cross-section we compensate by multiplying the outflow by a factor β, such that $\beta \cdot q_2 = 0.9$ Sv at present, where 0.9 Sv is observed present day outflow (Bryden et al., 1994). Furthermore, to conserve the total mass in the Mediterranean the total inflow q_1 is related to the outflow plus compensation for net evaporation and sea level rise

$$q_1 = q_2 + (E - P - R) + \frac{dH_{\text{Strait}}}{dt}. \tag{2.21}$$

The extra amount of water inflowing because of a (realistic) sea level rise $\frac{dH_{\text{Strait}}}{dt} << (E - P - R)$ in the Mediterranean. Therefore this term can be neglected. To simplify the strait we assume $h_1 = h_2 = \frac{H_{\text{Strait}}}{2}$. At present on average this is approximately the case. The average depth of the interface between in and outflow is approximately 147 m (Tsimplis & Bryden, 2000), while the depth of the Strait H_{Strait} is 284 m at present (Bryden et al., 1994). Mikolajewicz (2011) derived an expression showing that the outflow is linearly dependent on the strait depth, as long as variations in the salinity of the Mediterranean are small. As variations in the salinity of the Mediterranean in our model are small this justifies for our model purpose the assumption that $h_1 = h_2 = \frac{H_{\text{Strait}}}{2}$ which linearizes the outflow equation. The depth of the Strait can now be adjusted to include sea level variations. Note that the thickness of the layers in the Mediterranean stays constant. This a reasonable assumption as the depth of the Strait determines the properties of the Mediterranean. At the Strait the sea level rise changes the in- and outflow significantly. In the rest of the Mediterranean the thickness of the layers would slightly change. The effect of this is that it takes slightly longer for the layers to adjust to a new temperature or salinity. However, the change in depth of the

Mediterranean due to the sea level rise is only small compared to the total depth of the Mediterranean. Therefore we can take the sea level and layer thicknesses to be constant in the Mediterranean.

2.3 Model calibration

The box model (Appendix A.1) is programmed in Fortran 90, and is calibrated in the following way (Figure 2.3). Initial values are set for temperature and salinity of the different boxes, taken from the MEDAR database. From literature initial average values for E,P,R,H, and κ are found. A simple forward timestep model is used to calculate the changes in time. With the initial parameter values, changes in temperature, salinity and flow are calculated for a time step of $dt = 1$ day. The changes are then added to the intial value after which the process is repeated. We have chosen for time steps of days to make sure seasonal variations can be implemented, while the total calculation time of the model stays reasonable. Smaller time steps have also been tried but do not influence the outcome of the model anymore and do increase calculation time. The model is first given time to stabilize. After this stabilization time the model outcome is compared to data from the MEDAR database. The model is calibrated by including seasonal climatic variations which have been observed over the last 50 years (again data from the MEDAR database). This results in an error between data and model. We try to minimize this error by adjusting E,P,R,H, and κ within the range of the literature. This process is repeated iteratively until the error is minimized. Once the model is calibrated well-based estimates can be made of the precessional climatic variations. With these well-based estimates we can look at the possible impact of climatic variations on deep-water fo1

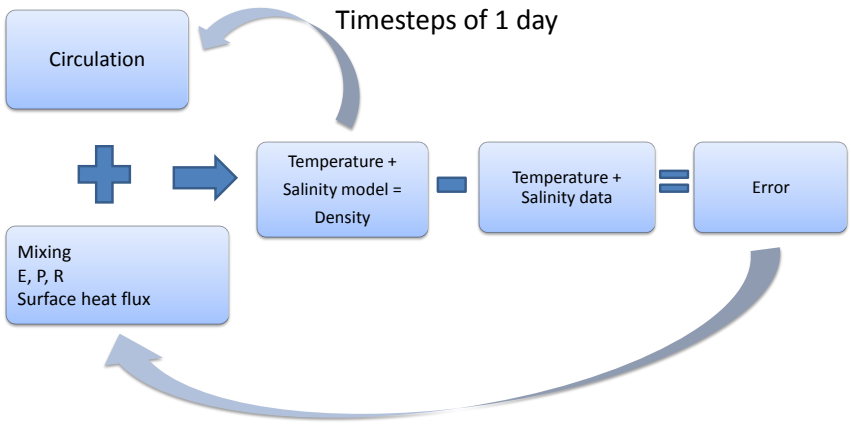

Figure 2.3: A schematic representation of the calibration process.

Chapter 3

Model parameters

Now that the model has been described the next step is to quantify all the parameters, and check the validity of the model. This requires a three step approach. The first step is to obtain measured data about temperature and salinity of the Mediterranean sea. For this the MEDAR database (MEDAR group, 2002) has been used. This data will be used to calibrate the model. The second step is to quantify the evaporation (E), precipitation (P), river runoff (R), heat exchange (H), mixing (κ), and the in- and outflow from the Atlantic (p_c). Various papers have been used to obtain realistic values for these parameters. The final step is to quantify the deep- and intermediate-water formation via the parameter μ. Once all parameters have been defined the model can be calibrated to the MEDAR data of the Mediterranean data. Section 3.1 will start by explaining how the average temperature and salinity are obtained from the MEDAR database. In Section 3.2 the temperature and salinity will be used to obtain the density in the Mediterranean. Section 3.3 will quantify the climatic forcing including seasonal and precessional climatic variations. Finally in this section we will discuss and quantify the flow and mixing.

3.1 Temperature and salinity

The MEDAR database contains measured information of the salinity and temperature of the Mediterranean and part of the Atlantic at 25 different depth points. The grid contains datapoints at a distance of 0.2 degrees latitude and 0.2 degrees longitude apart from each other. Temperature and salinity have been measured from 1945 up to 2002. The database contains both monthly averages and yearly averages.

A program (Appendix A.2) has been written to obtain the average monthly and yearly temperature and salinity between two specified depths. This program works as follows. Each datapoint is assumed to represent a volume. In this way we obtain a 3-D grid. A schematic representation of the grid is shown in Figure 3.1. The height $h(k)$ of each grid volume cell of layer k at depth $d(k)$ is

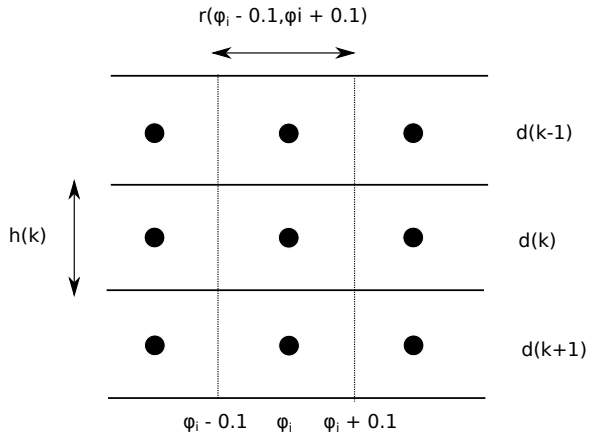

Figure 3.1: Schematic 2-D representation of the grid that is made to determine the average temperature and salinity in the Mediterranean. The dots represent the data points, d(k) is the depth of the data point k, and h(k) is the height of the cell which has the characteristics of the data point. $r(\phi_i - 0.1, \phi_i + 0.1)$ is the width of the data cell. The third dimension, the longitude, is not represented in this figure but is analogue to the latitude.

$$h(k) = \left| \frac{d(k+1) - d(k-1)}{2} \right|. \tag{3.1}$$

Then the area of each grid cell is calculated. This is done by using the haversine formula to determine the east-west and north-south dimension of the cell. The distance between two points is

$$r(\phi_1, \phi_2, \lambda_1, \lambda_2) = 2R \arcsin\left(\sqrt{\sin^2\left(\frac{\phi_2 - \phi_1}{2}\right) + \cos(\phi_1)\cos(\phi_2)\sin^2\left(\frac{\lambda_1 - \lambda_2}{2}\right)} \right), \tag{3.2}$$

with $R = 6371 \cdot 10^3$m the radius of the Earth, ϕ_1 and ϕ_2 the latitude of point 1 and point 2, and λ_1 and λ_2 the longitude of point 1 and point 2. Because the grid contains datapoints at a distance of 0.2 degrees latitude and 0.2 degrees longitude apart $\phi_1 = \phi_i - 0.1$, $\phi_2 = \phi_i + 0.1$, $\lambda_1 = \lambda_j - 0.1$, $\lambda_2 = \lambda_j + 0.1$, with ϕ_i and λ_j the latitude and longitude at the data point. The area of each data cell is

$$A(\phi_i, \lambda_j) = r(\phi_i - 0.1, \phi_i + 0.1, \lambda_j, \lambda_j) \cdot r(\phi_i, \phi_i, \lambda_j - 0.1, \lambda_j + 0.1). \tag{3.3}$$

Now that we have the area and the height of each data cell the volume is simply

$$V(k, \phi_i, \lambda_j) = h(k) \cdot A(\phi_i, \lambda_j). \tag{3.4}$$

The average temperature (T) between two layers k_n and k_m can now be calculated in the following way

$$T_{av}(k_n, k_m) = \frac{\sum_k \sum_i \sum_j (T(k, \phi_i, \lambda_j) \cdot V(k, \phi_i, \lambda_j))}{\sum_k \sum_i \sum_j V(k, \phi_i, \lambda_j)}. \tag{3.5}$$

The salinity (S) between layer k_n and k_m can be calculated in similar fashion

$$S_{av}(k_n, k_m) = \frac{\sum_k \sum_i \sum_j (S(k, \phi_i, \lambda_j) \cdot V(k, \phi_i, \lambda_j))}{\sum_k \sum_i \sum_j V(k, \phi_i, \lambda_j)}. \tag{3.6}$$

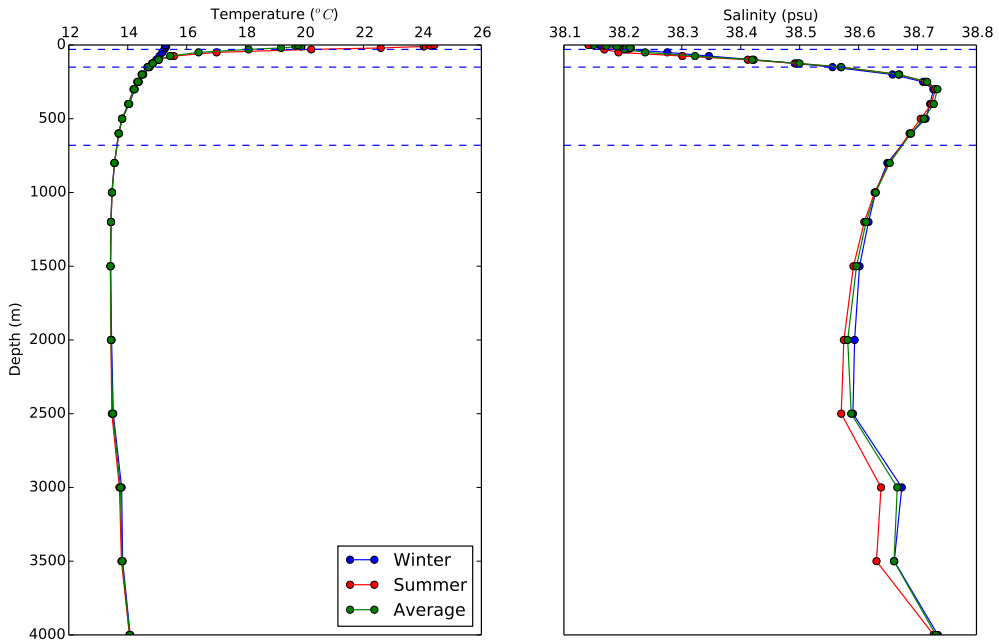

Figure 3.2: Average temperature and salinity depth profile in the Mediterranean. The dashed lines represent the box boundaries.

By specifying the coordinates the average temperature and salinity in a certain layer can now be calculated.

With the described method the temperature and salinity of the different layers has been calculated. Figure 3.2 shows the annual, summer and winter average temperature-depth and average salinity-depth profile in the Mediterranean. The depth of the different box boundaries is also shown in these figures.

If we now take the volume average in the boxes we obtain Figure 3.3. This figure gives respectively the average winter, summer and yearly temperature and salinity. If we look at the mean temperature we see in general a stably stratified column. The temperature is around 5.5^{o}C higher near the surface than at large depth. Salinity is lower near the surface by around 0.4 psu. The temperature of the Atlantic inflowing water is higher than the temperature of the outflowing water. This means that the Atlantic eventually heats the Mediterranean water. The salinity of the Atlantic inflowing water is lower than the salinity everywhere in the Mediterranean, thus the Atlantic inflow reduces the salinity of the Mediterranean.

If we look at the summer and winter temperature in the boxes it becomes clear that there are seasonal variations in temperature of the Upper layer and the Formation layer. The mean Formation layer temperature varies between 15^{o}C during winter and 23^{o}C during summer. The Upper layer has a seasonal temperature difference of 1^{o}C and varies between 15^{o}C and 15.9^{o}C. There is no significant change in salinity associated with seasonal fluctuations.

Apart from the temperature and salinity variations in depth, it is also interesting to

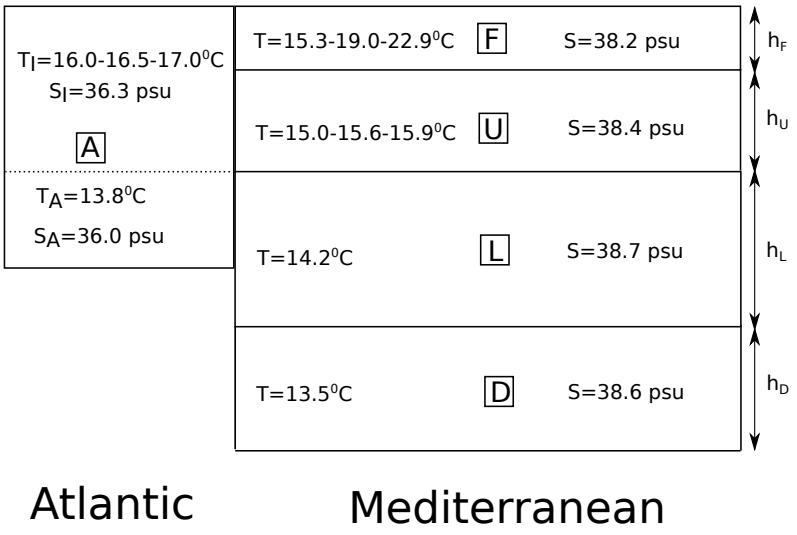

Figure 3.3: Box model of Mediterranean with average winter-annual-summer temperature and salinity calculated from MEDAR database. If only 1 temperature or salinity is denoted the temperature/salinity of the layer is constant through the year.

look at spatial temperature and salinity variations. These spatial variations can not be implemented easily into the box model, however these do tell us a lot about the flow and processes in the Mediterranean. Figure 3.4, and Figure 3.5 show the temperature in the Mediterranean at a depth of 5 meters. Temperature in the winter varies between 10-11^{o}C in the North to around 17-18^{o}C in the East in winter. In summer these temperatures vary between 20^{o}C in the North to 28^{o}C in the East. As cold temperatures cause a high density of the water the Northern locations favor deep-water formation. Figure 3.6 shows the annual average salinity at 5 meters depth. This graph clearly shows the inflow of low saline Atlantic water in the West. Salinity varies spatially between 36 and 39.3 psu, a much larger range than the salinity variations in depth. The Northern areas also show a lower salinity. This is due to river inflow of the Po, the Rhone, and inflow from the Black sea, which all have a very low salinity. If we look at the salinity at a depth of 500 meters in Figure 3.7 we see that the spatial variations have more or less disappeared. To look at possible locations of deep-water formation it is best to look at the density. This we will do in the next section.

3.2 Density

Now that the temperature and salinity of the Mediterranean are known, Equation 2.2 can be used to calculate the density of the layers. What is even more of interest is the density difference between the surface and the deep water layer, as $\rho_F > \rho_D$ initiates the deep-water formation. In this section we will look at this density difference in the Mediterranean during different seasons. In Figure 3.8, and 3.9 the density difference between water at 500 m depth and water at 5 m depth ($\rho_{500m} - \rho_{5m}$) is plotted. Figure 3.10 gives a depth-density profile in summer and winter. From these figures it becomes

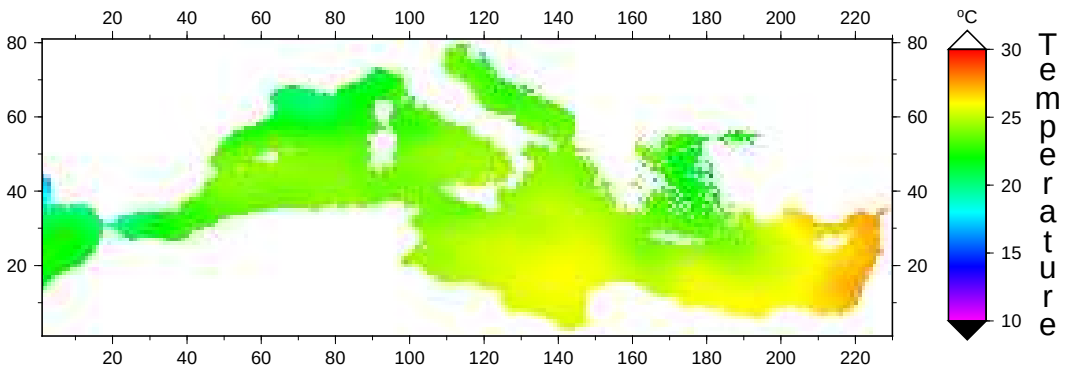

Figure 3.4: Temperature at 5 m depth during summer.

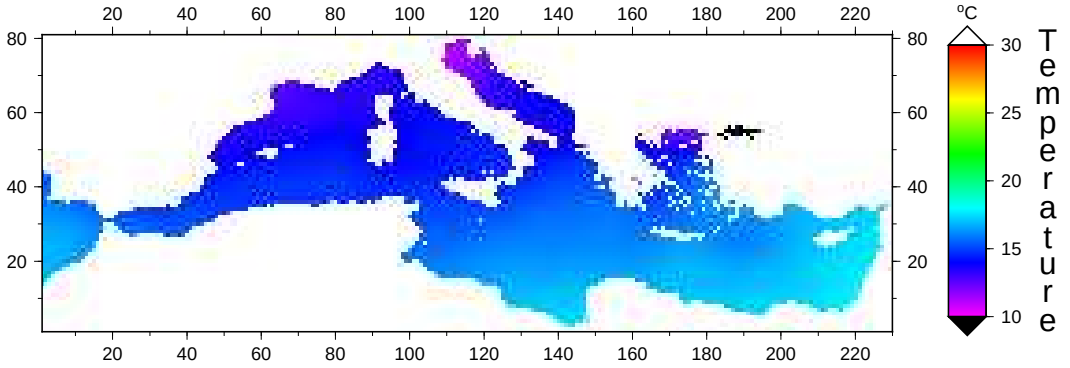

Figure 3.5: Temperature at 5 m depth during winter.

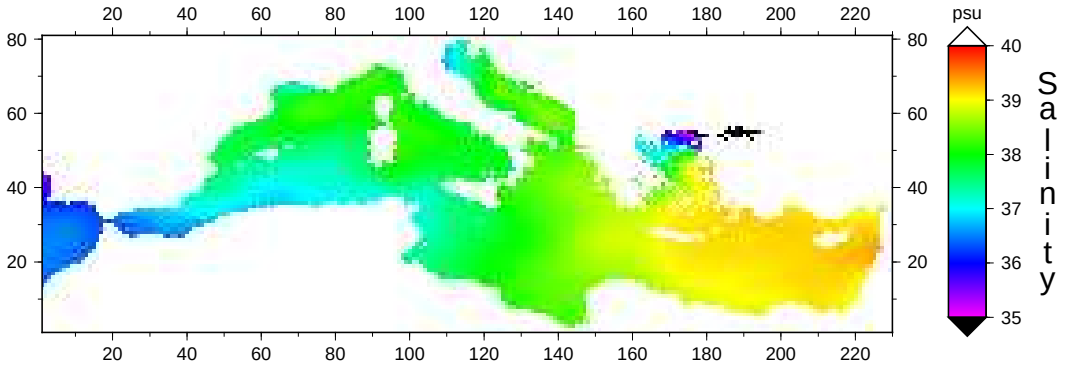

Figure 3.6: Yearly average salinity at 5 m depth.

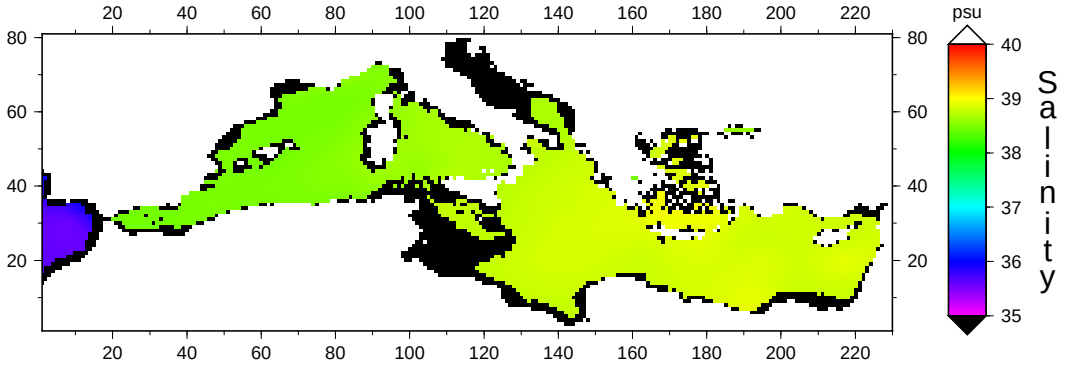

Figure 3.7: Yearly average salinity at 500 m depth.

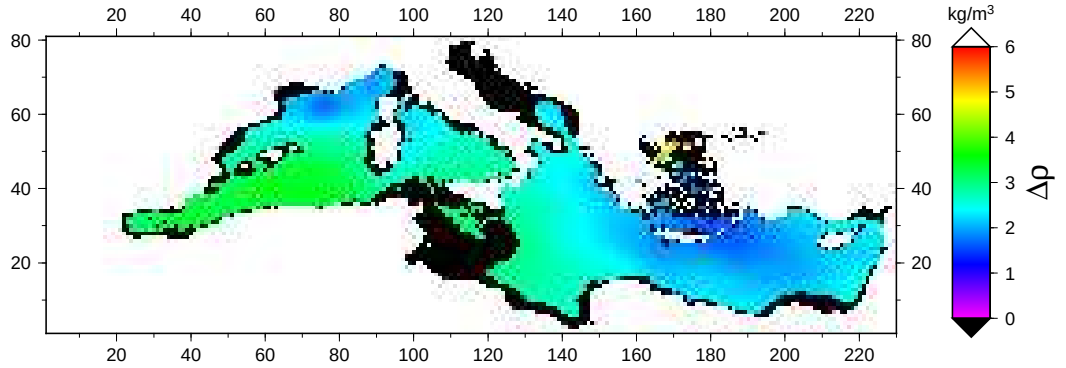

Figure 3.8: Density difference in summer between 5 m depth and 500 m depth ($\rho_{500m} - \rho_{5m}$).

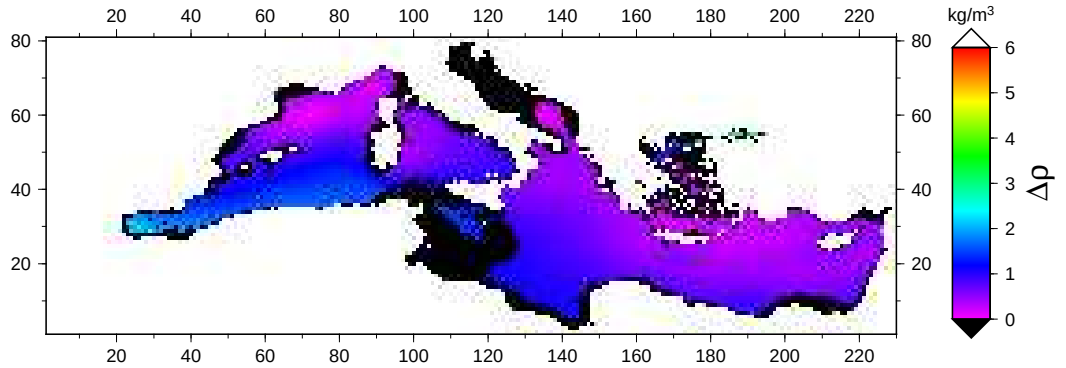

Figure 3.9: Density difference in winter between 5 m depth and 500 m depth ($\rho_{500m} - \rho_{5m}$).

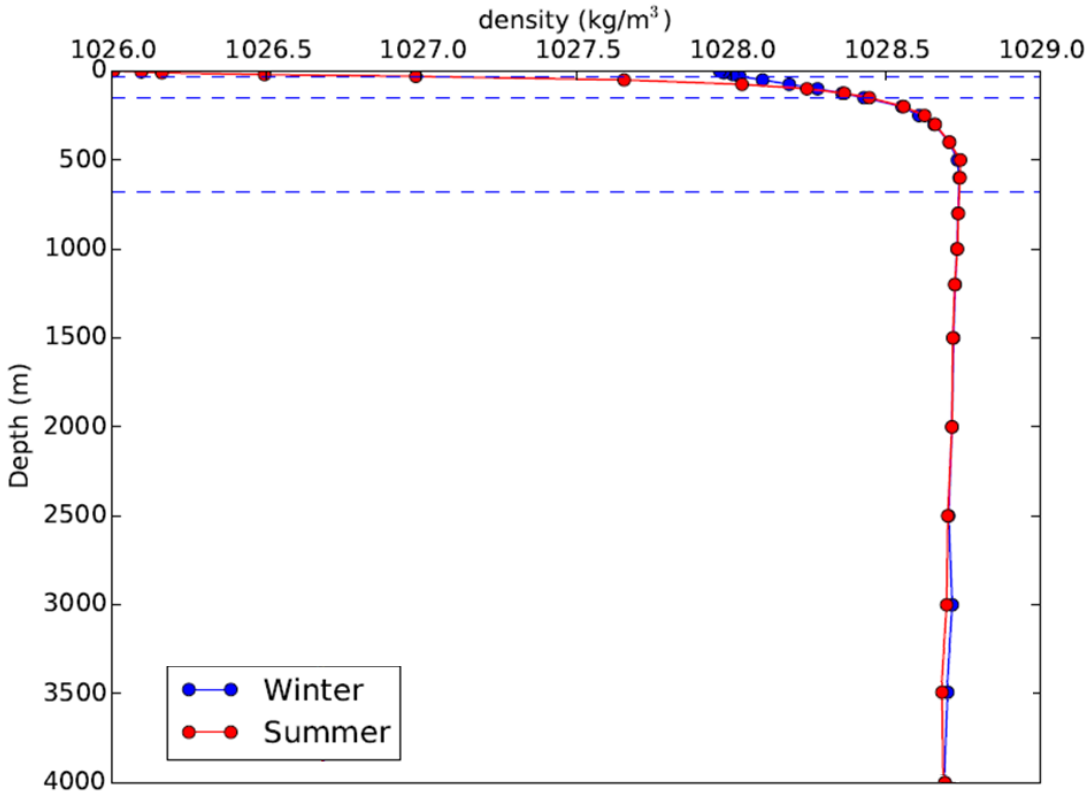

Figure 3.10: Density depth profile in summer and winter. The dashed lines represent the box boundaries.

clear that during summer there is a high density difference between the layers. The density is on average around 2.5 kg/m^3 lower near than surface than at depth. This suggests that the water column is stably stratified, and there is no large source of deep-water formation. However, during winter the density difference is around 0.7 kg/m^3 between the surface and the deep water. In the Northern parts of the Mediterranean the density difference between the surface and 500 m depth is close to 0. This suggests that there could be deep-water formation as dense surface waters tend to go down and mix with the deep water. When the surface water gets denser than the deep water there is deep-water formation. As the dense surface water sinks when it becomes denser than the deep water the difference between the surface water and the deep water is close to zero. The main reason for the surface water to get dense is the large heat loss during winter. The deep-water formation at these Northern spots during winter is in agreement with recent literature about circulation in the Mediterranean (Pinardi & Masetti, 2000).

3.3 Water and heat budget

The Mediterranean sea has a net water loss from the surface. This water loss results from the difference between evaporation (E) and precipitation (P) plus river runoff (R). There

is no consensus over the net yearly average evaporation, precipitation and river runoff however. The literature also contains a wide range of estimates over the Mediterranean heat budget (H). To obtain realistic values for E-P-R and H the following method has been used. First from literature the range is found for the yearly average E-P-R and H. From this range an average value is taken for the parameters as model input. The model is run without seasonal or Milankovitch variations. The outcome temperature and salinity of the model with these parameter values is compared to the temperature and salinity of the MEDAR database. By means of iteration the difference between the model outcome and the MEDAR database is minimized. After the yearly average E-P-R and H are found, seasonal variations are included. Initial seasonal variations in E-P-R and H are found by making a fit to literature data. Afterwards the parameters are fine-tuned to minimize the difference between the model outcome and the MEDAR seasonal data. The parameter values always stay within the range of values found in literature.

Estimates of E-P include 0.65 m/yr (Boukthir & Barrier, 2000), 0.5-0.7 m/yr (Mariotti et al., 2002), 1.1 m/yr (Bethoux & Gentili, 1999), and 0.9 m/yr (Romanon & Tselioudis, 2010). In this model a calibrated average of these estimates will be used of $E - P = 0.77$ m/yr. An annual average river influx of 0.17 m/yr will be used (Meijer & Tuenter, 2007).

The estimated yearly average heat budget of the Mediterranean varies between -11 W/m^2 (Castellari et al., 1998) and 29 W/m^2 (Garrett et al., 1993). A average yearly heat loss of 4 W/m^2 gives realistic temperatures in the box model.

3.3.1 Seasonal variations

The ECMWF Re-analysis project (ERA; Gibson et al., 1997) used data from 1979 to 1993 to obtain seasonal variations in E-P-R. The resulting data are plotted in Figure 3.11. The seasonal variations in E-P-R of the ECMWF can be approximated by a sinusoid

$$[E - P - R](t)_s = [E - P - R]_{av} - \Delta[E - P - R] \sin\left(\frac{2\pi(t - \Delta\Phi)}{\text{year}}\right). \tag{3.7}$$

$\Delta\Phi$ corrects the phase of the fit. The sinusoid fits the data best if $[E - P - R]_{av} =$ 0.5m/yr, and $\Delta[E - P - R] = 0.35$m/yr. However after calibrating the model output temperature and salinity a slightly higher average E-P-R of 0.6 m/yr, and a slightly higher sinusoidal amplitude of 0.4 m/yr fit the MEDAR data better. Therefore these values will be used.

The surface heat flux also has seasonal variations. This heat flux is incorporated in the term $\frac{H(t)}{C_{\text{Water}}\rho_F}$ in Equation 2.16. The NCEP climatological dataset has been used to analyse the net heat flux from the Mediterranean surface (Criado-Aldeanueva et al., 2012). Their datapoints are plotted in Figure 3.12. Again the seasonal pattern is clearly

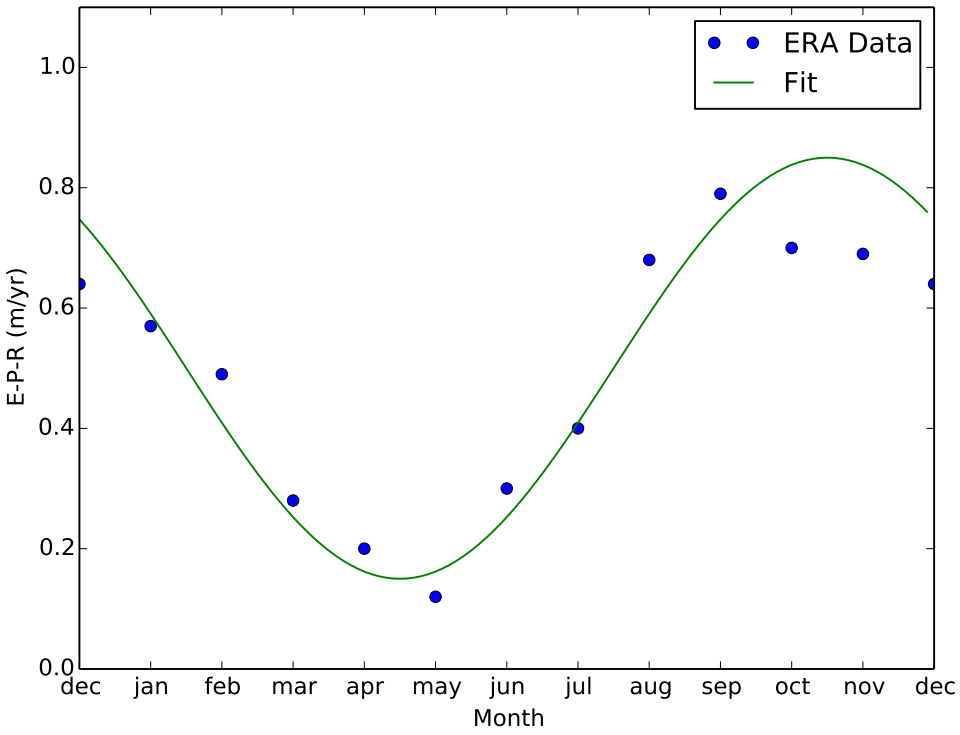

Figure 3.11: Seasonal variation in E-P-R. The green line is a fit to the data points (data points from Gibson et al., 1997).

sinusoidal and a fit is made:

$$H(t)_s = -H_{\max} \cos\left(\frac{2\pi t}{\text{year}}\right), H(t) > 0. \tag{3.8}$$

$$H(t)_s = -f_{\text{loss}} H_{\max} \cos\left(\frac{2\pi t}{\text{year}}\right), H(t) < 0. \tag{3.9}$$

$H_{\max} = 143$ W/m^2 is the maximum heat gain of the Mediterranean during summer. f_{loss} is a factor which can adjust for the fact that during winter the heat loss is different than the heat gain during summer. With $f_{\text{loss}} > 1$ there is a net surface heat loss over the year in the Mediterranean, while $f_{\text{loss}} < 1$ represents a situation in which there is a net surface heat gain in the Mediterranean. In this model $f_{\text{loss}} = 1.05$. This way the sinusoid fits the data points best, and we obtain realistic seasonal temperature variations. The average yearly heat flux including seasonal variations now is 2.3 W/m^2.

Finally, the temperature of the incoming water of the Atlantic also has seasonal fluctuations. From the MEDAR database we can obtain these seasonal fluctuations and the

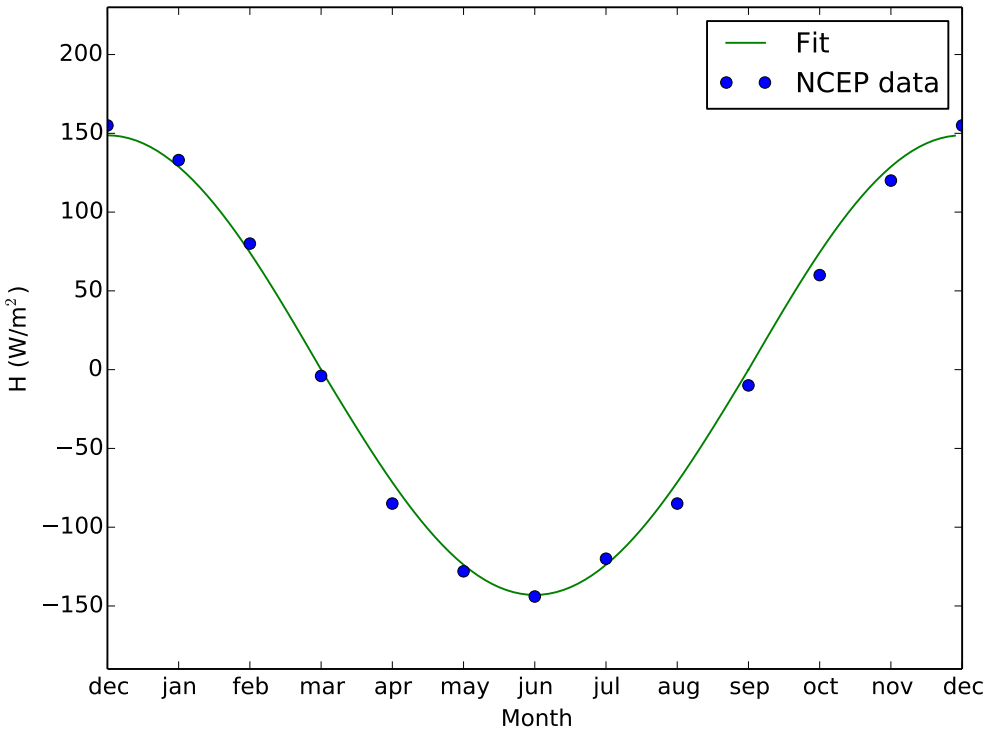

Figure 3.12: Seasonal variation in H. The green line is a fit to the data points. (data points from Criado-Aldeanueva et al., 2010)

yearly average. The average temperature of the incoming water of the Atlantic (T_{Iav}) of the upper 150 meters is around 16.5^{o}C, while the fluctuations (ΔT_I) are around 1^{o}C with:

$$T_I(t)_s = T_{Iav} - \Delta T_I \sin\left(\frac{2\pi t}{year}\right). \tag{3.10}$$

With these seasonal variations a model can be run which shows variations in deep-water formation on the timescale of years. If we want to model over a longer timespan of a precession cycle, the climatic variations due to this precession cycle also need to be included.

3.3.2 Precessional variations

In the beginning of the 20th century Milutin Milankovitch described that changes of the Earth's movement have effect upon its climate. He recognized three different long term movements the Earth has namely eccentricity, axial tilt, and precession. The precessional movement of the Earth seems to correlate with the formation of Sapropels in the Mediterranean (Rohling & Hilgen, 1990). To model climate variations in the

precession cycle we first have to understand what influence this precession cycle has on the climate. Therefore we first have to understand the precession cycle. The precession is the trend in the direction of the Earth's rotation axis relative to fixed stars. This axial precession has a period of around 26.000 years. The gyroscopic motion is caused by tidal forces exerted by the sun and the moon on the earth (Huybers, 2006). When the axis/north pole points towards the sun in perihelion the northern hemisphere has a larger difference between seasons, while the southern hemisphere has milder seasons (Bard et al., 2002). This is called a Northern hemisphere precession minimum. If the axis points away from the sun in perihelion it is the other way around. This is called a Northern hemisphere precession maximum. At present the perihelion occurs during southern hemisphere summer, meaning that we are in a precession maximum and the southern hemisphere has more extreme seasons than the northern hemisphere. In addition to the axial precession the orbital ellipse itself precesses in space as a result of interaction with Jupiter and Saturn. This smaller effect shortens the period of the precession to around 21.000 years (Huybers, 2006).

The precession cycle has 2 main effects. The first effect of a precession minimum is warm summers and cold winters, thus an increase in insolation difference between summers and winters. Figure 3.13 b) shows how the summer insolation varies over the last 120 kyr. The shape of the insolation fluctuations shows a sinusoidal pattern with a period of the precession cycle. The winter insolation will show the same pattern, with a lower insolation during a precession minimum. In the model this will be captured in the following way:

$$H_m = H_s \cdot (1 + \Delta H_m) - \Delta H_m \cdot H_s \cos\left(\frac{2\pi t}{t_m}\right), \tag{3.11}$$

where H_m is the precession dependent heat flux, $t_m = 21.000$ years, H_s is the seasonal dependent heat flux of Equation 3.8, and 3.9, and ΔH_m is the difference in summer and winter insolation between a precession minimum and a precession maximum. ΔH_m can vary depending on the precession cycle as can be seen from Figure 3.13 b). Therefore we will model the effects on deep-water formation for differences in insolation up to 30%.

The second climatic effect is that during a precession minimum various sources of extra freshwater have been identified. Both precipitation and river runoff increased during a precession minimum. Estimates are that precipitation and river runoff were both around 0.1-0.2 m/yr higher during the last precession minimum (Meijer & Tuenter, 2007). However the magnitude of variations in net evaporation has varied for different precession cycles. Therefore we will model a range of values for the increase of precipitation and river runoff between 0 and 0.6 m/yr. The shape of these variations in precipitation and river runoff is unknown. Therefore we will look both at a sinusoidal change and at a more sudden change. The sinusoidal change is incorporated in the

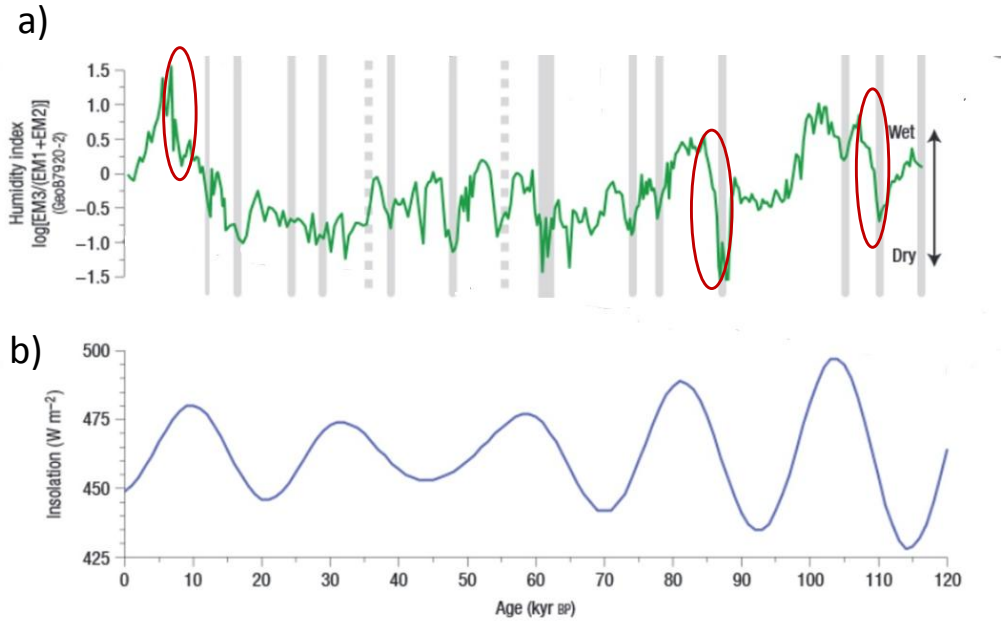

Figure 3.13: a) Humidity index in Northern Africa. Precession minima coincide with a high humidity in Northern Africa, which leads to a high river runoff. b) Summer insolation at 30°N. A high summer insolation insolation coincides with the precession minima and sapropel formation. (Tjallingii et al., 2008)

model in the following way:

$$P_m = P_s^* \cdot (1 + \Delta P_m \cdot P_{av}) - \Delta P_m \cdot P_{av} \cos\left(\frac{2\pi t}{t_m}\right), \tag{3.12}$$

$$R_m = R_s^* \cdot (1 + \Delta R_m \cdot R_{av}) - \Delta R_m \cdot R_{av} \cos\left(\frac{2\pi t}{t_m}\right), \tag{3.13}$$

P_s^* and R_s^* are adjusted in such a way that we are currently in a precession maximum. As mentioned we will model for different ΔP_m and ΔR_m. In Figure 3.13 a) we see the humidity index of Northern Africa, which shows that an increase in river runoff (and precipitation) may have taken place in a short period of time. This more sudden change in net evaporation will be modelled both as a decreasing slope in net evaporation of around 1000 years, and as a step function.

3.3.3 Flow and mixing

Vertical diffusivity is one of the key parameters controlling the circulation of the Mediterranean sea, and in particular the strength of the overturning circulation (Bryan, 1987). In circulation models normally a single value for the vertical diffusivity is used (Marotzke, 1997). The general background level of mixing is considered to be 0.1 cm/s^2 (Gregg, 1987). In previous box models background diffusivity values of 0.05-0.1 cm/s^2 have been used (Tziperman & Speer, 1994; Matthiesen & Haines., 2003). In general we will

use a background diffusivity of $\kappa = 0.1$ cm/s^2, but we will also investigate the effects of having a different background diffusivity.

To quantify the in- and outflow from the Mediterranean into the Atlantic the pressure constant p_c is used. $p_c = 2 \cdot 10^{-7}\text{m}^4(\text{kg}\cdot\text{s})$ and is calibrated in such a way that the outflow corresponds to a present day observed value of 0.9 Sv (Bryden et al., 1994). The deep- and intermediate water formation is quantified with the parameter μ. There is no literature available on the magnitude of the deep- and intermediate water formation. These flows do have an impact on the temperature and the salinity of the layers. Therefore we calibrated the magnitude of deep- and intermediate-water formation by comparing the model outcome temperature and salinity to the MEDAR database temperature and salinity. With this method we find $\mu = 1 \cdot 10^{-6}\text{m}^4(\text{kg}\cdot\text{s})^{-1}$.

Chapter 4

Results

In this section we use the model to try to understand the processes that cause deep-water formation in the Mediterranean. If we can understand what initiates deep-water formation, and how the process works, the model can be used to explain the formation of sapropels. To get a better understanding of sapropel deposition, the influence of the following events on deep-water formation in the Mediterranean will be investigated:

1) The influence of evaporation, precipitation, river runoff, heat inflow, mixing and the temperature and salinity of the Atlantic ocean. To investigate the effects of these parameters a sensitivity analysis is done.

2) The effect of seasonal variations in the parameters. A model which includes the seasonal variations will be run for a year. The model outcome will be used for calibration.

3) The effects due to climate variations caused by the Milankovitch precession cycle. A model which includes precessional variations will be run for 21.000 years. Focus will be on the effects of increased precipitation, and increasing variations in seasonal surface heat flow.

4) The effects of several processes during the last precession cycle. Sea level variations over the last 20.000 years will be implemented in the model. Also the opening of a connection between the Black sea and the Mediterranean around 8.500 BP is implemented in the model. In this way we can investigate if these event may have had significant influence on the formation of S1.

This chapter is divided into 4 corresponding sections.

4.1 Parameter sensitivity analysis

This section checks the sensitivity and influence on deep-water formation of a change in a single parameter. The model is first brought to an equilibrium. The parameter values that have been used are shown in Table 4.1. Before changes in parameters are applied we will first look at the outcome of the model in equilibrium (constant model).

The model results for the constant model are shown in Figure 4.1. The temperature in the constant model is approximately the same for all layers, around 13.9^oC. This is also the average temperature calculated from the MEDAR database in the Mediterranean. Temperature variations between the layers mainly follow from seasonal differences in surface heating which are not yet applied in this model. Due to mixing the temperature variations in this model are very small. Average salinity in the model is around 38.4 psu, which is very close to the average salinity of the Mediterranean of 38.6 psu. The average density in the model is 1028.5 kg/m^3, which is very close to the average of the Mediterranean of around 1028.7 kg/m^3. The outflow q_2 is calibrated with p_c to be around 0.9 Sv. There is a constant deep-water formation in this model of 0.6 Sv. The absolute amount of deep-water formation in the model is not meaningful as deep-water formation does only take place in the Mediterranean at specified locations. The box model contains no spatial variations, hence the absolute amount of deep-water formation is not a good indicator. What is a good indicator is the relative amount of deep-water formation. We can analyse the influence of events by looking at the amount of increase or decrease in deep-water formation. Note that the absolute amount of deep-water formation also depends crucially on the mixing, while the trend in deep-water formation does not. There is no intermediate-water formation in this constant model. Intermediate-water is only formed in the model when the density of the surface water is not high enough to result in deep-water formation. As there are no spatial variations, and there is deep-water formation, there is no intermediate-water formation in this constant model. However, there is a flow from the Upper layer to the Lower layer which compensates for the outflow. This flow is not a result of an unstable water column, but is there to balance the amount of water in each box. We will continue by looking at the sensitivity of deep-water formation to the parameters E-P-R, H, κ, T_I, and S_I.

4.1.1 Sensitivity in E-P-R

First we will look at the effects of a change in E-P-R. A Timescale of 1000 years is chosen to look at these changes as there is enough time to reach a new equilibrium after the change has been applied. Figure 4.2 shows what happens when suddenly the precipitation goes up by 0.2 m/yr. During a precession minimum E-P-R is expected to be lower than at present (Meijer & Tuenter, 2007). The increase in Precipitation causes a decrease in temperature of all layers and a decrease in salinity of all layers. The salinity in the Mediterranean decreases because there is a higher influx of fresh water. As a result of lower salinity in the Mediterranean the water is less dense and the

Parameter	Value
h_F^*	30 m
h_U^*	120 m
h_L^*	500 m
h_D^*	850 m
T_I^{**}	16.5 ^oC
κ^{***}	$2 \cdot 10^{-5} m^2 s^{-1}$
d_{FU}^*	75 m
d_{UL}^*	310 m
d_{LD}^*	750 m
p_c^{***}	$2 \cdot 10^{-7} m^4 (kg \cdot s)^{-1}$
μ^{***}	$1 \cdot 10^{-6} m^4 (kg \cdot s)^{-1}$
E-P-R*	0.6 m/yr
H*	4 W/m^2

Table 4.1: Table containing the parameters used in the box model for sensitivity analysis. Parameters with a * are obtained from literature, parameters containing ** are obtained from the MEDAR database, and parameters containing *** follow from optimisation of the model, by comparing model results with measured data of the Mediterannean.

outflow from the relatively cold Mediterranean water into the Atlantic reduces. This in turn causes the inflow from the relatively warm water of the Atlantic to reduce. This means the temperature of the layers will also decrease. The reduced salinity of the surface water causes the deep-water formation to stop as surface water becomes less dense. Only when the mixing has also caused the lower layers to become less saline the deep water-formation starts again. This means that a (sudden) change in E-P-R is the main reason the deep water-formation stops and not the value of E-P-R. The deep-water formation also depends on the rate of change of E-P-R. A fast change implies a sudden change in salinity and temperature, which can stop deep-water formation immediately. A more gradual change gives the sea more time to adapt to the changes in salinity and temperature, and has less impact on the deep-water formation. In the period of no deep-water formation the surface water is still dense enough to form intermediate-water formation. The density difference between the Formation layer and the Lower layer slowly increases in this period, increasing the intermediate-water formation. After approximately 200 years the density of the Formation layer is higher than the density of the Deep layer and deep-water formation starts again.

4.1.2 Sensitivity in H

The effect of an increase in surface heat loss of the Formation layer on the deep-water formation is a bit more difficult to describe. The results of changing the heat loss from 4 W/m^2 to 6 W/m^2 are shown in Figure 4.3. An increase in heat loss of course causes a decrease in temperature of all layers. This decrease in temperature causes the the

-	E-P-R ↑	H ↑	κ ↑	T_I ↑	S_I ↑
T_F	↑	↓	↑	↑	↑
T_U	↑	↓	↓	↑	↑
T_L	↑	↓	↓	↑	↑
T_D	↑	↓	↑	↑	↑
S_F	↑	↓	↓	↑	↑
S_U	↑	↓	↑	↑	↑
S_L	↑	↓	-	↑	↑
S_D	↑	↓	↓	↑	↑
q_{FD}	↑	↓↑	↓	↑	↑
q_{FL}	↑	↓↑	↓	↑	↑
q_2	↑	↑	↑	↓	↑

Table 4.2: Table with the influence of an increase in E-P-R, H, κ, T_I and S_I on the temperature, salinity, deep and intermediate water formation, and outflow into the Atlantic.

density of all layers to increase. The higher density of the Lower layer causes an increase in outflow into the Atlantic and thus an increase of inflow from the Atlantic into the Mediterranean. The net effect of outflow of the relatively cold Lower layer water and inflow of the relatively warm Atlantic water is heating of the Mediterranean. This heating effect can not compensate for the surface heat loss, but it reduces its effect. Another effect of this in- and outflow from the Atlantic is that the Mediterranean becomes less salty. The inflow water has a lower salinity, decreasing the salinity of the Mediterranean. The effect of the decrease in temperature and the effect of the increase of salinity can have an equal but opposite effect on the density of the layers. Therefore the change in density of the layers is small, which means the effect on deep-water formation does not have to be large. The first effect an increase in surface heat loss has on deep-water formation is an increase. The surface water becomes denser which causes deep-water formation to increase. Once the situation stabilizes again there might be an increase or decrease in deep-water formation depending on the amount of heat loss (and the mixing, E-P-R etc. that go along with it).

4.1.3 Sensitivity in mixing

The effect of an increase in mixing is first of all that the temperature and salinity of all layers get closer to each other. This also means that the densities of all layers get closer to each other. Figure 4.4 shows the effect of increasing the mixing from $2 \cdot 10^{-5}$ m^2s^{-1} to $4 \cdot 10^{-5}$ m^2s^{-1}. In a system with constant evaporation and heat loss this means that there is a decrease in deep-water formation. However if seasonal forcing is applied an increase in mixing causes deep-water formation to increase. The reason for this will be explained in the next section.

Table 4.2 summarizes the influence of all parameters. The influence of E-P-R, H, and κ we have discussed. The influence of T_I, and S_I are very straightforward. Increasing

the temperature of Atlantic inflow water will increase the temperature of the Upper and Formation layer. This decreases the density of these layers and reduces deep-water formation. An increase in salinity of the Atlantic inflowing water will increase salinity of the Upper and Formation layer. The density of these layers will increase and thus deep-water formation will increase as well.

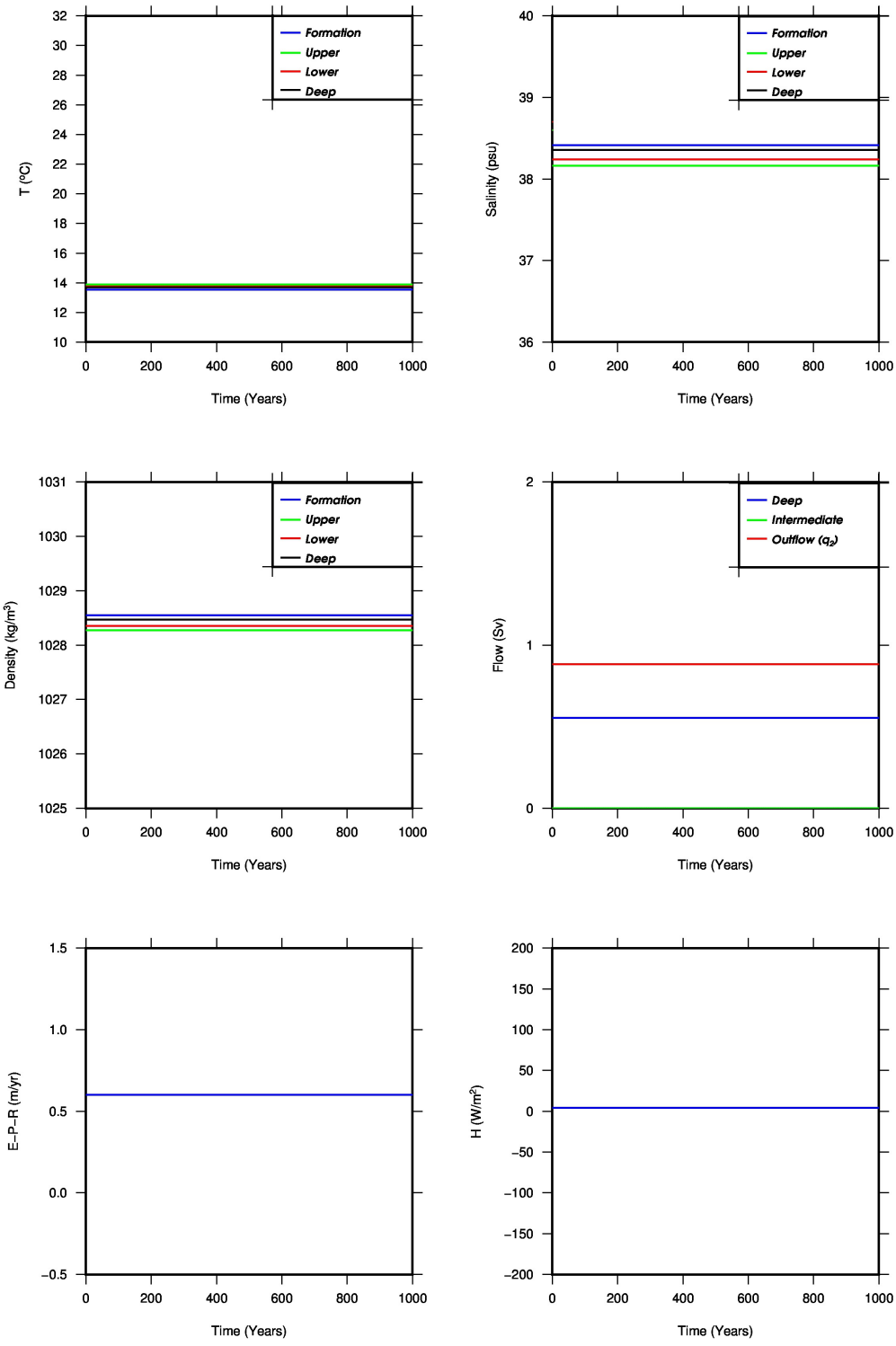

Figure 4.1: Model results with all parameters taken constant with values of Table 4.1.

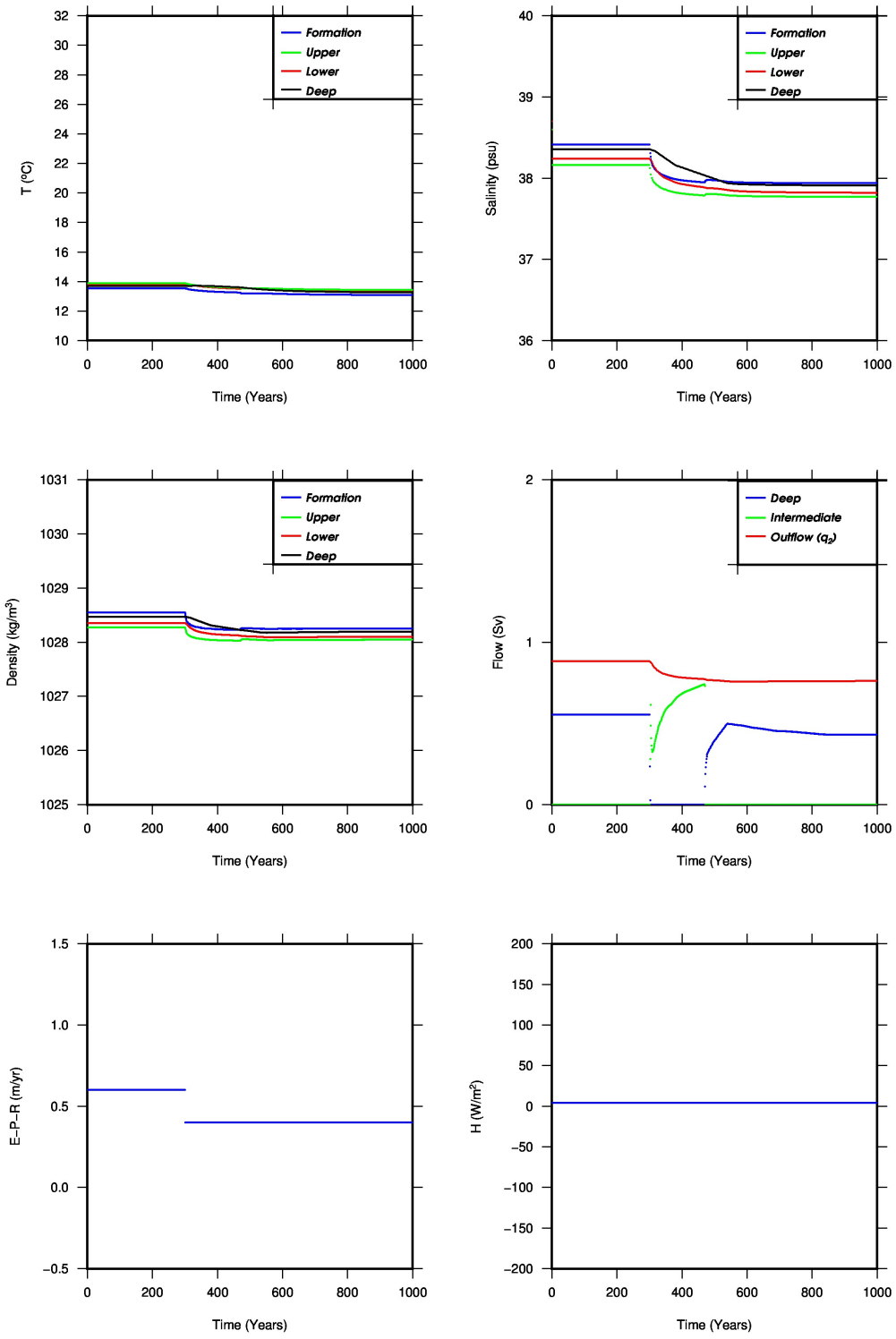

Figure 4.2: Model results changing E-P-R from 0.6 m/yr to 0.4 m/yr.

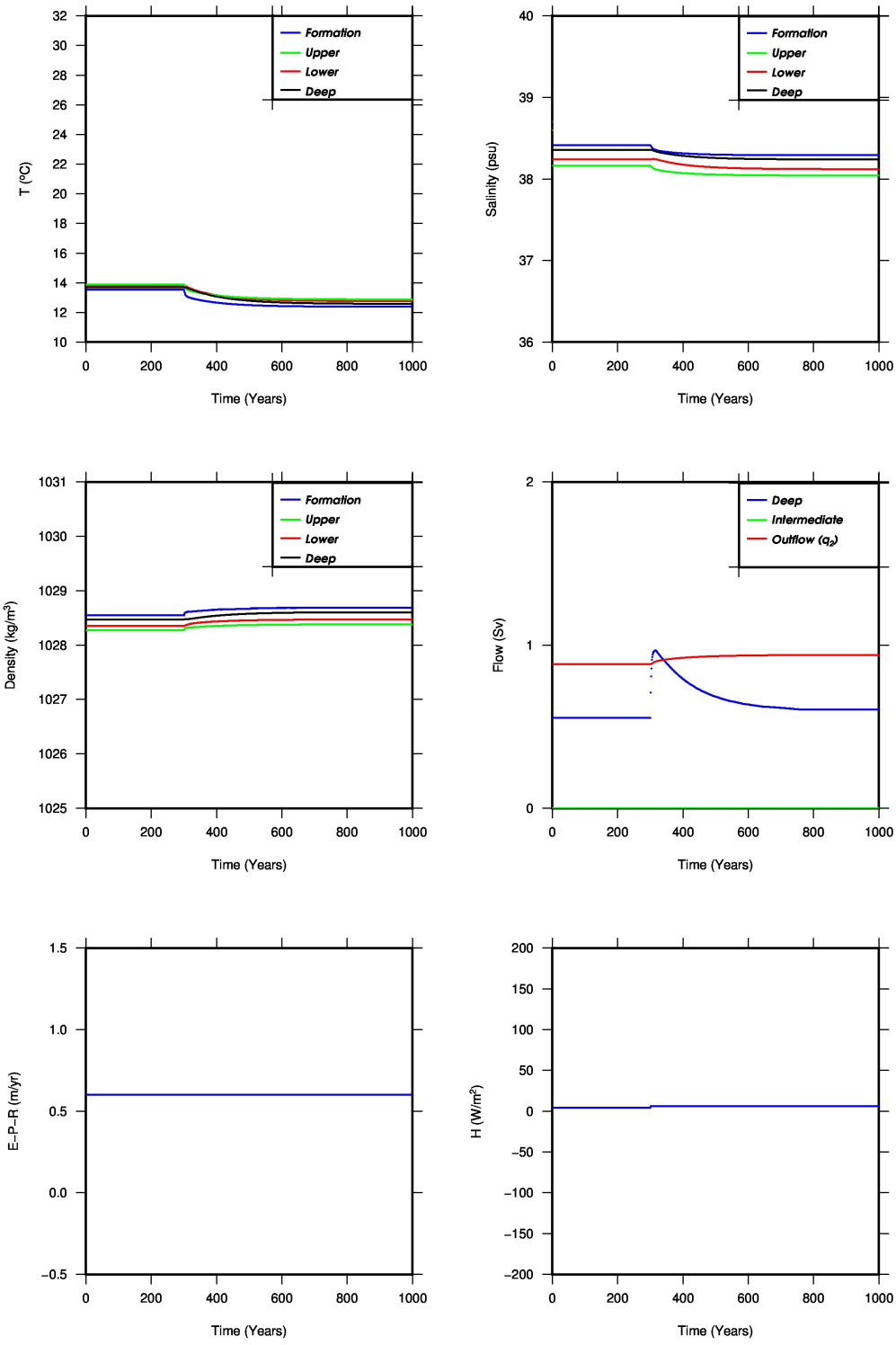

Figure 4.3: Model results changing H from 4 W/m^2 to 6 W/m^2.

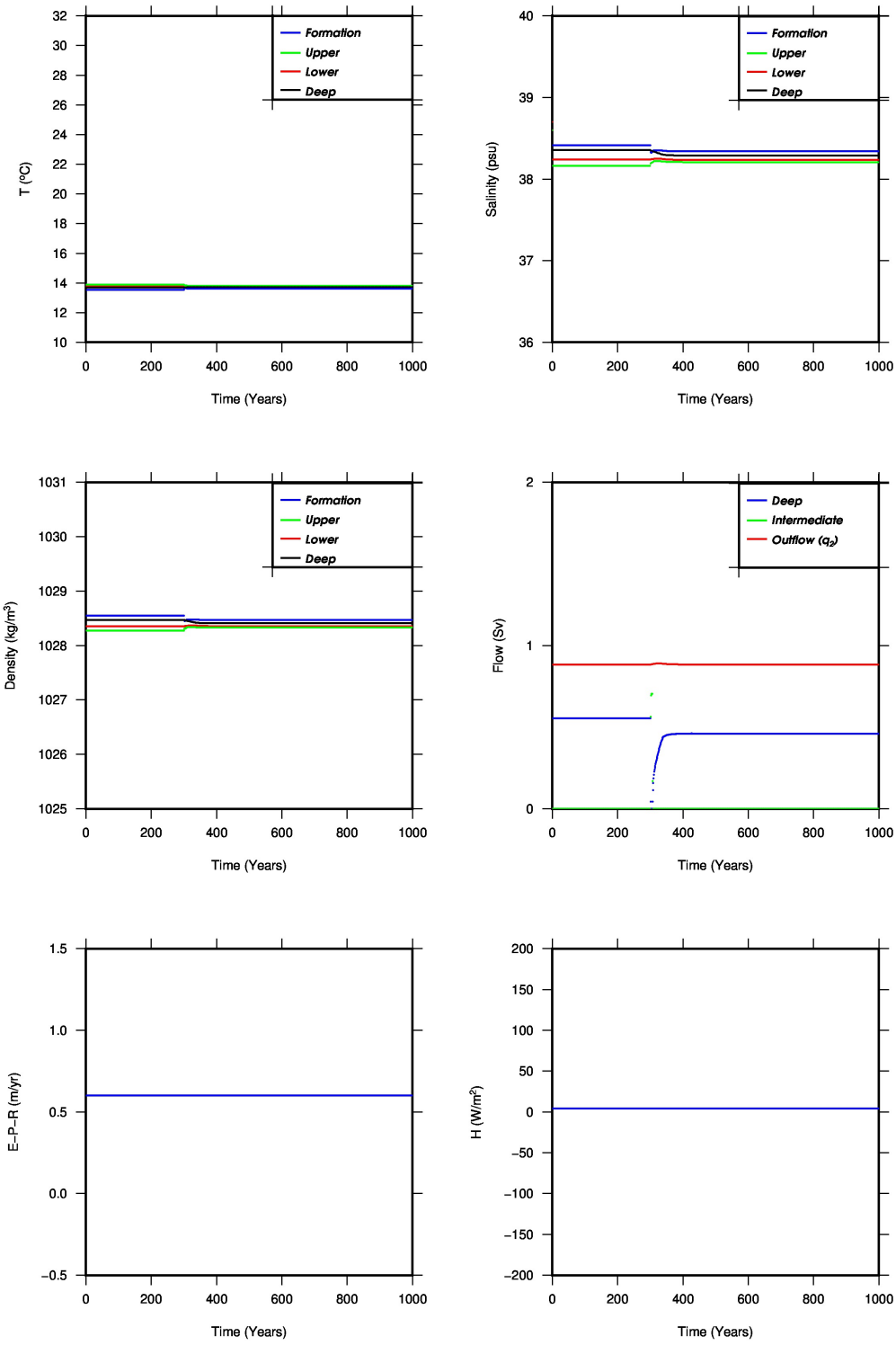

Figure 4.4: Model results changing κ from $2 \cdot 10^{-5}\mathrm{m}^2\mathrm{s}^{-1}$ to $4 \cdot 10^{-5}\mathrm{m}^2\mathrm{s}^{-1}$.

4.2 Seasonal variations

Due to the seasons on Earth there are variations in E, P, R, H, and T_I. The influence of the seasons on these parameters has been described in Section 3.3.1. First we will look at the separate effects of seasonal variations in these parameters, after which the effects will be combined.

Figure 4.5 shows the effects of seasonal fluctuations in E-P-R. The first month is the start of the winter in December. This means the first 3 months represent winter, months 4-6 are spring, months 7-9 are summer and months 10-12 are autumn. The only effect a fluctuation on E-P-R has on both temperature and salinity is a small variation of the surface salinity. During summer and autumn E-P-R is higher. However, there is a lag between the minimum in surface salinity and the minimum in E-P-R as surface salinity will keep on decreasing as long as E-P-R is below average. Deep-water formation is directly linked to the surface salinity as the density of the Formation layer is lowest during spring and therefore the deep-water formation is also lowest. There is intermediate-water formation when the deep-water formation stops.

Figure 4.6 shows the effect of the seasonal fluctuations in H. These fluctuations have a large effect on the temperature of the layers. For the first time now there is a substantial temperature difference between the layers in the model. The Formation layer is coldest during winter and this is also when deep-water formation takes place due to the high density of this layer. There is intermediate-water formation for a shorter period in spring and autumn.

If the effects of variations in H, and variations in E-P-R are now combined we obtain Figure 4.7. Deep-water formation takes place in the winter. This means the temperature effect of the surface heat loss during winter dominates the effect that E-P-R has on the surface salinity. Referring back to Section 4.1.3 if the mixing term is increased in the seasonal model the deep-water formation also increases. The density of the Deep layer goes down because salinity of the Deep layer becomes lower and the temperature becomes higher. The density of the Formation layer during winter however is not affected much by this increase in mixing. This is due to the following reason. During winter the Upper layer decreases the density of the Formation layer via mixing, because the Upper layer is warmer and less saline. If the mixing term is increased the salinity of the Upper layer increases, because both salinity of the Formation layer and of the Lower layer are higher. The temperature of the Upper layer decreases if there is more mixing. Thus the density of the Upper layer increases if there is more mixing in the Mediterranean. If there is more mixing in the Mediterranean the Formation layer would mix more with the Upper layer, but the effect of mixing would be less as the density of the Formation layer and Upper layer are closer to each other. Therefore by increasing the mixing term the density of the Formation layer during winter does not change significantly. The density of the Deep layer does reduce if the mixing term is increased so deep-water formation will increase.

Intermediate-water formation takes place during autumn and spring in this model. Both temperature and salinity of the Formation water during periods of intermediate-water formation are higher than temperature and salinity of the Deep layer. Therefore

we can say that it is the high salinity of the Formation layer that causes the density of the Formation layer to be higher than the density of the Deep layer. The salinity initiates the intermediate-water formation. A problem with intermediate-water formation in this model is the lack of spatial variations. Intermediate-water formation can only take place in periods when there is no deep-water formation. In the Mediterranean however spatial variations allow both to take place at the same time in different regions. The implications of this will be discussed in Chapter 5.

The model is fine-tuned as is explained in Chapter 3. The temperature of the Deep layer is around 13.2^oC while in reality the temperature is around 13.5^oC. The Lower layer has a temperature of 14.3^oC in the model, while the temperature is 14.2^oC in reality. The Upper layer temperature fluctuates by around 1^oC in the model with an average of 16.1^oC. Again the reality is not far off with an average temperature of 15.6^oC, and fluctuations of around 1^oC. The Formation layer is more difficult to compare to the data. Spatial variations of this layer are large. The difference between winter and summer is around 10^oC in the model. These temperature variations we also see in the measured data. The average temperature in the Formation layer in the model is around 17.0^oC, which is around 2^oC different from the average measured temperature of 19^oC. All together the temperature of the model agrees well with reality.

The salinity of the layers contains less variance due to seasons. In the model we see a salinity of around 38.4 psu of both the Deep and the Lower layer, a bit lower than the salinity in the Mediterranean in these layers which is around 38.6 psu. The Upper layer has a salinity of 38.2 psu in the model, also a bit lower than the 38.4 in the Mediterranean. The Formation layer has a salinity of 38.5 psu in the model, while the average is 38.2 psu in the Mediterranean. Fluctuations in salinity of the Formation layer of around 0.1 psu in the model are also measured. There is one difference between the model salinity and the Mediterranean average. In the model the Formation layer has the highest salinity (although not much higher than the Lower layer and Deep layer) while the measurements show it is the least saline layer. This can be explained by looking at Figure 3.6. The average surface salinity also includes the western waters, where surface salinity is largely influenced by the low saline inflowing water from the Atlantic. In the model the Atlantic water does not flow into the Formation box. The Formation box can therefore be seen as a box that excludes the region near the Strait of Gibraltar. Including this region would distort the process of deep-water Formation due to the very low salinity of the inflowing water. In the Mediterranean deep- and intermediate water formation also do not take place near the Strait of Gibraltar. In the discussion we will elaborate on the consequences of the lack of these spatial variations in our model.

In general the salinity and temperature in the model give a realistic representation of the Mediterranean. The model can predict deep-water formation in the winter and shows what paramaters prove to be essential for this deep-water formation. The model can now be used to predict deep-water formation during a precession cycle.

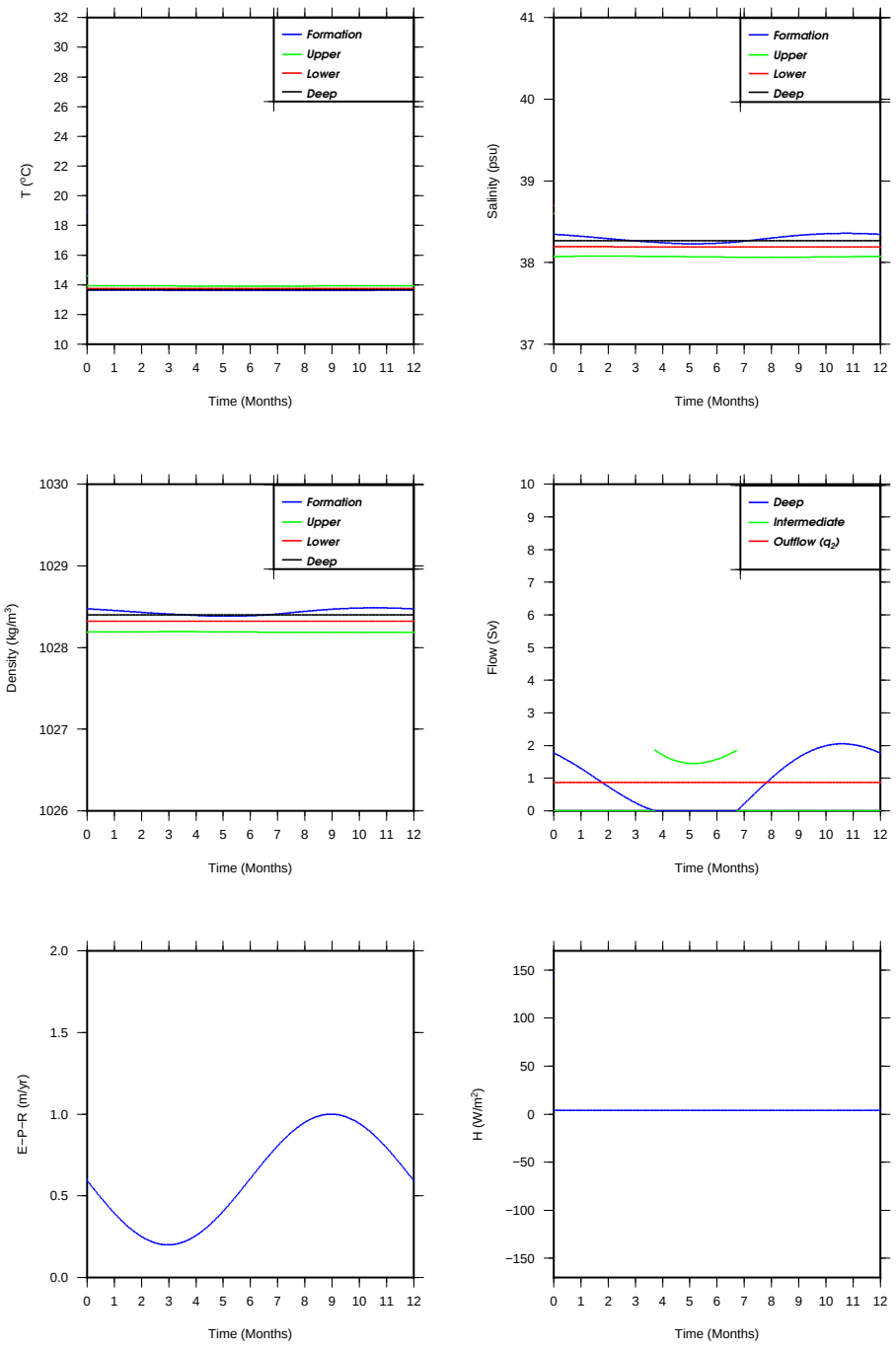

Figure 4.5: Model results with seasonal variations in E-P-R.

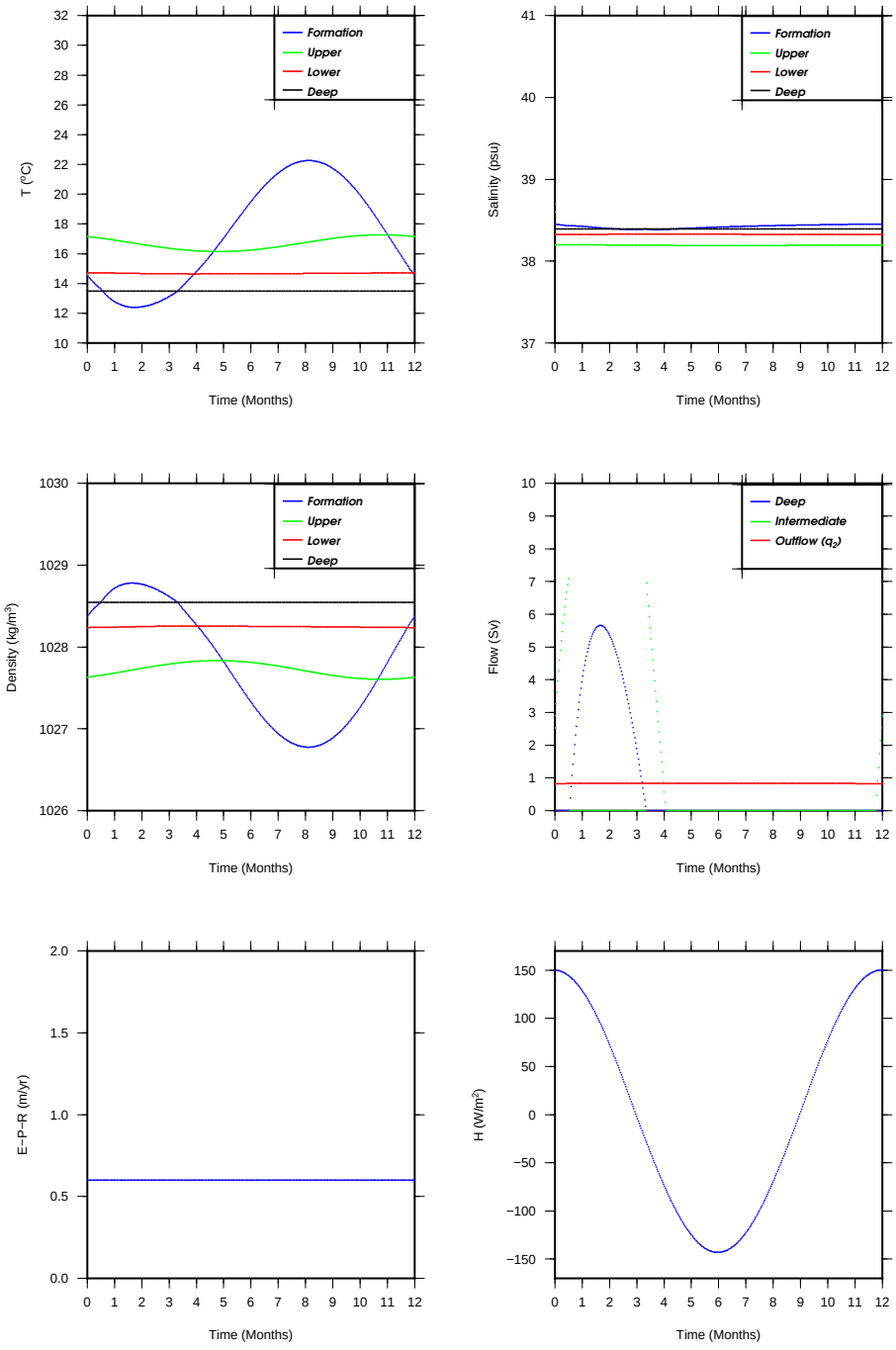

Figure 4.6: Model results with seasonal variations in H.

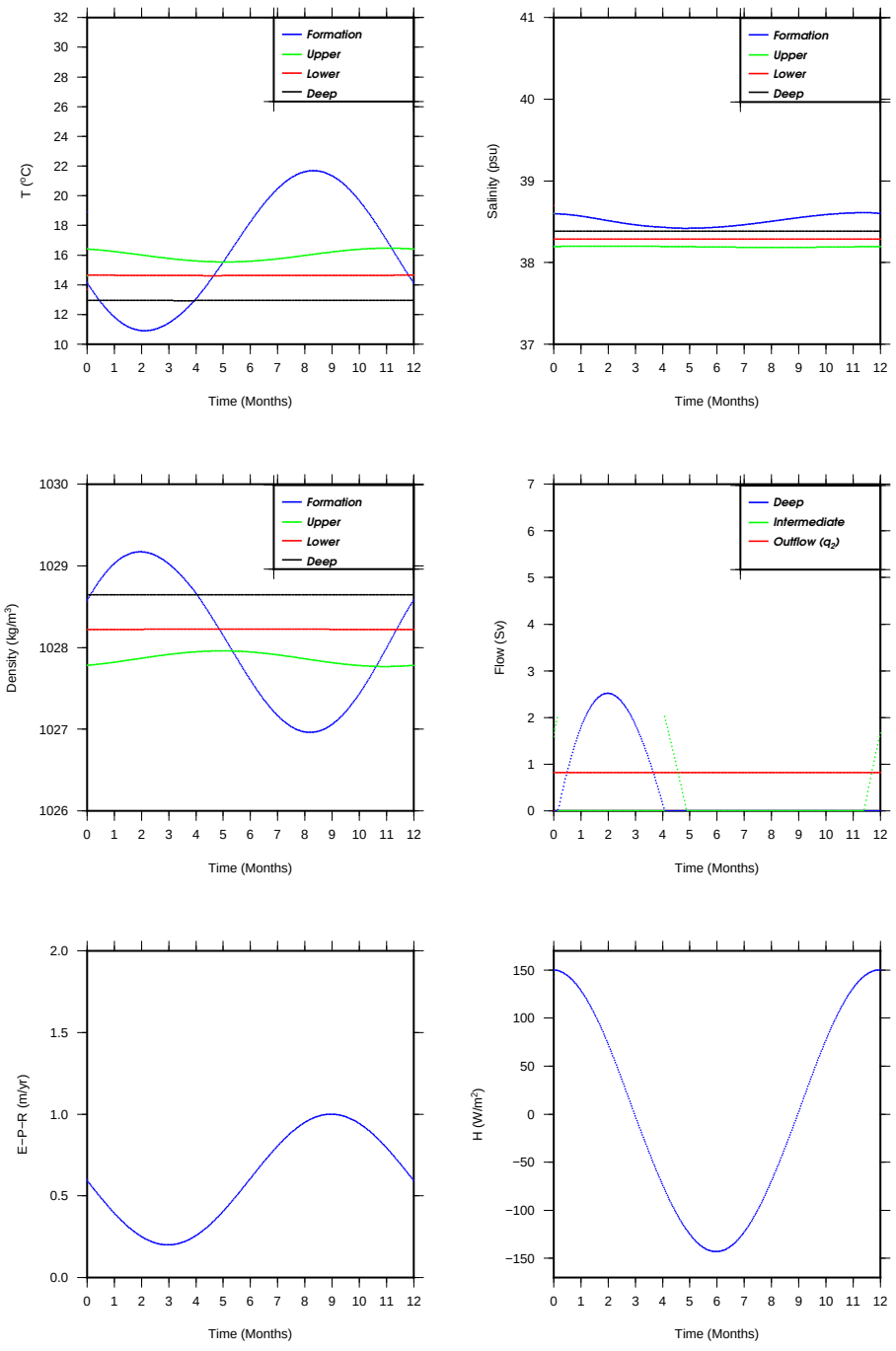

Figure 4.7: Model results with both seasonal variations in E-P-R and H.

4.3 Precessional variations

In Chapter 3 we have seen that the precession cycle has 2 effects on the climate. During the precession minimum we have cold winters and warm summers, and an increased precipitation and river runoff. The effects of these climatic variations on deep-water formation will be modelled separately, starting with the precessional heating effect.

4.3.1 Surface heating

In the first model precessional effects on surface heating are implemented. The model is run for 21.000 years with a precession minimum at 10.500 years. Figure 4.9 shows the results of the model of a summer insolation increase, and winter insolation decrease of 20%. This is already a large estimate if we look at Figure 3.13. As expected the temperature difference of the surface layer between summer and winter becomes larger. The effects on both salinity and temperature however are small. Due to the gradual variation in surface heating, the sea has time to adapt the temperature and salinity of all layers to a quasi-equilibrium situation. Therefore changes in both deep- and intermediate water formation are small. Table 4.3 shows the change in deep- and intermediate water formation if the summer- and winter insolation is changed by a factor f and a new equilibrium is reached. For all f the effect of the surface heating on deep- and intermediate water formation is small. Changes in intermediate-water formation are larger as the properties of the Lower layer are affected more by the changing outflow from the Mediterranean into the Atlantic.

The explanation for the small changes due to the summer- and winter insolation change is as follows. The Mediterranean has a net heat loss from surface heating. If seasonal heating effects are amplified, the net heat loss increases slightly. Therefore the temperature of the layers slightly decreases and the density increases. Outflow from the Lower layer into the Atlantic will increase as there is a higher density difference between these waters. Inflow from the Atlantic ocean then also increases. The incoming water from the Atlantic is warmer than the outflowing water from the Mediterranean. Therefore the net effect of the increased in- and outflow is an increase in temperature of the Mediterranean. As a result in general the temperature of the Mediterranean will not change significantly. This effect, together with the slow change in surface heating explain that the changing insolation is most likely not responsible for the stop or large change in deep-water formation.

4.3.2 Increased precipitation and river runoff

An increase in precipitation and river runoff will result in a decreased surface salinity. By lowering the surface salinity, the density of the Formation layer is lowered, and the water column is stabilized. Therefore an increased precipitation and river runoff will directly result in less deep-water formation. It is known that during a precession minimum there is an increased precipitation and river runoff (Meijer & Tuenter, 2007). In this section the change in net evaporation will be modelled with two different approaches. First the

	c_{FD}			c_{FL}		
f	Year 1	Year 2	Equilibrium	Year 1	Year 2	Equilibrium
1.25	+80.3%	+150.8%	+9.8%	-18.4%	-36.7%	+28.6%
1.20	+65.6%	+123.0%	+6.6%	-20.4%	-32.7%	+24.5%
1.15	+52.4%	+93.4%	+4.9%	-20.4%	-24.5%	+14.3%
1.10	+36.1%	+63.9%	+3.3%	-16.3%	-20.4%	+4.1%
1.05	+19.7%	+32.8%	-3.3%	-10.2%	-12.2%	-8.2%
0.95	-21.3%	-37.7%	-4.9%	+12.2%	+18.4%	-18.4%
0.90	-42.6%	-100.0%	-8.2%	+26.5%	+140.8%	-30.6%
0.85	-100%	-100.0%	-11.4%	+161.2%	+73.5%	-34.7%

Table 4.3: The change in deep- and intermediate water formation after 1 year, 2 years and in equilibrium, resulting from changing the amplitude of summer and winter insolation by a factor f.

change in net evaporation will be modelled as a gradual sinusoidal change. Afterwards we will model more rapid changes in net evaporation as may have been the case during a precession minimum looking at Figure 3.13.

Gradual change net evaporation

First we will look at the influence of climatological variations in E-P-R on deep-water formation due to the precession cycle without seasonal fluctuations. In this way we can see the effects of an increased precipitation and river runoff. Because deep-water formation is initiated in winter periods it is important to include seasonal fluctuations. This will be the next step.

Figure 4.10 shows the effect of a gradual decrease in net evaporation with a magnitude of 0.6 m/yr during the precession minimum. The salinity in the Mediterranean decreases, which in turn causes the density of the layers to decrease. The reduced density of the Lower layer causes a reduced outflow of water into the Atlantic. Inflow from the Atlantic also reduced and again this results in a net decrease in temperature and salinity of the Mediterranean. The salinity of the Surface water will decrease first if the net evaporation decreases. Therefore there is less deep-water formation during the precession minimum.

In Figure 4.11 seasonal variations in E-P-R and H are included. Again the net evaporation is decreased gradually, which first reduces the Formation layer salinity. Deep-water formation reduces due to the lower density of the Formation layer. Once mixing has reduces the salinity of the lower layers outflow into the Atlantic will also reduce. Therefore we have less inflow of the Atlantic waters, again causing a reduction in temperature of the Mediterranean layers. Once the net evaporation starts increasing again at the precession minimum the deep-water formation immediately increases. The Deep layer has had time to adjust to the lower salinity. Increasing the net evaporation increases the Formation layer salinity. Therefore it is during the a period of fast increase in net evaporation that the deep-water formation is highest. The intermediate-water formation is also lowest around the precession minimum. However the intermediate-

	c_{FD}			c_{FL}		
$E-P-R$	Year 1	Year 2	Equilibrium	Year 1	Year 2	Equilibrium
+0.6 m/yr	+39.3%	+123.0%	+11.5%	-2.0%	-22.4%	+40.8%
+0.4 m/yr	+26.2%	+83.6%	+8.2%	-8.2%	-20.4%	+26.5%
+0.2 m/yr	+14.8%	+42.7%	+4.9%	-6.1%	-12.2%	12.2%
-0.2 m/yr	-13.1%	-47.5%	-3.3%	+6.1%	+20.4%	-16.3%
-0.4 m/yr	-27.9%	-100.0%	-9.8%	+12.2%	+114%	-30.6%
-0.6 m/yr	-42.6%	-100.0%	-19.7%	+20.4%	+63.3%	-46.9%

Table 4.4: The change in deep- and intermediate water formation after 1 year, 2 years and in equilibrium, resulting from changing the net evaporation with a step function.

water formation curve lags the deep-water formation curve. The reason for this is that while at first water is not dense enough to form deep water, it may still be dense enough to form intermediate water. Table 4.4 shows the change in deep-water formation resulting from a change in net evaporation after reaching an equilibrium, and after the first 2 years. The changes in equilibrium are small. However after the first 2 years changes are much larger. From this it can be concluded that it is not exclusively the magnitude of change in net evaporation that can stop deep-water formation. Changes in intermediate-water formation again are larger as the properties of the Lower layer are affected more by the changing outflow from the Mediterranean into the Atlantic. In the next section a more rapid change of net evaporation will be applied.

Rapid change net evaporation

The effects of a more rapid change in net evaporation are different from the effects of a gradual change. Figure 4.12 shows how a rapid change in net evaporation results in a stop of deep-water formation for a period of 100's of years. The immediate decrease in net evaporation causes the salinity of the Formation layer to decrease. The Deep layer still retains it higher salinity until mixing has lowered the salinity of the Deep layer as well. While deep-water formation stops, the water is still dense enough to form intermediate water in winter periods.

There are two main parameters that determine the length of the stop of deep-water formation which are the mixing and the magnitude of decrease of net evaporation. In Figure 4.8 the duration of the stop of deep-water formation is plotted against the magnitude of decrease of net evaporation, for different κ. The duration of the stop in deep-water formation for a realistic change of E-P-R (0.1-0.6 m/yr (Meijer & Tuenter, 2007; Tjallingii et al., 2008)) is 100's to 1000's of years. Already for a small decrease in net evaporation deep-water formation stops. An increased mixing leads to a decrease of the length of stop of deep-water formation. By decreasing the deep-water formation in steps there may have been periods of 1000's of years with no deep-water formation. Sapropel records are also formed over periods of several 1000's of years. A further effect of the stop of deep-water formation may be that mixing also decreases, as the column is more stable. This would lengthen the period of no deep-water formation.

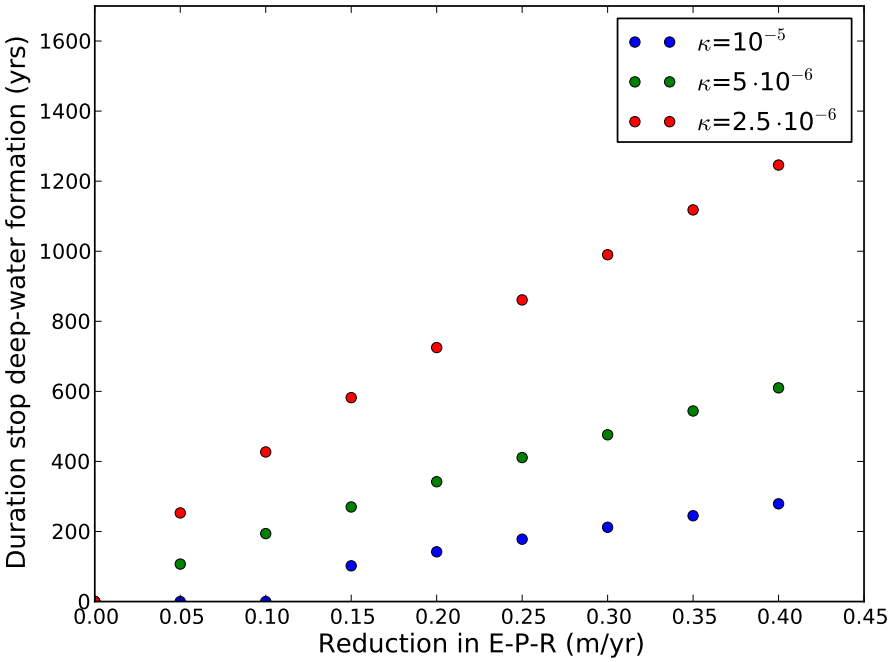

Figure 4.8: The duration of the stop of deep-water formation plotted against the magnitude of the change in net evaporation, for different background diffusion coefficients κ .

To conclude, according to the box model it is more likely that sapropels were formed in periods of a fast increase in precipitation and river runoff. A fast increase can stop deep-water formation for a period of 100's to 1000's of years. This scenario is more likely than that a gradual change of net evaporation caused the sapropel formation.

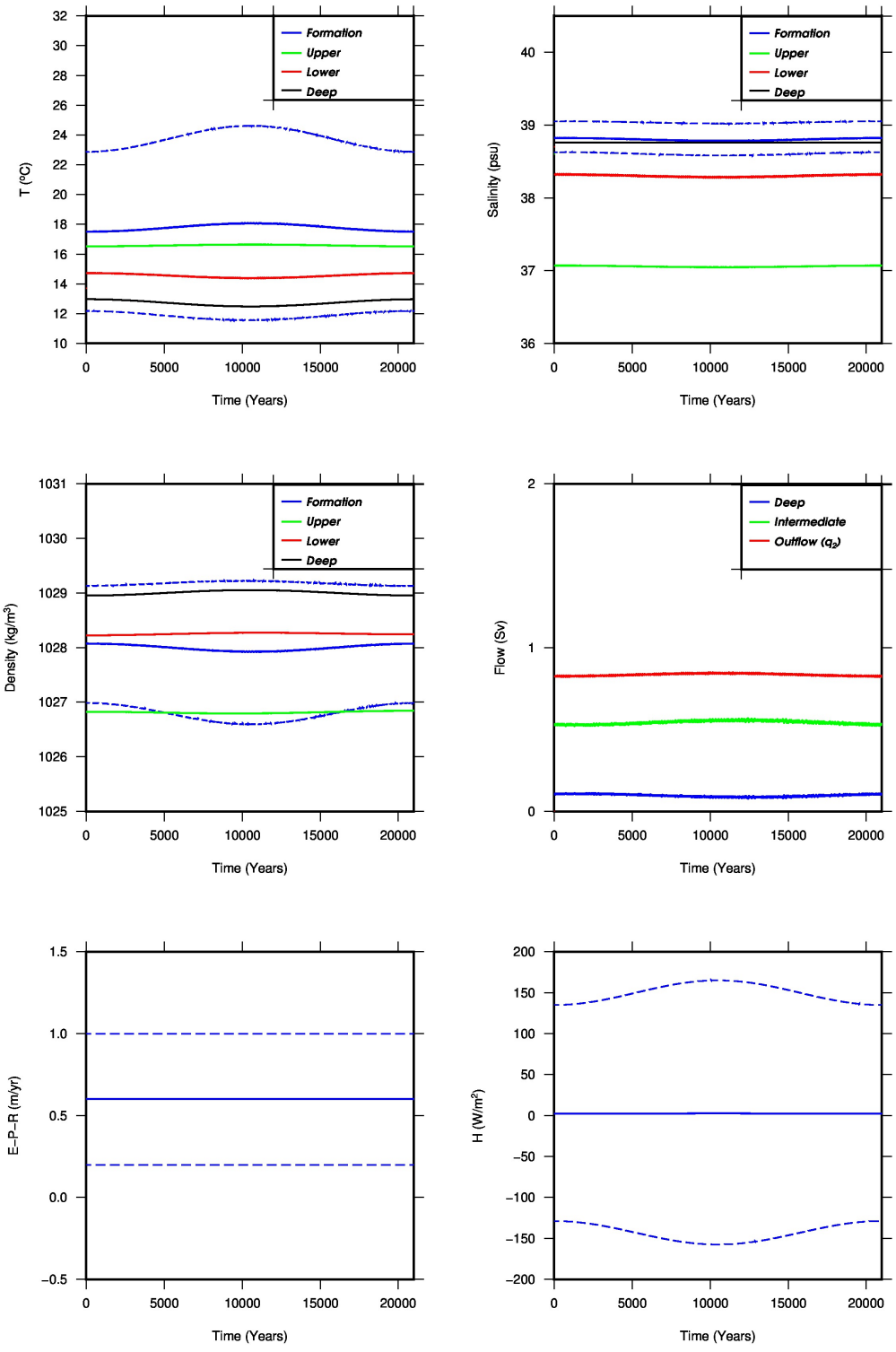

Figure 4.9: Model results for seasonal variations in E-P-R, and H and precessional variations in H. All graphs present yearly averages of the parameters. The dashed lines represent the seasonal maximum and minimum.

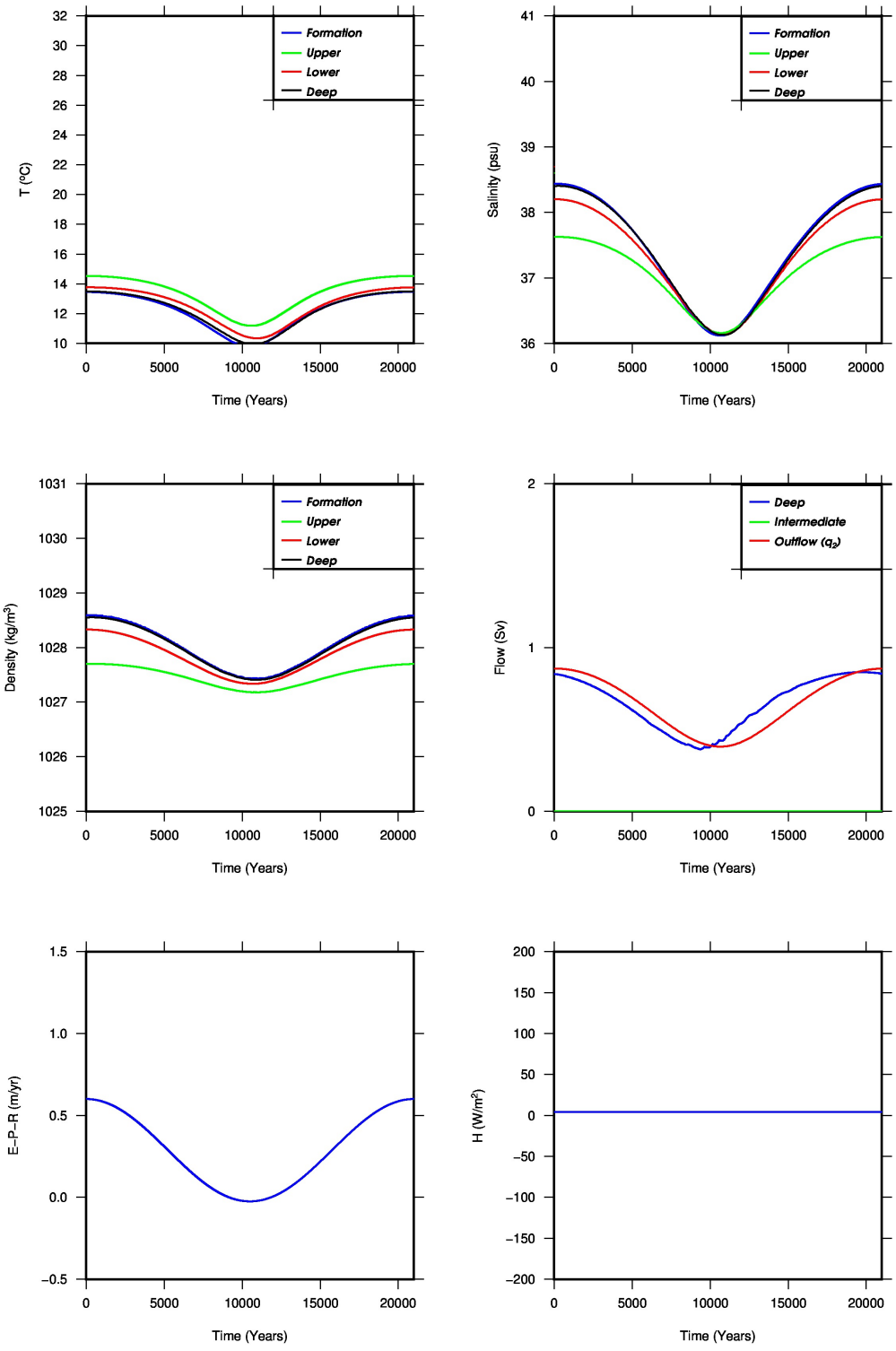

Figure 4.10: Model results for precessional variations in E-P-R, with no seasonal variations.

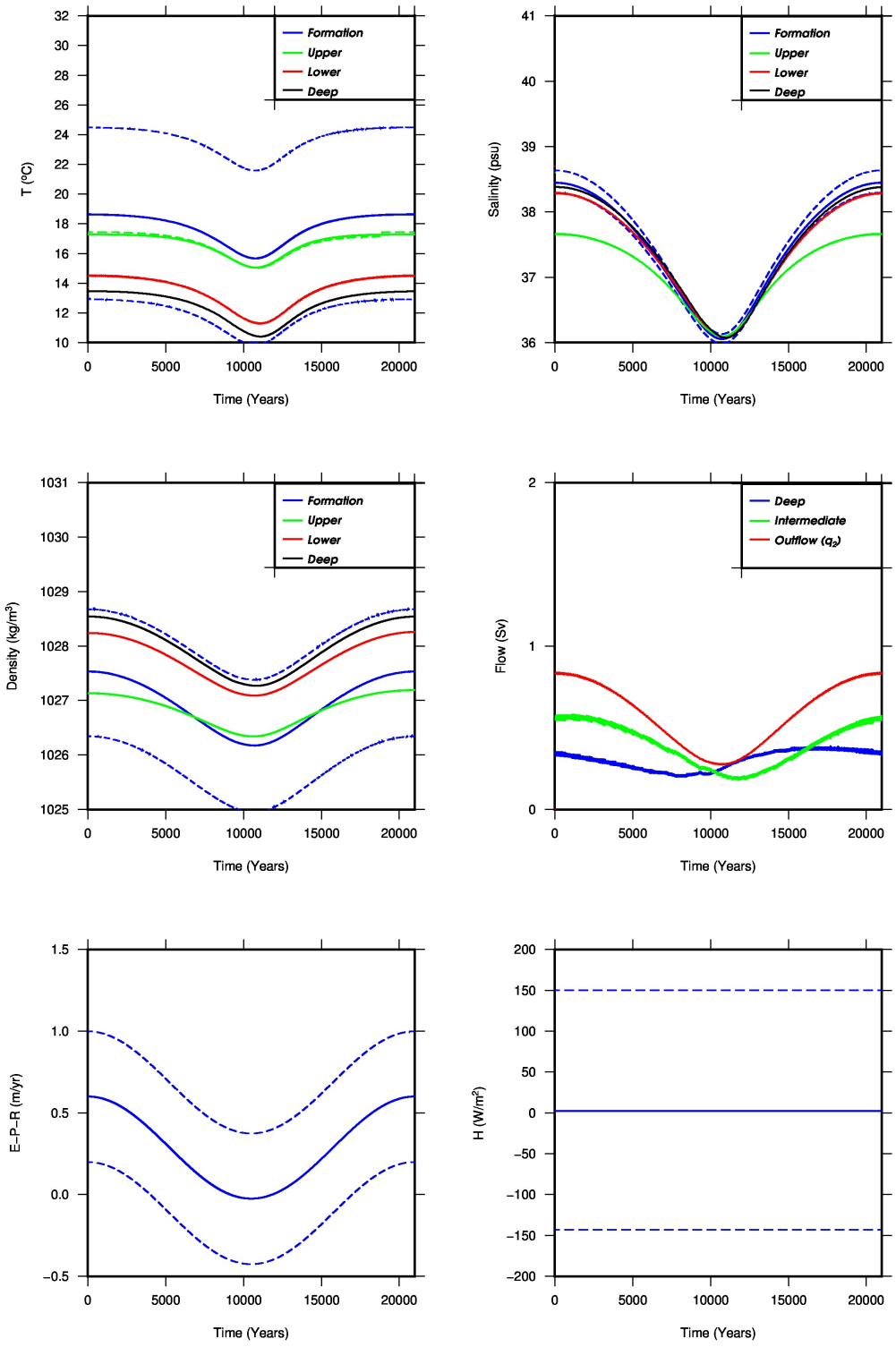

Figure 4.11: Model results for precessional variations in E-P-R. All graphs present yearly averages of the parameters. The dashed lines represent the seasonal maximum and minimum.

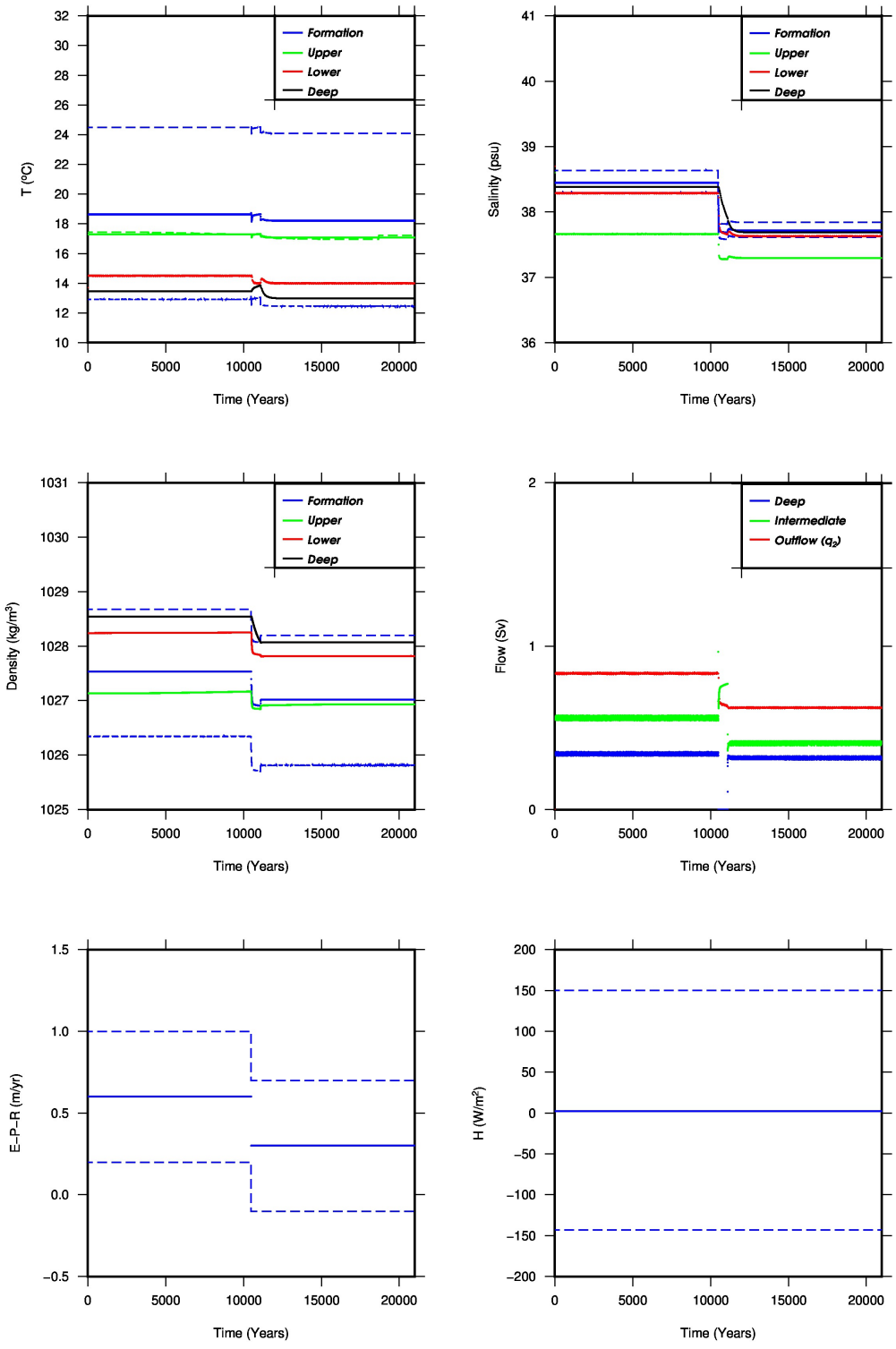

Figure 4.12: Model results for a sudden decrease in net evaporation. All graphs present yearly averages of the parameters. The dashed lines represent the seasonal maximum and minimum.

4.4 S1 sapropel

The most recently deposited sapropel (S1) was deposited between 9 and 6.5 ka (De Lange et al., 2008). The last precession minimum was around 11 ka, thus the S1 sapropel was deposited after the precession minimum. Three major events during the last precession cycle may have influenced the formation of the last sapropel. Due to the orbitally forced change in short-wave radiation the Intertropical convergence zone and the associated rainfall belt might have migrated north giving rise to the African Humid period from 9 to 5.5 ka (Tjallingii et al., 2008). Speleotherm data have shown a very wet interval in the Mediterranean region between 8.2 and 7.3 ka (Spotl et al., 2010). The increased rainfall in Northern Africa and the humid interval in the Mediterranean region have also lead to an increase in river runoff during this period. A second event which caused increased influx of fresh water into the Mediterranean is the connection between the Black sea and the Mediterranean sea which formed between 8.5 and 5 ka (Lane-Serff et al., 1997). Initially the Black sea consisted of fresh water. On top of these two events which have caused an increased influx of fresh water, the sea level rose during the last precession cycle due to deglaciation by around 120 m (Fairbanks, 1989). This sea level rise was most rapid during two periods, which are called Meltwater pulse 1A and 1B. Figure 4.13 summarizes the events and shows the timing. The effects of a fast increase in precipitation and river runoff have been investigated in the last section. In this section we will look at the impact of the sea level rise and the opening of a connection between the Black sea and the Mediterranean sea.

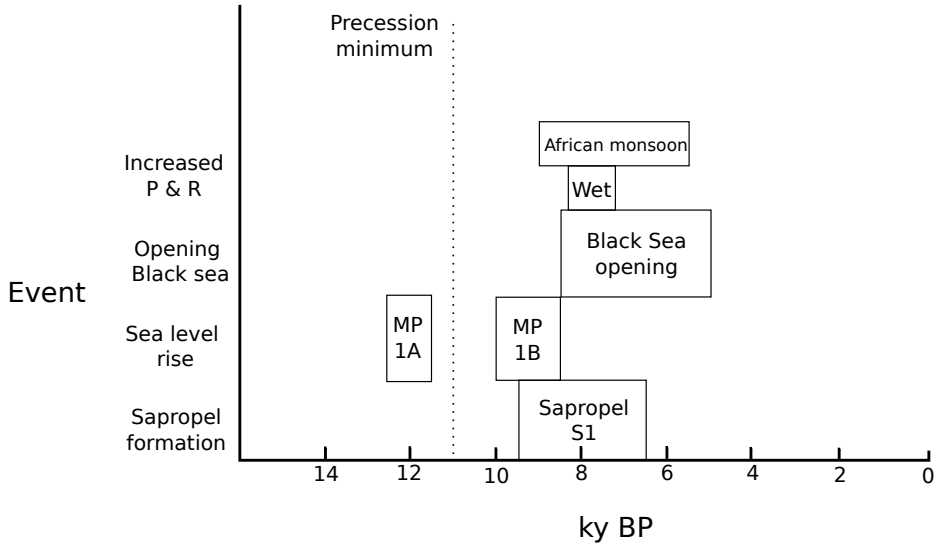

Figure 4.13: All events that may have caused the formation of the S1 sapropel and the timing of the events.

4.4.1 Sea level rise

By implementing hydraulic control theory at the Strait of Gibraltar the effects of sea level variations on deep-water formation during the last precession cycle can be investigated. The sea level curve that is used comes from a paper of Fairbanks (1989). Figure 4.14 shows the sea level variations over the last 18.000 years. These variations have been implemented into the model by changing the total depth of the strait H_{Strait}. The depth of the Strait is taken to be 284 m at present (Bryden et al., 1994). The sea level rise is rapid during two periods of deglaciation. The first period of rapid sea level change took place around 12.500 years ago when the sea level rose around 24 m in less than 1000 years. This period is termed melt-water pulse 1A. Around 10.000 years ago a second rapid sea level rise was initiated. Within 1500 years the sea level rose with around 30 m. This period is termed melt-water pulse 1B. Meltwater pulse 1A took place before the Northern hemisphere precession cycle insolation maximum which is dated at around 11.000 years BP. Meltwater pulse 1B took place after this insolation maximum.

The resulting effects of the sea level rise on the temperature, salinity & circulation are shown in Figure 4.15. This model includes seasonal variations. The direct result of this sea level rise is an increase in in- and outflow from the Atlantic. The incoming water from the Atlantic lowers the salinity of the Upper layer. Mixing causes the salinity of the Formation layer to decrease. It takes much longer to decrease the salinity of the Lower and Deep layer. Therefore the rapid increase in sea level during the two meltwater pulses causes the deep-water formation to reduce. From around 8.000 year BP until now the effects of the changing sea level have no significant effect on deep-water formation. While the sea level rise does have an effect the deep-water formation the effect is not large enough to stop it. This is in agreement with Figure 4.13, where we see that sapropels were not being formed during the periods of rapid sea level variations yet. A sea level rise also could not be the main cause for sapropel formation, as they do not necessarily relate to precession minima, and are not present during many precession cycles when sapropels have been formed (Fairbanks, 1989).

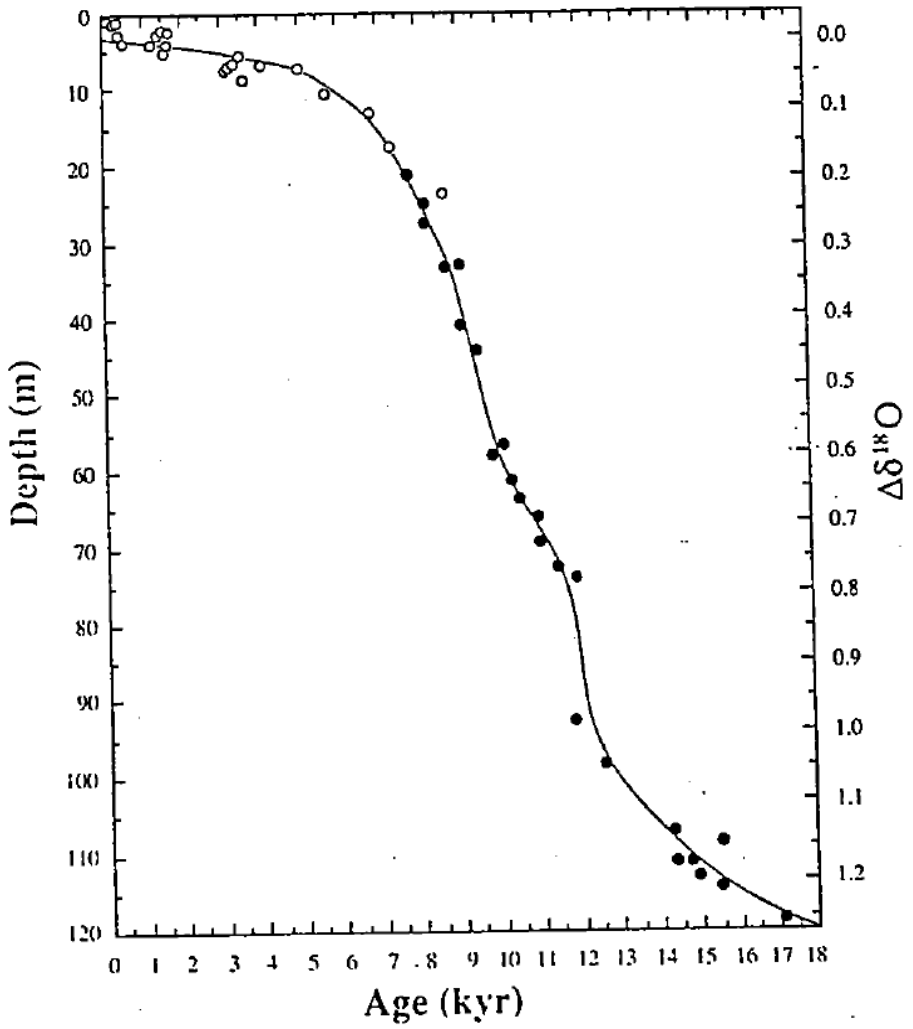

Figure 4.14: Sea level rise over the last 18.000 years. (Fairbanks, 1989).

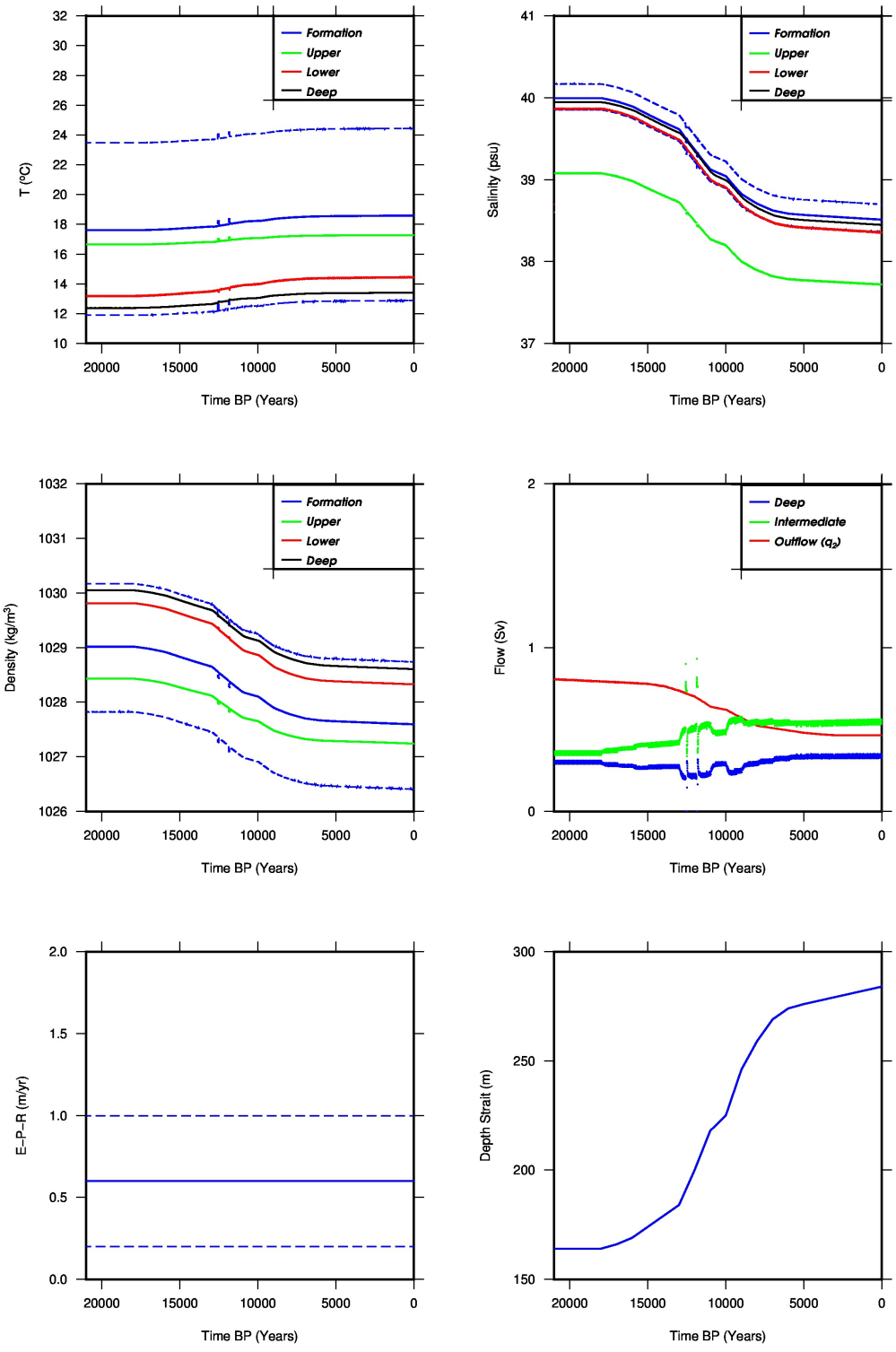

Figure 4.15: The effects of a sea level rise during the last precession cycle. Sea level variations are modelled from 18.000 BP till present. All graphs present yearly averages of the parameters. The model includes seasonal variations, the dashed lines present the seasonal maximum and minimum value.

4.4.2 Opening of the connection to Black Sea

Between 8500 year BP and 5000 year BP a connection between the Black sea and the Mediterranean Sea formed (Lane-Serff et al., 1997). Before the connection was formed the Black Sea was still a lake containing fresh water. The connection therefore entailed a new source of fresh water for the Mediterranean. In this section we model the opening of the Black sea with two different scenario's. The first scenario models the gradual opening of the Black Sea based on the work of Lane-Serff et al. (1997). Between 8.500 year BP and 6.750 year BP the influx of fresh water linearly increased to 15.000 m^3/s, which corresponds to a increase in river runoff of 0.2 m/yr over the whole basin. The inflow from the Black Sea gradually becomes saltier as the Black sea becomes saltier. After 6.750 year BP the extra inflow of fresh water starts linearly decreasing again until at 5.000 year BP it reaches the same level as before the opening of the Black Sea. The second scenario models a more catastrophic opening of the Black Sea, based on the work of Matthiesen & Haines (2003). Before the opening of the Black Sea there was a missing influx of fresh water, which means the excess net evaporation would have been around 0.15 m/yr larger than today. At around 7.000 BP the outflow from the Black Sea was established, decreasing excess evaporation by 0.35 m/yr. Afterwards it linearly returns to the present day value in the next 1.750 years. Both models include seasonal variations.

The results of the first gradual scenario of the opening of the Black Sea are plotted in Figure 4.16. The decrease in excess evaporation results in a lower deep-water formation between 8.500 year BP and 6.750 year BP. When the excess evaporation starts increasing again at around 6.750 year BP deep-water formation is even higher than before the opening of the Black Sea. The explanation for this is as follows. It is the increase in fresh water that decreases deep-water formation by reducing the salinity of the Formation layer. When the inflow of fresh water starts decreasing again the Deep layer has had time to adapt to the lower salinity in the Mediterranean. The Formation layer starts increasing in salinity again and the difference between the salinity of the Formation layer and of the Deep box is higher than before the opening of the Black Sea.

The results of the catastrophic scenario are plotted in Figure 4.17. This time deep-water formation completely stops after 7000 year BP because of the immediate inflow of fresh water. However deep-water formation starts again after around 500 years because of the increase in net evaporation. Both scenario's are consistent with formation of sapropels between 9.000 year BP and 6.500 year BP, as both scenario's have a decrease or stop of deep-water formation up till around 6.500 year BP. However, the connection between the Black sea and the Mediterranean can not be the only and main reason sapropels have formed, as sapropel formation started 9.000 year BP. The connection of the Black Sea and the Mediterranean Sea could have been one of the reason sapropel formation stopped 6.500 BP, as this is the period the increased net evaporation caused by the Black Sea connection increased deep-water formation.

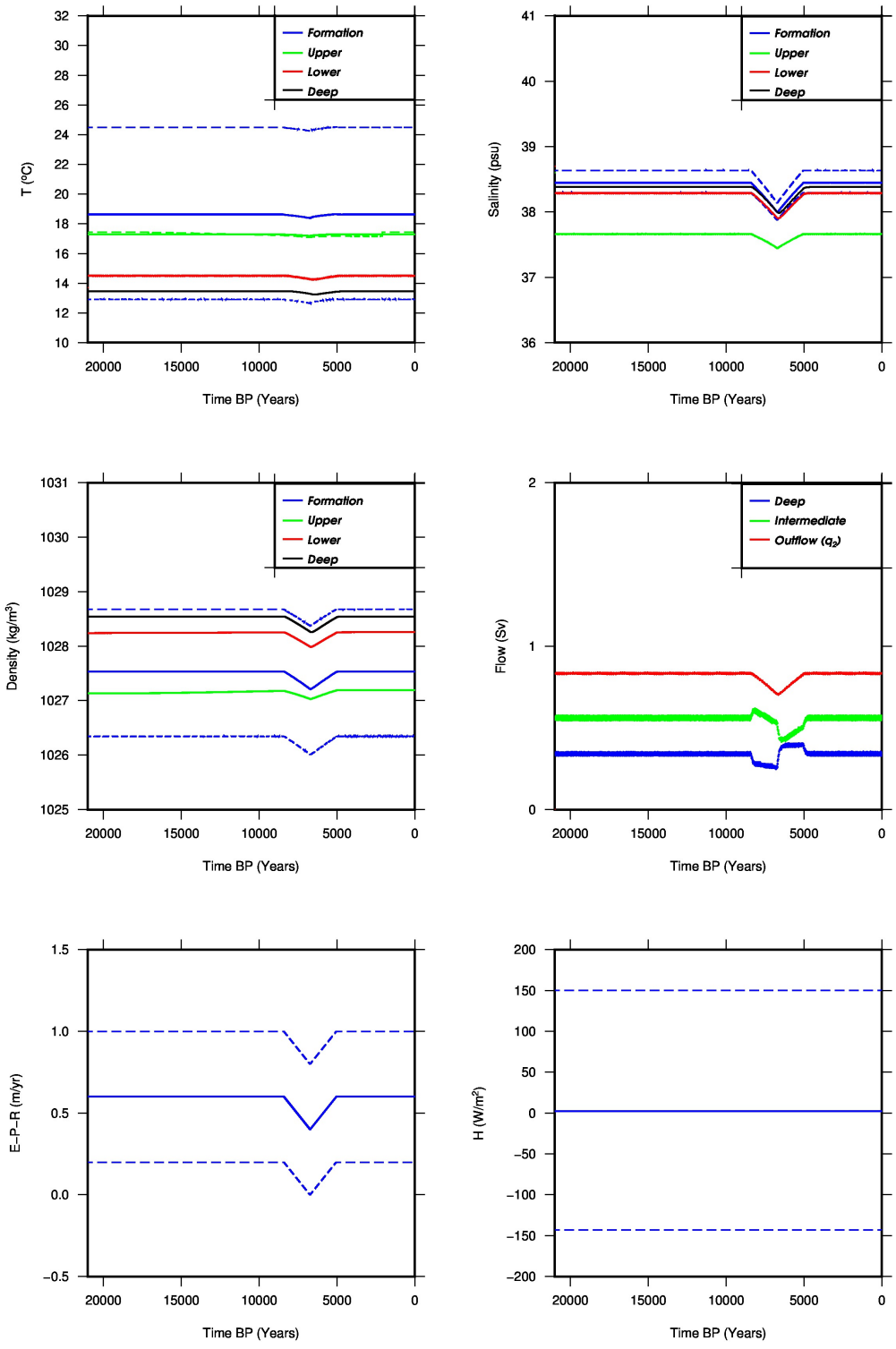

Figure 4.16: Effects of a gradual increase in river runoff due to the opening of the connection between the Black sea and the Mediterranean. All graphs present yearly averages of the parameters. The model includes seasonal variations, the dashed lines present the seasonal maximum and minimum value.

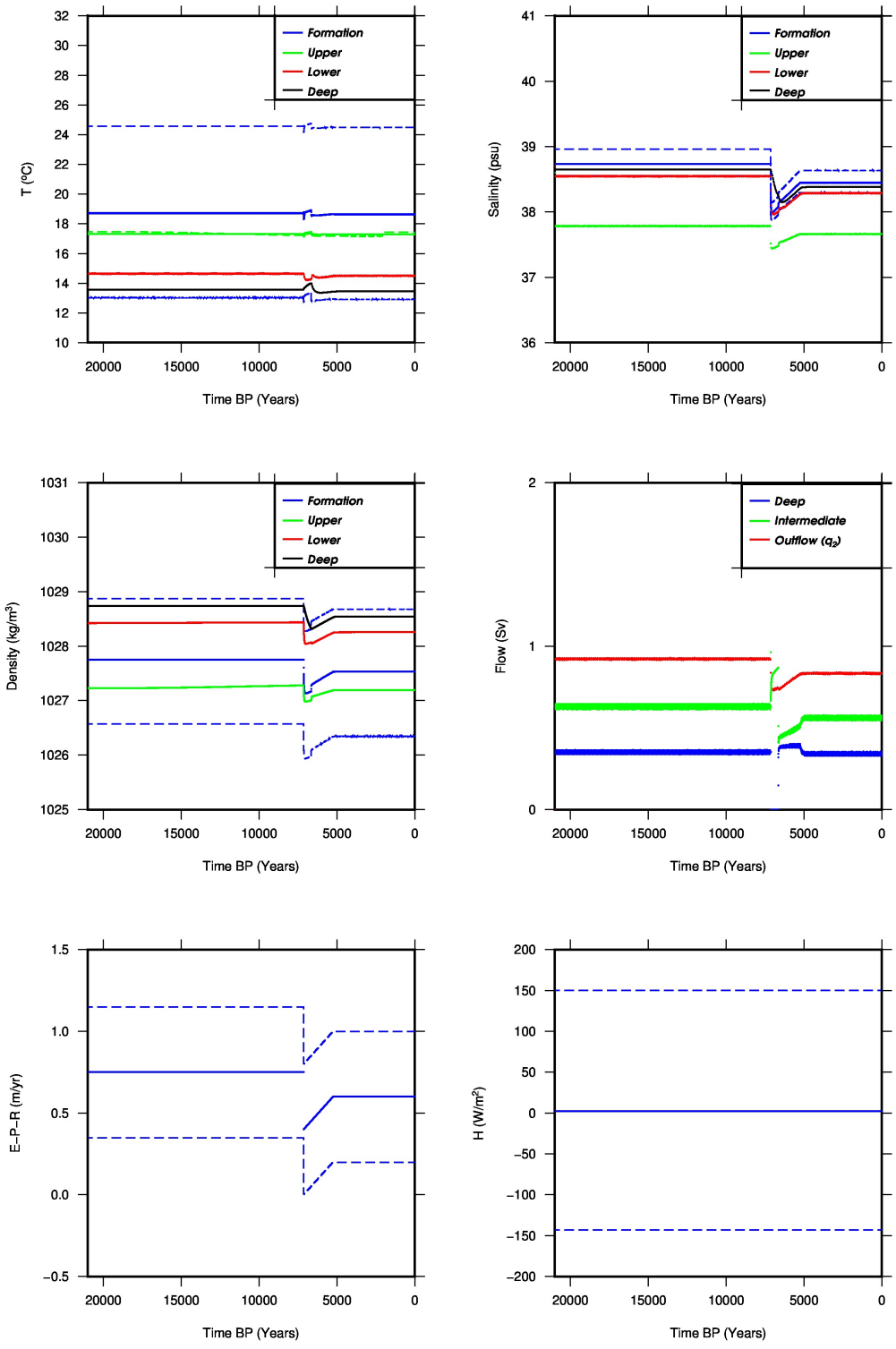

Figure 4.17: Effects of an abrupt increase in river runoff due to the opening of the connection between the Black sea and the Mediterranean. All graphs present yearly averages of the parameters. The model includes seasonal variations, the dashed lines present the seasonal maximum and minimum value.

4.4.3 Concluding remarks

The S1 sapropel was formed between 9.000 and 6.500 year BP. Most likely MP1B created a more stable water column, but the increasing precipitation and river runoff caused deep-water formation to stop. We have seen in the previous chapter that an increase of precipitation and river runoff can cause a stop of deep-water formation of 100-1000 yrs. The increase of precipitation and river runoff started around 9.000 years ago, at the same time the North African humid period started (Tjallingii et al., 2008). Most likely the increase in precipitation and river runoff during this period initiated the stop of deep-water formation and the start of the S1 sapropel deposition. The connection between the Black sea and the Mediterranean formed during the period of sapropel formation and may have possibly extended the period. When the precipitation, river runoff, and fresh water supply from the Black decreased deep-water formation could start again. The time-lag between the last precession minimum and the formation of the S1 sapropel can be explained. However it is uncertain if this time-lag can also be applied to other precession minima. According to the model results it is most likely that during other precession minima there was also a period of rapid increase of precipitation and river runoff, which initiated sapropel formation. For this time-lag to be applied to other precession minima an increase in precipitation and river runoff is expected to have been largest after the precession minimum.

Chapter 5

Discussion

5.1 3 Layer box model

In this research a box model with 4 layers has been used. Many authors (Tziperman & Speer, 1994; Matthiesen & Haines, 2003) have used a 3 layer box model. These models do not have a deep water box and are therefore not suitable to model deep-water formation. It is possible to make a 3-layer model with a deep box. For this we have to combine the Upper and Lower layer of the 4-layer model. In this model in- and outflow of the Atlantic take place from the same box. We have tested this approach.

Figure 5.1 schematically represents the 3-layer model. The combined Upper and Lower layer of the 4-layer model we now call the Lower layer. As inflow from the Atlantic goes into the Lower layer this layer will have a higher temperature than before. Because outflow also takes place from this layer and the outflow is driven by a density difference between the lower layer and the Atlantic, the outflow is also influenced by this simplification. The difference in temperature between the top and bottom of the lower layer in reality is around 4 degrees Celsius, and 0.4 psu. We have tested the influence of E-P-R, H, the mixing terms and T and S of Atlantic inflow in the 3 layer box model and compared this with the 4-layer box model.

In Figure 5.2 we see the seasonal results of the 3-layer model. Apart from missing the fourth layer and therefore having a slightly different temperature and salinity in the three other layers, the model does show deep-water formation during winter. Therefore for explaining deep-water formation on the scale of years the 3-layer model is good enough. On this short time scale, the temperature and salinity of the Lower layer and thus the outflow and inflow do not change much in the model.

By including (gradual) Milankovitch precessional fluctuations in the model we obtain Figure 5.3. Again the temperature and salinity give a realistic image of the Mediterranean. The model does show a different picture for deep-water formation. While deep-water formation is lowest when the net evaporation is lowest, the deep-water formation in the 3-layer model shows a direct relation with the net evaporation, and not with the change in net evaporation. As the 'Upper' layer and the 'Lower' layer of the

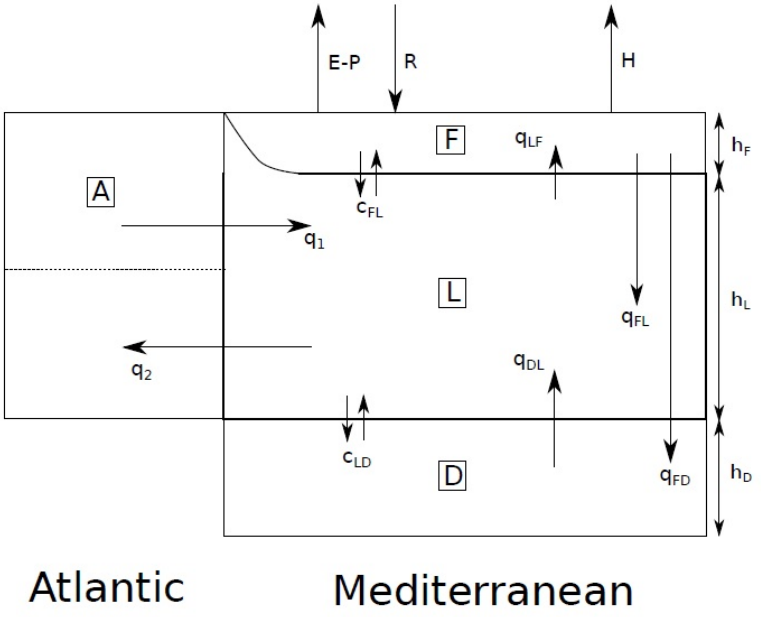

Figure 5.1: Box model with 3 layers.

4-layer model are combined in the 3-layer model there is inflow and outflow in the 3-layer model from the same layer. If the density of the layer becomes higher the outflow increases and thus the inflow increases. The inflow consists of less dense water. Therefore the density of this layer is immediately reduced again. Because there is no division between the Upper and the Lower layer, the Lower layer is in contact with both the Formation layer and the Deep layer. The Lower and Deep layer of the 3-layer model are therefore much easier brought to their equilibrium temperature and salinity. Because of the tendency of the model to go to an equilibrium situation very fast (and we have seen that changes in deep- and intermediate-water formation in equilibrium are small) , deep-water formation is not as strongly affected by changes in climate anymore.

Table 5.1 shows the influence of the parameters in the 3-layer box model. The main difference between the 3-layer model and the 4-layer model is that in the 4-layer model the deep-water formation is dependent upon the Atlantic inflow temperature and salinity. In the 3-layer model a change in T_I, and S_I do not have much influence on deep-water formation. The Strait of Gibraltar has no significant effect in the 3-layer model. Therefore the 4-layer model is advised in further research.

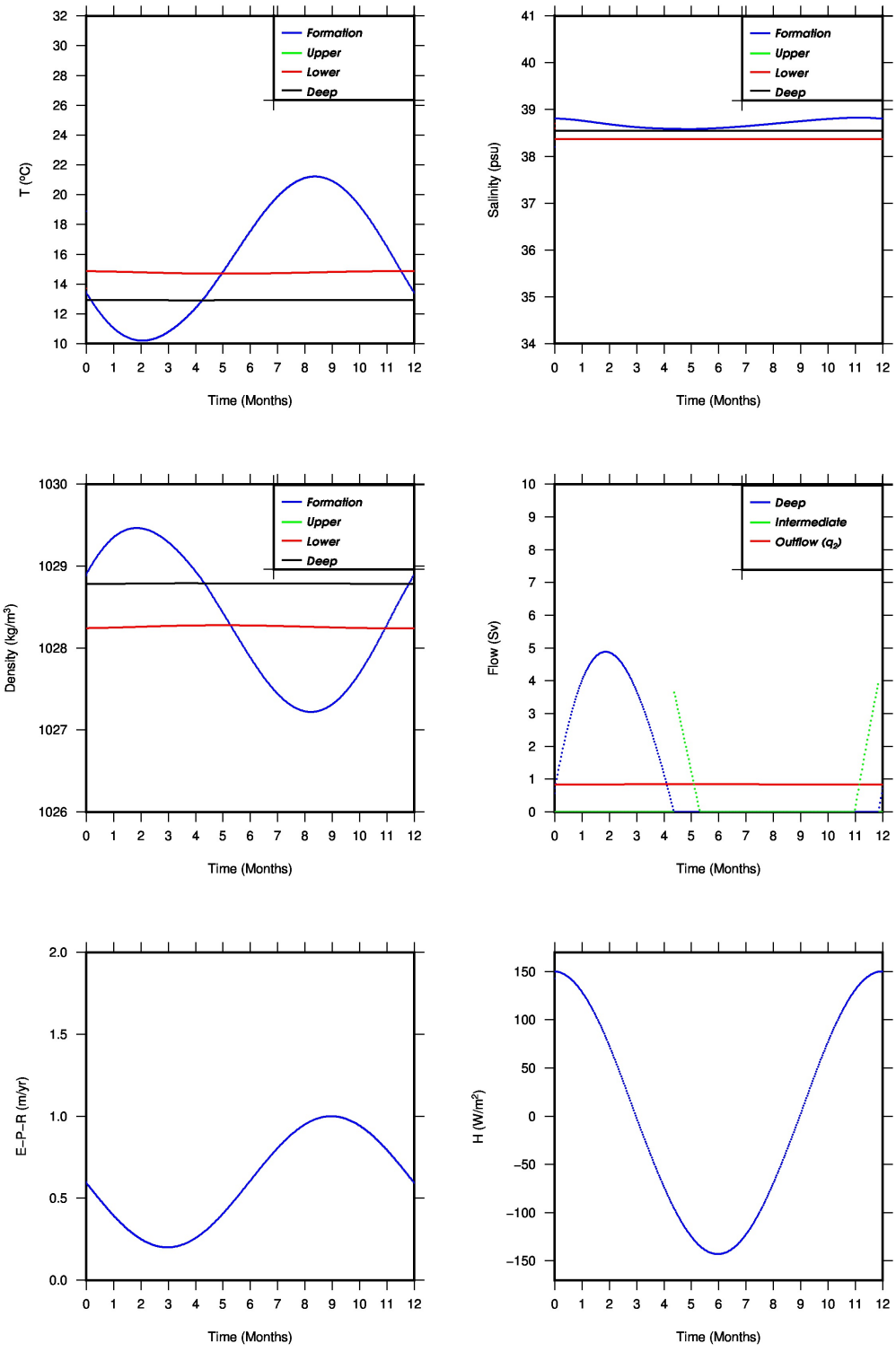

Figure 5.2: Seasonal model results for the 3-layer model.

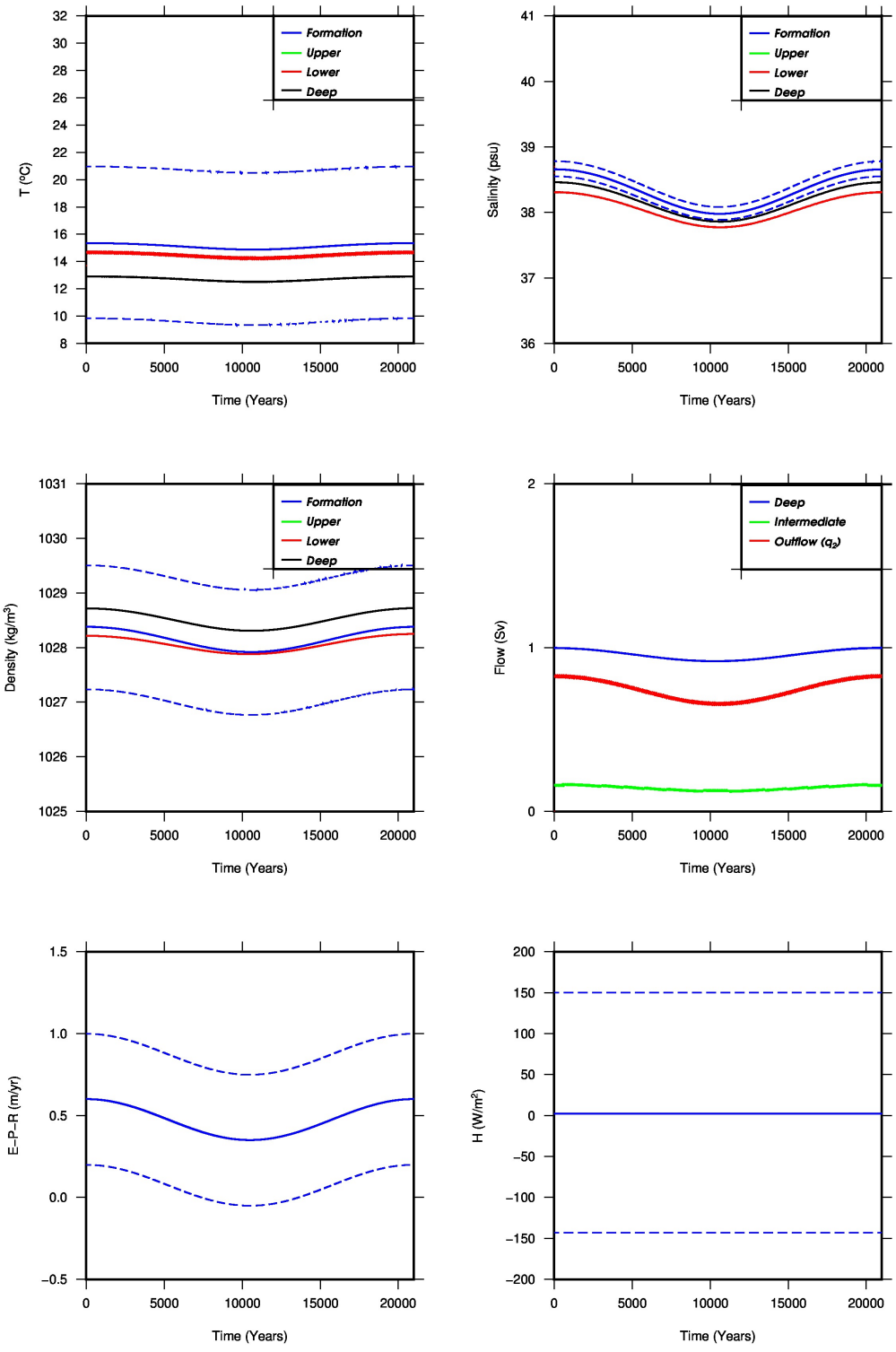

Figure 5.3: Model results of the 3-layer model with precessional variations in E-P-R. All graphs present yearly averages of the parameters. The dashed lines represent the seasonal maximum and minimum.

-	E-P-R ↑	H ↑	κ ↑	d_{FL} ↑	d_{LD} ↑	T_I	S_I
T_F	↑	↓	↑	↓	↓	↑	↑
T_L	↑	↓	-	-	-	↑	↑
T_D	↑	↓	↑	↓	↓	↑	↑
S_F	↑	↓	↓	↑	↑	↑	↑
S_L	↑	↓	↑	-	-	↑	↑
S_D	↑	↓	↓	↑	↑	↑	↑
q_{FD}	↑	↓↑	↓	↑	↓	-	-
q_{FL}	↑	↓↑	↓	↑	↓	-	-
q_2	↑	↑	↑	-	-	↓	↑

Table 5.1: Table with the influence of E-P-R, H and the mixing terms in the 3-layer model on temperature, salinity, and deep and intermediate water formation.

5.2 Limitations box model

5.2.1 Spatial limitations

The model contains only two dimensions. Therefore spatial variations can not be included in the model. The surface water of the Mediterranean does spatially vary in temperature by around 8-10 ^{o}C and in salinity by around 3 psu. Deeper waters contain less spatial variations in temperature and salinity but do still contain variations. Due to these spatial variations the Mediterranean contains area's where deep- and intermediate-water formation takes place. In the model there is either deep- or intermediate-water formation everywhere or nowhere. An implication of this is that in the model we will only have deep-water formation if the average density of the Formation layer is high enough. In the Mediterranean deep-water formation could be more local, explaining also why some sapropels are local (Martinez-Ruiz et al., 2002). Also the evaporation, precipitation, river runoff, and surface heating have local variance in the Mediterranean but not in the model.

A possible method to include some spatial variations is to include the Strait of Sicily in the model and divide the Mediterranean into and Eastern part and a Western part. With this division also a difference in river runoff and heat flux can easily be implemented in the model. Spatial variations such as the lack of an organic rich layer deposition during S1 in the Western Mediterranean (Martinez-Ruiz et al., 2002) can then possibly be explained. The Western Mediterranean was mostly affected by the sea level rise. This event alone might not have been a reason for deep-water formation to stop. The connection of the Black sea and the increased river runoff from African rivers did only affect the Eastern Mediterranean. The increased fresh water input could have caused a more stable column in the Eastern Mediterranean causing the regional differences in Sapropel formation.

5.2.2 Constant layer thickness

In the model all layers have a constant thickness. The constant layer thickness is achieved by applying extra circulation terms to keep the water budget in each layer constant. This is in contrast to the models of Tziperman & Speer (1994) and Matthiesen & Haines (2003), where the layers have a variable thickness. There are several arguments for keeping a constant layer thickness. The main argument is that we do not know the the absolute value of deep- and intermediate-water formation. Therefore it would be unjustified to let the layer thicknesses vary because of these two flow terms. A second reason to not implement varying layer thicknesses is that a highly artificial parameterization feedback mechanism is necessary to make sure the box volumes do not deviate too far from their specified average values. If this artificial method to keep the box volumes close to their average is not used, the volume of some boxes would diverge, and the volume of other boxes would converge to 0. There is no justification for applying this artificial feedback mechanism, except that otherwise the model would not work. A third reason for the constant layer thickness is that the model contains four layers. A three layer model requires a variable layer thickness, if outflow into the Atlantic takes place from the deepest box. Otherwise the outflow into the Atlantic would be equal to the deep-water formation. In a four layer box model we do not have this problem.

Tziperman & Speer (1994) state that in their model variable box volumes would allow the volume of the upper water box to increase owing to the inflow during the summer, and decrease again during the winter water mass formation events. The volume of the lower box would reduce as it loses water to outflow during summer, while the volume increases as it regains the water in winter deep-water formation events. This seasonal relation in outflow is not observed however (Sannino et al., 2002).

Including (slightly) variable layer thicknesses would have a small effect on the temperature and salinity of the layers and thus on the flow. There is no accurate method to include variable layer thicknesses in the model though. As the effects would probably be small, the assumption to have constant layer thicknesses in the four layer box model therefore seems justified.

Chapter 6

Conclusion

A 4-layer box model has been made to gain insight into the basic physical mechanisms of deep-water formation. The Neogene sedimentary record of the Mediterranean basin is characterised by an alternation of organic rich sapropels and marine marls. Oxygen depleted zones in the deep sea may have been the cause for increased conservation of organic materials, and thus sapropel formation. These oxygen depleted zones may have formed as a result of a decrease or stop of deep-water formation. The box model has linked deep-water formation to climatic conditions to test if the climatic conditions initiate this stop of deep-water formation.

The box model has first been calibrated by comparing temperature and salinity data from the MEDAR database with the model output. Seasonal variations in the model have also been calibrated with MEDAR data. The outcome of the model is that deep water is formed in the winter due to a temperature driven increase in density of the surface water. The temperature change is caused by the seasonal variations of surface heat flux. This agrees well with observations.

On the time-scale of the precessional Milankovitch cycle (21.000 years) the changes in deep-water formation are driven by changes in evaporation, precipitation and river runoff. A sudden increase in precipitation and river runoff is most likely to have been the cause for deep-water formation to stop. The increased fresh water influx with relatively low density may have stabilized the water column and caused the stop of deep-water formation. During precession minima precipitation it is found that precipitation and river runoff in the Mediterranean region increases (Tjallingii et al., 2008). An increase of river runoff and/or precipitation of 0.1-0.6 m/yr can cause a stop of deep-water formation of 100-1000's yrs. The increased summer and decreased winter insolation during a precession minimum are less likely to be the cause of the stop of deep-water formation. In the model these insolation variations have less effect on deep-water formation.

During the last sapropel deposition (S1) (9.000-6.500 BP) an increase in both river runoff and precipitation have been observed (Tjallingii et al., 2008). Most likely the increase in precipitation and river runoff 9.000 year BP initiated the stop of deep-water formation and the start of the S1 sapropel deposition. The connection between the Black

Event	Influence on deep-water formation
Precipitation/river runoff	++
Surface heat flux	0
Sea level rise	+
Black sea	++

Table 6.1: This table summarizes the influence of single events on sapropel formation in both the Eastern and Western Mediterranean. ++ is large influence, + is significant influence, and 0 is no significant influence.

sea and the Mediterranean formed during the period of sapropel formation (around 8.500 BP) and may have extended the period. Sea level variations during the last precession minimum could have lead to a more stable water column, but are probably not the main cause for the stop of deep-water formation. Table 6.1 summarizes the influence of the events on the S1 formation in the Mediterranean sea.

Apart from an oxygen-depleted zone due to a stop of deep-water formation, another cause of sapropel formation may have been the increased biological production associated with higher nutrient supply to the euphotic zone (Bard et al., 2002). However these two theories do not have to be mutually exclusive (Emeis and Sakamoto, 1998). Sapropels may have been formed by a combination of increased precipitation in the whole Mediterranean and increased river runoff to both stabilize the water column and increase nutrient supply. To further investigate differences between the Eastern and Western Mediterranean sapropel formation, the box model could be extended to contain an Eastern and a Western part by including the Strait of Sicily.

Chapter 7

References

Bard, E., Delaygue, G., Rostek, F., Antonioli, F., Silenzi, S., Schrag, D.P. 2002. Hydrological conditions over the western Mediterranean during the deposition of the cold Sapropel 6. Earth and Planetary Science Letter 202, pp. 481-494.

Bethoux, J.P. 1993. Mediterranean sapropel formation, dynamic and climatic viewpoints. Oceanologica acta 16, pp. 127-133.

Bethoux, J.P., Gentili, B. 1999. Functioning of the Mediterranean Sea: past and present changes related to freshwater input and climatic changes. Journal of Marine Systems 20, pp. 33-47.

Boukthir, M., Barnier, B. 2000. Seasonal and inter-annual variations in the surface freshwater flux in the Mediterranean Sea from the ECMWF re-analysis project. Journal of Marine Systems 24, pp. 343-354.

Bryan, F., 1987. Parameter sensitivity of primitive equation ocean general circulation models. Journal Physical Oceanography 17, pp. 970-985.

Bryden, H.L., Candela, J., Kinder, T.H. 1994. Exchange through the Strait of Gibraltar. Progress in Oceanography 33, pp. 201-248.

Castellari, S., Pinardi, N., Leaman, K. 1997. A model study of air-sea interactions in the Mediterranean sea. Journal of Marine System 18, pp. 89-114.

Criado-Aldeanueva, F., Soto-Navarro, F.J., Garcia-Lafuente, J. 2012. Seasonal and interannual variability of surface heat and freshwater fluxes in the Mediterranean sea:budgets and exchange through the Strait of Gibraltar. International Journal of Climatology 32, pp. 286-302.

Emeis, K.C., Sakamoto,T. 1998. The sapropel theme of leg 160. Proceedings ODP Scientific Results 160, pp. 29-36.

Fairbanks, R.G. 1989. A 17.000 year glacio-eustatic sea level record: influence of glacial melting rates on the Younger Dryas event and deep-ocean circulation. Nature 342, pp. 637-642.

Garrett, C., Outerbridge, R., Thompson, K. 1993. Interrannual variability in Mediterranean heat and buoyancy fluxes. Journal of Climate 6, pp. 900-910.

Gascard, J. C. 1978. Mediterranean deep water formation, baroclinic instability and oceanic eddies. Oceanologica Acta 1, pp. 315-330.

Gascard, J.C. 1991. Open ocean convection and deep water formation revisited in the Mediterranean, Labrador, Greenland and Weddell seas. Elsevier Oceangraphy series 57, pp.157-181.

Gibson, J. K., Kallberg, P., Uppala, S., Hernandez, A., Nomura, A., Serrano, E. 1997. ERA description. ECMWF Re-Analysis Project 1, pp. 71.

Gregg, M.C., 1987. Diapycnal mixing in the thermocline: A review. Journal Geophysical Research 92, pp. 5249-5286.

GRID Arendal., 2013. Mediterranean Sea water masses: vertical distribution. State of the Mediterranean Marine and Coastal Environment.

Hilgen, F., 1991. Astronomical calibration of Gauss to Matuyama sapropels in the Mediterranean and implication for the Geomagnetic Polarity Time Scale. Earth and Planetary Science Letters 104, pp. 227-246.

Hilgen, F., Krijgsman, W., Langereis, C.G., Lourens, L.J., Santarelli, A., Zachariasse, W.J. 1995. Extending the astronomical (polarity) time scale into the Miocene. Earth and Planetary Science Letters 136, pp. 495-510.

Huybers, P. 2006. Early Pleistocene glacial cycles and the integrated summer insolation forcing. Science 313, pp. 508-511.

Jayne, S.R., St. Laurent, L.C., Gille, S.T. 2004. Connections between ocean bottom topography and Earth's climate. Oceanography 17, pp. 65-74.

Johnson, H. L., Marshall, D. P., Sprowson, D. A. J. 2007. Reconciling theories of a mechanically driven meridional overturning circulation with thermohaline forcing and multiple equilibria. Climate Dynamics 29, pp. 821-836.

P.D. Killworth. 1976. The mixing and spreading phases of MEDOC. Progress in Oceanography 7, Mrs. J.C. Swallow, ed. Pergamon Press, Oxford.

Lane-Serff, G. F., Rohling, E. J., Bryden, H. L., Charnock, H. 1997. Postglacial connection of the Black Sea to the Mediterranean and its relation to the timing of sapropel formation. Paleoceanography 12, pp. 169-174.

de Lange, G., Thomson, J., Reitz, A., Slomp, C.P., Principato, M.S., Erba, E., Corselli, C., 2008. Synchronous basin-wide formation and redox-controlled preservation of a Mediterranean sapropel. Nature Geoscience 1, pp. 606-610.

Lascaratos, A., Roether, W., Nittis, K., Klein, B. 1999. Recent changes in deep water formation and spreading in the eastern Mediterranean sea: a review. Progress in Oceanography 44, pp. 5-36.

Ledwell, J.R., Watson, A.J., Law, C.S. 1998. Mixing of a tracer released in the pycnocline. J. Geophysical Research 103, pp.499-529.

Ledwell, J.R., Montgomery, E.T. Polzin, K.L., St. Laurent, L.C., Schmitt, R.W., Toole, J.M. 2000. Evidence for enhanced mixing over rough topography in the abyssal ocean. Nature 403, pp. 179-182.

Mariotti, A., Struglia, M., Zeng, N., Lau, K.-M. 2002. The hydrological cycle in the Mediterranean region and implications for the water budget of the Mediterranean Sea. Journal of Climate 15, pp. 1674-1690.

Marinez-Ruiz, F., Paytan, A., Kastner, M., Gonzalez-Donoso, J.M., Linares, D., Bernasconi, S.M. Jimenez-Espejo, F.J. 2003. Paleoceanography, Paleoclimatology, Paleoecology 190, pp.23-37.

Marotzke, J., 1997. Boundary mixing and the dynamics of three-dimensional thermohaline circulation. Journal Physical Oceanography 27, pp. 1713-1728.

Matthiesen, S., Haines, K. 2003. A hydraulic box model study of the Mediterranean response to postglacial sea-level rise. Paleoceanography 18, pp. 8.1-8.12.

MEDAR Group, 2002 - MEDATLAS/2002 database. Mediterranean and Black Sea database of temperature salinity and bio-chemical parameters. Climatological Atlas. IFREMER Edition.

MEDOC group. 1970. Observation of formation of deep water in the Mediterranean sea. Nature 227, pp.1037-1040.

Meijer, P.T., Tuenter, E. 2007. The effect of precession-induced changes in Mediterranean freshwater budget on circulation at shallow and intermediate depth. Journal of Marine Systems 68, pp. 349-365.

Meijer, P.T. 2012. Hydraulic theory of sea straits applied to the onset of the Messinian Salinity Crisis. Marine Geology 326-238, pp. 131-139.

Millot, C. 1999. Circulation in the Western Mediterranean Sea. Journal of Marine Systems 20, pp. 423-442.

Mikolajewicz, U. 2011. Modeling Mediterranean Ocean climate of the Last Glacial Maximum. Climate of the Past 7, pp. 161-180.

Myers, P.G., Haines, K., Rohling, E.J. 1998. Modeling the paleocirculation of the Mediterranean: The last glacial maximum and the Holocene with emphasis on the formaiton of sapropel S1. Paleoceanography 13, pp. 586-606.

Paluszkiewicz, T., Garwood, R.W., Denbo, D.W. 1994. Deep convective plumes in the ocean. Oceanography 7, pp. 37-44.

N. Pinardi., E. Masetti, 2000. Variability of the large scale general circulation of the Mediterranean Sea from observations and modelling: a review. Palaeogeography, Palaeoclimatology, Palaeoecology 158, pp. 153-173.

Polzin, K.L., Toole, J.M., Ledwell, J.R., Schmitt, R.W. 1997. Spatial variability of turbulent mixing in the abyssal ocean. Science 276, pp. 93-96.

Rahmstorf, S. 2002. Ocean circulation and climate during the past 120,000 years. Nature 419, pp. 207-214.

Rohling E.J., Hilgen, F.J. 1990. The eastern Mediterranean climate at times of sapropel formation: a review. Geologie en mijnbouw 70, pp. 253-264.

Romanou, A., Tselioudis, G. 2010. Evaporation-Precipitation variability over the Mediterranean and the Black Seas from satellite and reanalysis estimates. Journal of Climate 23, pp. 5268-5287.

Ryan, W. B. F., Pitman, W. C., Major, C.O., Shimkus, K., Moskalenko, V., Jones, G. A., Dimitrov, P., Gorur, N., Sakinc, M., Yuce, H. 1997. An abrupt drowning of the Black Sea shelf. Marine Geology 138, pp. 119-126.

Sannino, G., Bargagli, A., Artale, V. 2002. Numerical modelling of the mean exchange through the Strait of Gibraltar. Journal of Geophysical Research 107, pp. 1-24.

Shaltout, M., Omsteds, A. 2011. Calculating the water and heat balances of the Eastern Mediterranean basin using ocean modelling and available meteorological, hydrological and ocean data. Oceanologia 54, pp. 199-232.

Spotl, C., Burns, S.J., Frank, N., Mangini, A., Pavuza, N. 2004. Speleothems from the highalpine Spannagel Cave, Zillertal Alps (Austria). In: Sasowsky, I.D., Mylroie, J. (Eds.), Studies of Cave Sediments. Physical and Chemical Records of Paleoclimate, Dortrecht, Kluwer, pp. 243-256.

Tjallingii, R., Claussen, M., Stuut, J.-B.W., Fohlmeister, J., Jahn, A., Bickert, T., Lamy, F., Rhl, U. 2008. Coherent high- and low-latitude control of the northwest African hydrological balance. Nature Geoscience 1, 670-675.

Tsimplis, M.N., Bryden, H.L. 2000. Estimation of the transports through the Strait of Gibraltar. Deep-Sea Research 47, pp. 2219-2242.

Tziperman, E., Speer, K. 1994. A study of water mass transformation in the Mediterranean Sea: analysis of climatological data and a simple three-box model. Dynamics of atmospheres and oceans 21, pp. 53-82.

Wehausen, R., Brumsack, H.J. 1998. The formation of Pliocene Mediterranean sapropels: constraints from high-resolution major and minor element studies. Proceedings of the Ocean Drilling Program, Scientific Results 160, pp. 207-217.

Appendix A

Fortran Programs

A.1 Box model

```
program sea_bas

implicit none

!Characteristics of the different layers
real :: h_F, h_U, h_L, h_D       !Depth of Formation layer (F), Upper layer (U), Lower layer (L), and Deep layer (D)
real :: T_F, T_U, T_L, T_D, T_A, T_A_I, T_A_I_season !Temperature of different layers, A is atlantic
real :: T_F_max, T_F_min, T_F_av, T_F_year !Maxima, minima and average for T, S
real :: T_U_max, T_U_min, T_U_av, T_U_year
real :: S_F_max, S_F_min, S_F_av, S_F_year
real :: T_L_init,S_L_init
real :: S_F, S_U, S_L, S_D, S_I, S_A !Salinity of different layers
real :: rho_F, rho_U, rho_L, rho_D, rho_A, rho_I, rho  !Denisty in different layers
real :: rho_diff_FL,rho_diff_FD, rho_diff_LA !Density difference
real :: rho_F_max, rho_F_min, rho_F_av, rho_F_year

! Changes in time in the model
real :: dh_F, dh_U, dh_L, dh_D !Change in thickness of layers
real :: dT_F, dT_U, dT_L, dT_D, dT_A_I !Change in temperature
real :: dS_F, dS_U, dS_L, dS_D !Change in salinity

!Constants
real :: A !Area off Meditteranean (A)
real :: kappa !Background diffusion (kappa)
real :: d_UL, d_FU, d_LD !effective diffusion length
real :: pressure_constant !Coefficient for flow from (L) to (A)
real :: mu, mu2     !coefficient for flow from formation layer to deep layer in  m^3 /(kg s)
real :: heat_capacity_water !water specific heat capacity
real, parameter :: day=24.*3600. !Day in seconds
real, parameter :: yr2sec= 365.25*24.*3600. !Year in seconds
real, parameter :: pi=3.1415

! Flow between different layers
real :: c_UF, c_FU, c_UL, c_LU, c_LD, c_DL, c_FD, c_FL !Mixing between the different layers
real :: c_FD_year,c_FD_total
real :: c_FL_year,c_FL_total
real :: c_FD_max, c_FD_av
real :: c_FL_max, c_FL_av
real :: q1, q2 !Inflow from Atlantic to Upper layer (q1), Outflow from Lower layer to Atlantic (q2)
real :: E, E_season, P, dE !Evaporation (E), and precipation (P) from formation layer (F), dE is change in evaporation due to seasons
real :: E_max, E_min, E_year, E_av
real :: E_precession !Evaporation varies due to Milankovic cycli
real :: R, R_average, dR !River runoff, with dR being seasonal differences
real :: R_max,R_min,R_av,R_year
real :: H_atm, H_season !Heat loss in (W/m^2) of formation layer (F), atm gives constant heat loss, season makes season dependent
real :: H_milank_fluc,E_milank_fluc,R_milank_fluc
real :: H_max, H_min, H_av, H_year

!Time
real :: time,time_total,dtime,maxtime !Time,steps in time and maximum time
real :: t_stabilize,t_measure_year, t_measure_milank !Time to stabilize
real :: t_measure
```

```
integer, parameter :: t_measure_milank_dum = 7665000

!Parameters for Strait Gibraltar
real :: dS !Salinity difference between upper and lower layer
real :: h1,h2,H, W !Depth of Inflow layer, outflow layer and total depth and width of strait
real :: delta !Difference parameter between height upper and lower layer
real :: U1,U2 !Velocity at strait
real :: g !gravitational constant
real :: a_solve,b_solve,enc_solve,d_solve !To solve U2
real, dimension(t_measure_milank_dum) :: sea_level_change

!Options
integer :: seasonal_fluctuations, milankovic_fluctuations !Choices if you want these fluctuations in the model or not
integer :: measurement, measurement_points
integer :: include_strait
integer :: include_sea_level
integer :: i
integer :: black_sea



!!!!!!!!!!!!!!!!!!!!!!!!!!!!!!!!!!!!!!!!!!!!!!!!!!!!!!!!!!!!!!!!!!!!!!!!!!!!!!!!!!!
!!!!!!!!!!!!!!!Choose if you want seasonal and Milankovic fluctuations!!!!!!!!!!!!!
!!!!!!!!!!!!!!!!!!!!!!!!!!!!!!!!!!!!!!!!!!!!!!!!!!!!!!!!!!!!!!!!!!!!!!!!!!!!!!!!!!!


! 1=yes, 0=no

seasonal_fluctuations=1
milankovic_fluctuations=1

!!!!!!!!!!!!!!!!!!!!!!!!!!!!!!!!!!!!!!!!!!!!!!!!!!!!!!!!!!!!!!!!!!!!!!!!!!!!!!!!!!!
!!!!!!!!!!!!!!!!!!!!!!!Choose how long you want to measure!!!!!!!!!!!!!!!!!!!!!!!!!
!!!!!!!!!!!!!!!!!!!!!!!!!!!!!!!!!!!!!!!!!!!!!!!!!!!!!!!!!!!!!!!!!!!!!!!!!!!!!!!!!!!


! 0 = 1 year, 1 = 21.000 years

measurement=1

!!!!!!!!!!!!!!!!!!!!!!!!!!!!!!!!!!!!!!!!!!!!!!!!!!!!!!!!!!!!!!!!!!!!!!!!!!!!!!!!!!!
!!!!!!!!!!!!!!!!!!!!!!!Choose to include strait!!!!!!!!!!!!!!!!!!!!!!!!!!!!!!!!!!!
!!!!!!!!!!!!!!!!!!!!!!!!!!!!!!!!!!!!!!!!!!!!!!!!!!!!!!!!!!!!!!!!!!!!!!!!!!!!!!!!!!!

! 0 = Not include strait, 1 = Include strait

include_strait=1


if (include_strait==1) then
open (83,file='sea_level_without_time.dat')
do i=1, t_measure_milank_dum
 read(83,*) sea_level_change(i)
end do
end if

!!!!!!!!!!!!!!!!!!!!!!!!!!!!!!!!!!!!!!!!!!!!!!!!!!!!!!!!!!!!!!!!!!!!!!!!!!!!!!!!!!!
!!!!!!!!!!!!!!!!!!!!!!!Choose to sea level variations!!!!!!!!!!!!!!!!!!!!!!!!!!!!!!
!!!!!!!!!!!!!!!!!!!!!!!!!!!!!!!!!!!!!!!!!!!!!!!!!!!!!!!!!!!!!!!!!!!!!!!!!!!!!!!!!!!

! 0 = Not include sea level variations, 1 = Include sea level variations

include_sea_level=1


!!!!!!!!!!!!!!!!!!!!!!!!!!!!!!!!!!!!!!!!!!!!!!!!!!!!!!!!!!!!!!!!!!!!!!!!!!!!!!!!!!!
!!!!!!!!!!!!!!!!!!!!!!!Choose to include black sea !!!!!!!!!!!!!!!!!!!!!!!!!!!!!!!!
!!!!!!!!!!!!!!!!!!!!!!!!!!!!!!!!!!!!!!!!!!!!!!!!!!!!!!!!!!!!!!!!!!!!!!!!!!!!!!!!!!!

! 0 = Not include Blac Sea, 1 = Include Black sea

black_sea=1

!!!!!!!!!!!!!!!!!!!!!!!!!!!!!!!!!!!!!!!!!!!!!!!!!!!!!!!!!!!!
!!!!!!!!!!!!!!!!!!!!!!!Parameters!!!!!!!!!!!!!!!!!!!!!!!!!!!!
!!!!!!!!!!!!!!!!!!!!!!!!!!!!!!!!!!!!!!!!!!!!!!!!!!!!!!!!!!!!


!Initial depth of layers
h_F=30.
h_U=120.
h_L=500.
h_D = 850.
```

```
!Depth strait
H=284.
h1=H*0.5 !Location of interface
h2=H-h1
W=12000 !Width of Strait
g=9.8 !Gravitational constant

!Defining initial temperature
T_F_max=0. !Initial values assigned for computational purpose
T_F_min=100.
T_F_av=0.
T_F_year=0.
T_U_max=0.
T_U_min=100.
T_U_av=0.
T_U_year=0.
T_F=18.9
T_U=14.6
T_L=13.7
T_D=13.6
T_A=13.8
T_A_I=16.3
T_L_init=13.7
dT_L=0.0
dT_A_I=1.0

!Defining initial salinity
S_F_max=0.
S_F_min=100.
S_F_av=0.
S_F_year=0.
S_F=38.2
S_U=38.6
S_L=38.7
S_D=38.6
S_I=36.3
S_A=36.0
S_L_init=38.7 ! Gedaan voor hogere precisie, meer dan 7 cijfers achter komma
dS_L=0.0

!Defining initial density
rho_F_max=0.
rho_F_min=5000.
rho_F_av=0.
rho_F_year=0.


rho_F=rho(T_F,S_F)
rho_U=rho(T_U,S_U)
rho_L=rho(T_L,S_L)
rho_D=rho(T_D,S_D)
rho_A=rho(T_A,S_A)
rho_diff_FL=rho_F-rho_L
rho_diff_FD=rho_F-rho_D
rho_diff_LA=rho_L-rho_A

!Defining constants
A = 2.4e12 !Area Meditteranean in m^2/s
kappa =2.5*10e-6 !Background diffusion
d_FU = 75. !effective diffusion length (m)
d_UL = 310. !effective diffusion length (m)
d_LD = 750. !effective diffusion length (m)
pressure_constant=2.e-7 !
mu = 3.e-6 !in m^3/(kg s)
heat_capacity_water=3993. !In joule/(kg K)

!Defining initial time
time = 0.0 !In days, time after stabilizing
time_total = 0.0 !Is the total time including stabilizing time
dtime = 1.0 !Time steps of 1 day
t_stabilize=7665000. !t_stabilize is mostly around 20.000 days 7665000
t_measure_year=365.*2
t_measure_milank=7665000. !Time after system has stabilized and you can start performing a measurement 7665000
if (measurement==0) then !Number of measurement points in graph if measuring for 1 year
  t_measure=t_measure_year
  measurement_points=1
else
  t_measure=t_measure_milank !Number of measurement points in graph if measuring for 21.000 years
  measurement_points=10000
endif
maxtime = t_stabilize+t_measure !After this time the calculation stops
```

```
!Evaporation, precipitation, heat loss
E = 1.25 !Evaporation in m/yr
E_max=0.
E_min=1.
E_av=0.
E_year=0.
P = 0.45 !Precipitation in m/yr
dE = 0.4 !Change in evaporation due to seasons, for computational purpose. This is actually d(E-P-R).
R_average=0.2 !River runoff
dR=0.00
R=R_average
R_max=0.
R_min=1.
R_av=0.
R_year=0.
H_atm=143. !Heat loss (W/m^2)
H_max=0.
H_min=0.
H_av=0.
H_year=0.

!Percentual fluctuations due to Milankovic cycle in E, R and H
E_milank_fluc=0.10
R_milank_fluc=0.10
H_milank_fluc=0.1


!Calculation of initial mixing
q2=pressure_constant*(rho_diff_LA)
q1=q2+(E_season-P-R)/yr2sec

 c_FD_max=0.
 c_FD_year=0.
  c_FD_av=0.
   c_FL_max=0.
 c_FL_year=0.
  c_FL_av=0.
 if (rho_F > rho_D) then
   c_FD=mu*(rho_F-rho_D)
 else
   c_FD=0.
 endif

 c_FL=0

 if (c_FD==0) then
  if (rho_F > rho_L) then
   c_FL=mu*(rho_F-rho_L)
  else
  c_FL=0
 endif
 endif

 c_FU=kappa/d_FU
 c_UF=kappa/d_FU+(E_season-P-R)/yr2sec+c_FL+c_FD
 c_UL=kappa/d_UL+q2-c_FL-c_FD
 c_LU=kappa/d_UL
 c_LD=kappa/d_LD
 c_DL=kappa/d_LD+c_FD

  !Calculate yearly average deep water formation
  if (time_total .ge. t_stabilize) then
  c_FD_total=c_FD_total+c_FD
  if (mod(int(time_total),365)==0) then
  c_FD_year=c_FD_total/365.
  c_FD_total=0.
  end if
  end if


!Printing initial paramaters
open(99,file='parameter_file.dat')
write (99,*), ""
write (99,*),"Initial parameters"
write (99,*), ""
write (99,*),"h_F =",h_F
write (99,*),"h_U =",h_U
write (99,*),"h_L =",h_L
write (99,*),"h_D =",h_D
write (99,*), ""
write (99,*),"T_F =",T_F
write (99,*),"T_U =",T_U
write (99,*),"T_L =",T_L
write (99,*),"T_D =",T_D
```

```
write (99,*),"T_A =",T_A
write (99,*), ""
write (99,*),"S_F =",S_F
write (99,*),"S_U =",S_U
write (99,*),"S_L =",S_L
write (99,*),"S_D =",S_D
write (99,*),"S_A =",S_A
write (99,*), ""
write (99,*),"rho_F =",rho_F
write (99,*),"rho_U =",rho_U
write (99,*),"rho_L =",rho_L
write (99,*),"rho_D =",rho_D
write (99,*),"rho_A =",rho_A
write (99,*), ""
write (99,*),"rho_diff_FL =",rho_diff_FL
write (99,*),"rho_diff_FD =",rho_diff_FD
write (99,*),"rho_diff_LA =",rho_diff_LA
write (99,*), ""
write (99,*), "kappa=", kappa
write (99,*), "d_FU=", d_FU
write (99,*), "d_UL=", d_UL
write (99,*), "d_LD=", d_LD
write (99,*), "pressure_constant=", pressure_constant
write (99,*), "mu=", mu
write (99,*), ""
write (99,*),"q1 =",q1*A/1000000, "Sv"
write (99,*),"q2 =",q2*A/1000000, "Sv"
write (99,*),"c_FU =",c_FU
write (99,*),"c_UF =",c_UF
write (99,*),"c_UL =",c_UL
write (99,*),"c_LU =",c_LU
write (99,*),"c_DL =",c_DL
write (99,*),"c_LD =",c_LD
write (99,*),"c_FD =",c_FD
write (99,*), ""
write (99,*), "E-P =",E-P
write (99,*), "H_atm =", H_atm
write (99,*),"R =", R
write (99,*), "dE=", dE
write (99,*),"dR =", dR
write (99,*), ""
write (99,*),"E_milank_fluc =", E_milank_fluc
write (99,*),"H_milank_fluc =", H_milank_fluc
write (99,*),"R_milank_fluc =", R_milank_fluc

print *, "performing calculations"

 !!!!!!!!!!!!!!!!!!!!!!!!!!!!!!!!!!!!!!!!!!!!!!!!!!!!!!!!!!!!!!!!!!!!!!!!!!!!!!!!!!!!
!!!!!!!!!!!!!!!!!!!!Writing initial data into a file !!!!!!!!!!!!!!!!!!!!!!!!!!!!!!!
!!!!!!!!!!!!!!!!!!!!!!!!!!!!!!!!!!!!!!!!!!!!!!!!!!!!!!!!!!!!!!!!!!!!!!!!!!!!!!!!!!!!!

! Salinity and temperature
open(20,file='t_S_T.dat')
write (20, '(a)') '> time, S_F, S_U, S_L, S_D, S_A, T_F, T_U, T_L, T_D, T_A'
write (20,*) time_total, S_F, S_U, S_L, S_D, S_A, T_F, T_U, T_L, T_D, T_A

!Density
open (21,file= 'density.dat')
write (21, '(a)') '>  time, rho(T_F,S_F), rho(T_U,S_U), rho(T_L,S_L), rho(T_D,S_D), rho(T_A,S_A)'
write (21,*) time, rho(T_F,S_F), rho(T_U,S_U), rho(T_L,S_L), rho(T_D,S_D), rho(T_A,S_A)

!Flow between different boxes
open (22,file= 'flow.dat')
write (22, '(a)') '>  time, c_UF, c_FU, c_UL, c_LU , c_DL, c_LD, c_FL, c_FD, q1, q2 '

!Depth of layers
open (23,file= 'depth.dat')
write (23, '(a)') '>  time, h_U, h_F, h_L, h_D'
write (23,*) time, h_U, h_F, h_L, h_D

!Deep water flow
open(24,file='c_FD.dat')

!Water outflow Meditteranean
open(25,file='q2.dat')
write (25,*) time, q2

!Salinity and temperature in separate files to plot.
open(31,file='S_F.dat')
write (31,*) time, S_F

open(32,file='S_U.dat')
write (32,*) time, S_U
```

```
open(33,file='S_L.dat')
write (33,*) time, S_L

open(34,file='S_D.dat')
write (33,*) time, S_D

open(35,file='T_F.dat')
write (35,*) time, T_F

open(36,file='T_U.dat')
write (36,*) time, T_U

open(37,file='T_L.dat')
write (37,*) time, T_L

open(38,file='T_D.dat')
write (38,*) time, T_D

!To plot sea level
open(154,file='sea_level_plot.dat')

!Heat flow, Evaporation-Precipitation and river runoff
open(40,file='H.dat')
write (40,*) time, H_atm

open(41,file='E_P.dat')
write (41,*) time, E-P

open(42,file='R.dat')
write (42,*) time, R

!Deep water flow
open(43,file='c_FL.dat')

!Yearly average  deep water flow
open(44, file='c_FD_year.dat')

!All maxima, minima and averages of T,S, c, H, E, R, rho
open(50,file='T_F_max.dat')
open(51,file='T_F_min.dat')
open(52, file='T_F_av.dat')
open(53,file='T_U_max.dat')
open(54,file='T_U_min.dat')
open(55, file='T_U_av.dat')
open(56,file='S_F_max.dat')
open(57,file='S_F_min.dat')
open(58, file='S_F_av.dat')
open(59, file='c_FD_max.dat')
open(60, file='c_FD_av.dat')
open(61, file='c_FL_max.dat')
open(62, file='c_FL_av.dat')
open(63,file='H_max.dat')
open(64,file='H_min.dat')
open(65, file='H_av.dat')
open(66,file='E_max.dat')
open(67,file='E_min.dat')
open(68, file='E_av.dat')
open(69,file='R_max.dat')
open(70,file='R_min.dat')
open(71, file='R_av.dat')
open(72,file='rho_F_max.dat')
open(73,file='rho_F_min.dat')
open(74, file='rho_F_av.dat')

open(150,file='rho_F.dat')
open(151,file='rho_U.dat')
open(152,file='rho_L.dat')
open(153,file='rho_D.dat')

!!!!!!!!!!!!!!!!!!!!!!!!!!!!!!!!!!!!!!!!!!!!!!!!!!!!!!!!!!!!!!!!!!!!!!!!!!!!!!!!
!!!!!!!!!!!!!!!!!!!!!!!!!!!Change in time!!!!!!!!!!!!!!!!!!!!!!!!!!!!!!!!!!!!!!!!
!!!!!!!!!!!!!!!!!!!!!!!!!!!!!!!!!!!!!!!!!!!!!!!!!!!!!!!!!!!!!!!!!!!!!!!!!!!!!!!!

do while (time_total .le. maxtime)

!!!!!!!!!!!!For constant model!!!!!!!!!!!!!!!!!!
H_season=4.
E_season=E
R=R_average
T_A_I_season=T_A_I

if (include_sea_level==1) then
H=164.
h1=H*0.5
```

```
h2=H*0.5
if (time_total>t_stabilize) then
H=284.
i=int(time_total)-int(t_stabilize)
H=H-sea_level_change(i)
h1=H*0.5
h2=H*0.5
end if
end if


!!!!!!!!!!!!Introduce seasonality in sea!!!!!!!!!!

if (seasonal_fluctuations==1) then
H_season=0.
H_season=H_atm*cos(2*pi*(time_total-t_stabilize)/365.) !365 days in a year
if (H_season > 0.) then
 H_season=1.05*H_season
endif
E_season=E-dE*sin(2*pi*(time_total-t_stabilize)/365.)
R=R_average+dR*sin(2*pi*(time_total-t_stabilize)/365.)
T_A_I_season=T_A_I-dT_A_I*sin(2*pi*(time_total-t_stabilize)/365.)
endif


!!!!!!!!!!Introduce Milankovic precession in sea!!!!!!!!

if (milankovic_fluctuations==1) then
!!!! To make sure that we are at a precession maximum
E_season=E_season-E_milank_fluc*E!*0.5
R=R-0.5*R_milank_fluc
H_season=H_season-H_milank_fluc*H_season*cos(2*pi*(time_total)/7665000.)
E_season=(E_season+E_milank_fluc*E*cos((pi*2*time_total)/7665000.))
end if


!Black sea opening

if (black_sea==1) then
if ((time_total>t_stabilize+0.6*(t_measure)).AND. (time_total<(t_stabilize+0.68*(t_measure)))) then
E_season=E_season-0.2*((time_total-(t_stabilize+0.6*(t_measure)))/(0.08*t_measure))
end if
if ((time_total>t_stabilize+0.68*(t_measure)).AND. (time_total<(t_stabilize+0.76*(t_measure)))) then
E_season=E_season-0.2*(1-((time_total-(t_stabilize+0.68*(t_measure)))/(0.08*t_measure)))
end if
end if

! Define in and outflow
q2=pressure_constant*(rho_diff_LA)
q1=q2+(E_season-P-R)/yr2sec



  !!!!!!!!!!!!!!!!!!!!Strait of Gibraltar!!!!!!!!!!!!!!!!!!!!

if (include_strait==1) then
rho_I=rho(T_A_I,S_I)
a_solve=h1**3+h2**3
b_solve=2.*E_season*h2**3
enc_solve=E_season**2*h2**3-(h1**3*h2**3*W**2*g*((rho_L-rho_I)/(rho_L)))
d_solve=b_solve**2-4*a_solve*enc_solve
U2=(-b_solve+Sqrt(d_solve))/(2*a_solve)
q2=0.4*(U2/A)
q1=q2+(E_season-P-R)/yr2sec
endif


!!!!!!!!!!!!!!!!!!!Calculation of initial mixing!!!!!!!!!!!!!!!!!!!!!!!!!
 if (rho_F > rho_D) then
   c_FD=mu*(rho_F-rho_D) !Transport in m/s
 else
   c_FD=0.
 endif

 c_FL=0

 if (c_FD==0) then
  if (rho_F > rho_L) then
   c_FL=mu*(rho_F-rho_L)
  else
  c_FL=0
 endif
 endif
```

```
 c_FU=kappa/d_FU
 c_UF=kappa/d_FU+(E_season-P-R)/yr2sec+c_FL+c_FD
 c_UL=kappa/d_UL+q2-c_FL-c_FD!+q1-((E_season-P-R)/yr2sec+c_FD) !Transport in m/s
 c_LU=kappa/d_UL
 c_LD=kappa/d_LD
 c_DL=kappa/d_LD+c_FD


  !!!!!!!!!!!!!!!!!!!!!!!!!Calculate Volume change!!!!!!!!!!!!!!!!!!!!!!!!
 dh_F=(-(E_season-P-R)/yr2sec+c_UF-c_FU-c_FD-c_FL)*day
 dh_U=(q1-c_UF+c_FU-c_UL+c_LU)*day
 dh_L=(-q2+c_DL-c_LD+c_UL-c_LU+c_FL)*day
 dh_D=(c_FD+c_LD-c_DL)*day

  !!!!!!!!!!!!!!!!!!!!!!!Calculate Salinity change!!!!!!!!!!!!!!!!!!!!!!!!
 dS_F=((S_F*(E_season-P-R)/yr2sec+c_UF*(S_U-S_F))/h_F)*day
 dS_U=(((S_I-S_U)*q1+(S_L-S_U)*c_LU+(S_F-S_U)*c_FU)/h_U)*day
 dS_L=(((S_U-S_L)*c_UL+c_DL*(S_D-S_L)+c_FL*(S_F-S_L))/h_L)*day+dS_L
 dS_D=(((S_F-S_D)*c_FD+(S_L-S_D)*c_LD)/h_D)*day

 !!!!!!!!!!!!!!!!!!!!!!!Calculate Temperature change in time!!!!!!!!!!!!!!!!!!
 dT_F=(((T_U-T_F)*c_UF)/h_F)*day - (H_season/(heat_capacity_water*rho_F*h_F)*day)
 dT_U=(((T_A_I_season-T_U)*q1+(T_L-T_U)*c_LU+(T_F-T_U)*c_FU)/h_U)*day
 dT_L=(((T_U-T_L)*c_UL+(T_D-T_L)*c_DL+c_FL*(T_F-T_L))/h_L)*day+dT_L
 dT_D=(((T_F-T_D)*c_FD+(T_L-T_D)*c_LD)/h_D)*day

!Calculate new h, T, S
h_F=h_F+dh_F
h_U=h_U+dh_U
h_L=h_L+dh_L
h_D=h_D+dh_D

S_F=S_F+dS_F
S_U=S_U+dS_U
S_L=S_L_init+dS_L
S_D=S_D+dS_D

T_F=T_F+dT_F
T_U=T_U+dT_U
T_L=T_L_init+dT_L
T_D=T_D+dT_D


!Calculate new density
rho_F=rho(T_F,S_F)
rho_U=rho(T_U,S_U)
rho_L=rho(T_L,S_L)
rho_D=rho(T_D,S_D)
rho_A=rho(T_A,S_A)
rho_diff_FL=rho_F-rho_L
rho_diff_FD=rho_F-rho_D
rho_diff_LA=rho_L-rho_A

!For making min and max graph and average
if (time_total > t_stabilize) then
if ((dT_F>0.) .AND. (T_F>T_F_max))then
T_F_max=T_F
end if
if ((dT_F<0.) .AND. (T_F<T_F_min))then
T_F_min=T_F
end if
T_F_year=T_F_year+T_F


if ((dT_U>0.) .AND. (T_F>T_U_max))then
T_U_max=T_U
end if
if ((dT_U<0.) .AND. (T_U<T_U_min))then
T_U_min=T_U
end if
T_U_year=T_U_year+T_U

if ((dS_F>0.) .AND. (S_F>S_F_max))then
S_F_max=S_F
end if
if ((dS_F<0.) .AND. (S_F<S_F_min))then
S_F_min=S_F
end if
S_F_year=S_F_year+S_F


if (c_FD>c_FD_max) then
 c_FD_max=c_FD
end if
```

```
 c_FD_year=c_FD_year+c_FD

 if (c_FL>c_FL_max) then
 c_FL_max=c_FL
end if
 c_FL_year=c_FL_year+c_FL



if (H_season>H_max) then
H_max=H_season
end if

if (H_season<H_min) then
H_min=H_season
end if

 H_year=H_year+H_season


 if (E_season>E_max) then
E_max=E_season
end if

if (E_season<E_min) then
E_min=E_season
end if

 E_year=E_year+E_season

  if (R>R_max) then
R_max=R
end if

if (R<R_min) then
R_min=R
end if

R_year=R_year+R


if (rho_F>rho_F_max) then
rho_F_max=rho_F
end if

if (rho_F<rho_F_min) then
rho_F_min=rho_F
end if

rho_F_year=rho_F_year+rho_F

end if

if ((time_total > t_stabilize) .AND. (mod(int(time_total), 365)==0)) then
T_F_av=T_F_year/365.
T_U_av=T_U_year/365.
S_F_av=S_F_year/365.
 c_FD_av=c_FD_year/365.
 c_FL_av=c_FL_year/365.
 H_av=H_year/365.
 E_av=E_year/365.
 R_av=R_year/365.
 rho_F_av=rho_F_year/365.

write (50,*) time/365, T_F_max
write (51,*) time/365, T_F_min
write (52,*) time/365, T_F_av
write (53,*) time/365, T_U_max
write (54,*) time/365, T_U_min
write (55,*) time/365, T_U_av
write (56,*) time/365, S_F_max
write (57,*) time/365, S_F_min
write (58,*) time/365, S_F_av
write (59,*) time/365, c_FD_max*A/1000000
write (60,*) time/365, c_FD_av*A/1000000
write (61,*) time/365, c_FL_max*A/1000000
write (62,*) time/365, c_FL_av*A/1000000
write (63,*) time/365, H_max
write (64,*) time/365, H_min
write (65,*) time/365, H_av
write (66,*) time/365, E_max-P
write (67,*) time/365, E_min-P
write (68,*) time/365, E_av-P
write (69,*) time/365, R_max
```

```
write (70,*) time/365, R_min
write (71,*) time/365, R_av
write (72,*) time/365, rho_F_max
write (73,*) time/365, rho_F_min
write (74,*) time/365, rho_F_av
write (150,*) time/365, rho_F
write (151,*) time/365, rho_U
write (152,*) time/365, rho_L
write (153,*) time/365, rho_D
write (154,*) time/365, H

T_F_max=0.
T_F_min=100.
T_F_year=0.

T_U_max=0.
T_U_min=100.
T_U_year=0.

S_F_max=0.
S_F_min=100.
S_F_year=0.

 c_FD_max=0
 c_FD_year=0

 c_FL_max=0
 c_FL_year=0

H_max=0.
H_min=0.
H_year=0.

E_max=0.
E_min=1.
E_year=0.

R_max=0.
R_min=1.
R_year=0.

rho_F_max=0.
rho_F_min=5000.
rho_F_year=0.

end if

 !Writing data into file
  if ((time_total .ge. t_stabilize) .AND. (mod(int(time_total), measurement_points)==0)) then
 write (20,*) time/365, S_F, S_U, S_L, S_D, S_A, T_F, T_U, T_L, T_D, T_A
 write (21,*) time/365, rho(T_F,S_F), rho(T_U,S_U), rho(T_L,S_L), rho(T_D,S_D), rho(T_A,S_A)
 write (22,*) time/365, c_UF*A/1000000, c_FU*A/1000000, c_UL*A/1000000, c_LU*A/1000000 , c_DL*A/1000000, c_LD*A/1000000, q2*A/1000000!, c_FD*A/
 write (23,*) time/365, h_U, h_F, h_L, h_D
 write (24,*) time/365, c_FD*A/1000000
 write (25,*) time/365, q2*A/1000000
 write (31,*) time/365, S_F
 write (32,*) time/365, S_U
 write (33,*) time/365, S_L
 write (34,*) time/365, S_D
 write (35,*) time/365, T_F
 write (36,*) time/365, T_U
 write (37,*) time/365, T_L
 write (38,*) time/365, T_D
 write (40,*) time/365, H_season
 write (41,*) time/365, E_season-P-R
 write (42,*) time/365, R
 write (43,*) time/365, c_FL*A/1000000
  end if

!Time change
if (time_total>t_stabilize) then
  time= time + dtime
end if

 time_total=time_total+dtime
 if (mod(int(time_total), 1000000)==0) then
 print *, "time=", time_total
 end if

 end do

 end
! ........................................
```

```
real function rho(T,S)

! linear equation of state to determine density of sea water from Johnson et al. (2007)

implicit none

real :: T, S
real, parameter :: rho0= 1027.5e0, alpha= 2.e-4, beta= 8.e-4
real, parameter :: T0= 5.e0, S0= 35.e0

rho= rho0*(1.e0 - alpha*(T-T0) + beta*(S-S0))

return
end
```

A.2 Temperature/Salinity program

```
program average

use, intrinsic :: iso_fortran_env


implicit none

character(len=1) :: filenumber
character(len=1024) :: filename_T, filename_S
character(len=1024) :: format_string_T, format_string_S
integer, parameter :: arraylen = 18630
integer, parameter :: nrlayers = 25
real, dimension(arraylen) :: lon, lat, depth, T, S
real, dimension(nrlayers) :: layer_thickness, layer_T, layer_S
real, dimension(26) :: layer_depth
real :: T_total, T_average, S_total, S_average
integer ::  num,i,j,k,l,m, readcode

real :: to_radian,radian
real :: haversine, haversine_test
real :: width_cell=0.2
real :: volume_total

real :: rho
real , dimension(arraylen) :: density, density_dummy , density_difference
real, dimension(nrlayers) :: density_total

real, dimension(nrlayers) :: area_cell_total, volume_layer
real, dimension(nrlayers) :: T_volume,T_add, T_vol_av, S_volume, S_add, S_vol_av
real, dimension(arraylen) :: area_cell,distance_lat,distance_lon,volume_cell
real, dimension(arraylen) :: T_vol_cell, S_vol_cell


real :: T_between_layers,volume_between_layers_add,T_between_layers_add
real :: S_between_layers,S_between_layers_add

integer :: layer_1, layer_2

!!!!!!!!!!!!!!!!!!!!!!!!!!!!!!!!!!!!!!!!!!!!!!!!!!!!!!!!!!!!!!!!!!!!!!!!!!!
!Between these two layers you want to determine the average temperature!
!!!!!!!!!!There are 25 layers ranging between 0 and 4000 m!!!!!!!!!!!!!!
!!!!!!!!!!!!!!!!!!!!!!!!!!!!!!!!!!!!!!!!!!!!!!!!!!!!!!!!!!!!!!!!!!!!!!!!!!!

layer_1=17
layer_2=25



!Setting parameters to 0
do i=1,25
 volume_layer(i)=0.
 T_add(i)=0.
 T_vol_av(i)=0
end do

do i=1,26
 layer_depth(i)=0
end do
!!!!!!!!!!!!!!!!!!!!!!!!!!!!!!!!!!!!!!!!!!!!!!!!!!!!!!!!
!!!!!!!Calculate average Temperature!!!!!!!!!!!!
!!!!!!!!!!!!!!!!!!!!!!!!!!!!!!!!!!!!!!!!!!!!!!!!!!!!!!!!
```

```
open (2, file="temperature_clim_surf.dat")
open (3, file="salinity_clim_surf.dat")

layer_depth(1)=4000.
layer_depth(2)=3500.
layer_depth(3)=3000.
layer_depth(4)=2500.
layer_depth(5)=2000.
layer_depth(6)=1500.
layer_depth(7)=1200.
layer_depth(8)=1000.
layer_depth(9)=800.
layer_depth(10)=600.
layer_depth(11)=500.
layer_depth(12)=400.
layer_depth(13)=300.
layer_depth(14)=250.
layer_depth(15)=200.
layer_depth(16)=150.
layer_depth(17)=125.
layer_depth(18)=100.
layer_depth(19)=75.
layer_depth(20)=50.
layer_depth(21)=30.
layer_depth(22)=20.
layer_depth(23)=10.
layer_depth(24)=5.
layer_depth(25)=0.
layer_depth(26)=0.

do i=2,25
layer_thickness(1)=250.
layer_thickness(i)=(layer_depth(i-1)-layer_depth(i+1))/2
end do

i=0

print *, "layer_thickness=",layer_thickness

do k=25,49
j=0
T_total=0.
volume_total=0.
      if (k < 34) then
            format_string_T = "(A14,I1,A4)"
        else
            format_string_T = "(A14,I2,A4)"
        endif

        write (filename_T,format_string_T) "clim.med.temp.",k-24,".xyz"

        open (k, file = trim(filename_T))

ReadLoop: do i=1, ArrayLen

   read (k, *, iostat=ReadCode ) lon(i), lat(i), depth(i), T(i)

  !Write Temperature of single layer to file
   if (k==48) then

   write (2,*) T(i)
   end if

   !T>10 degrees becuase there are some weird data points, and lon>-5.29 to avoid Atlantic ocean
   if (T(i)> 1.0 .and. lon(i)<-5.29) then
    !print *, lon(i), lat(i), depth(i), T(i)
    T_total=T_total+T(i)
    !Calculate the total area size of each cell using haversine function to determine distance
    !between two points,
    distance_lon(i)=haversine(lat(i),lon(i)-width_cell/2,lat(i),lon(i)+width_cell/2)
    distance_lat(i)=haversine(lat(i)-width_cell/2,lon(i),lat(i)+width_cell/2,lon(i))
    area_cell(i)=distance_lat(i)*distance_lon(i)
    volume_cell(i)=area_cell(i)*layer_thickness(k-24)
    volume_layer(k-24)=volume_layer(k-24)+volume_cell(i)
    T_vol_cell(i)=volume_cell(i)*T(i)
    T_add(k-24)=T_add(k-24)+T_vol_cell(i)

   !Keep track of the amount of data points
   j = j+1
   end if

   if ( ReadCode /= 0 ) then
      if ( ReadCode == iostat_end ) then
```

```
         exit ReadLoop
      else
         write ( *, '( / "Error on read: ", I0 )' )  ReadCode
         stop
      end if
   end if
   num = num + 1

end do ReadLoop

T_average = T_total/j
layer_T(k-24)=T_average
!layer_depth(k-24)=depth(1)
T_vol_av(k-24)=T_add(k-24)/volume_layer(k-24)
print *, 'T_average',depth(1),'m =', T_average
!print *, 'T_average_volume',depth(1),'m =', T_vol_av(k-24)

close (k)

end do

!Now determine the average temperature between two layers
T_between_layers=0.
T_between_layers_add=0
volume_between_layers_add=0.

do i=layer_1, layer_2


T_between_layers_add=T_between_layers_add+T_add(i)
volume_between_layers_add=volume_between_layers_add+volume_layer(i)
end do

T_between_layers=T_between_layers_add/volume_between_layers_add


print *,"Average temperature between ", layer_depth(layer_2),"m depth and", layer_depth(layer_1),"m depth =", T_between_layers
print *,


num=0


!!!!!!!!!!!!!!!!!!!!!!!!!!!!!!!!!!!!!!!!!!!!!!!!!!!
!!!!!!!!Calculate average Salinity!!!!!!!!!!!!!!!!
!!!!!!!!!!!!!!!!!!!!!!!!!!!!!!!!!!!!!!!!!!!!!!!!!!!

do i=1,25
  volume_layer(i)=0.
  S_add(i)=0.
  S_vol_av(i)=0
 end do


do k=50, 74
j=0
S_total=0.

  if (k < 59) then
           format_string_S = "(A14,I1,A4)"
       else
           format_string_S = "(A14,I2,A4)"
       endif

       write (filename_S,format_string_S) "clim.med.psal.",k-49,".xyz"

       open (k, file = trim(filename_S))

ReadLoop2: do i=1, ArrayLen

   read (k, *, iostat=ReadCode ) lon(i), lat(i), depth(i), S(i)



   if (k==60) then

   write (3,*) S(i)
   end if


   if (S(i)> 30.0 .and. lon(i)>-5.29) then !5.29
   !if (lon(i)>-7.) then
    !print *, lon(i), lat(i), depth(i), S(i)
    S_total=S_total+S(i)
```

```
    distance_lon(i)=haversine(lat(i),lon(i)-width_cell/2,lat(i),lon(i)+width_cell/2)
    distance_lat(i)=haversine(lat(i)-width_cell/2,lon(i),lat(i)+width_cell/2,lon(i))
    area_cell(i)=distance_lat(i)*distance_lon(i)
    volume_cell(i)=area_cell(i)*layer_depth(k-49)
    volume_layer(k-49)=volume_layer(k-49)+volume_cell(i)
    S_vol_cell(i)=volume_cell(i)*S(i)
    S_add(k-49)=S_add(k-49)+S_vol_cell(i)
    j = j+1
   !end if
   end if
   if ( ReadCode /= 0 ) then
      if ( ReadCode == iostat_end ) then
         exit ReadLoop2
      else
         write ( *, '( / "Error on read: ", I0 )' )  ReadCode
         stop
      end if
   end if

   num = num + 1

end do ReadLoop2



S_average = S_total/j
layer_S(k-49)=S_average
S_vol_av(k-49)=S_add(k-49)/volume_layer(k-49)
print *, 'S_average',depth(1),'m =', S_average

close (k)

end do

!Now determine the average temperature between two layers
S_between_layers=0.
S_between_layers_add=0
volume_between_layers_add=0.

do i=layer_1, layer_2
S_between_layers_add=S_between_layers_add+S_add(i)
volume_between_layers_add=volume_between_layers_add+volume_layer(i)
end do

S_between_layers=S_between_layers_add/volume_between_layers_add


print *,"Average salinity between ", layer_depth(layer_2),"m depth and", layer_depth(layer_1),"m depth =", S_between_layers
print *,




!!!!!!!!!!!!!!!!!!!!!!!!!!!!!!!!!!!!!!!!!!!!!!!!!!!!!!!!!!!!!!!!!!!!!!
!!!!!!!!!!!!!!!!!Calculate density!!!!!!!!!!!!!!!!!!!!!!!!!!!!!!!!!!!!
!!!!!!!!!!!!!!!!!!!!!!!!!!!!!!!!!!!!!!!!!!!!!!!!!!!!!!!!!!!!!!!!!!!!!!

do i=1,25
  density_total(i)=0.
  density_dummy(i)=0
end do

open (1, file="density_difference_summ.dat")

do k=75,99
l=0
m=0


!We are going to calculate density difference between this layer and surface layer
if (k==85) then
do i=1, ArrayLen
density_dummy(i)=density(i)
end do
end if



  if (k < 84) then
            format_string_T = "(A14,I1,A4)"
            format_string_S = "(A14,I1,A4)"
```

```
        else
            format_string_T = "(A14,I2,A4)"
            format_string_S = "(A14,I2,A4)"
        endif


write (filename_T,format_string_T) "wint.med.temp.",k-74,".xyz"
        write (filename_S,format_string_S) "wint.med.psal.",k-74,".xyz"



         open (k, file = trim(filename_T))
        open (k+25, file = trim(filename_S))

do i=1, ArrayLen
   read (k, *, iostat=ReadCode ) lon(i), lat(i), depth(i), T(i)
   read (k+25, *, iostat=Readcode)  lon(i), lat(i), depth(i), S(i)


   if (T(i)> 5.0  .and. lon(i)>-5.29) then
   density(i)=rho(T(i),S(i))
   else if (T(i).NE.T(i)) then
   density(i)=0.
   end if



   if (k==98) then
   if (density_dummy(i)>0.) then
   write (1,*) density_dummy(i) - density(i)
   else if (density_dummy(i)==0. .and. density(i)==0.) then
   write (1,*) 1000.00000000
   else if (density_dummy(i)==0 .and. density(i)>0.) then
   write (1,*) -100.00

   end if
  end if


  if (T(i)> 10.0  .and. lon(i)>-5.29) then
   density_total(k-74) = density_total(k-74) + density(i)
   l=l+1
   end if


   end do
   density_total(k-74)=density_total(k-74)/real(l)
   print*,'Average density',depth(1),'m =', density_total(k-74)
   close (k)
   close(k+25)
end do


end program



!---------------------------------------------------------------------

!Functions to determine distance between points, when longitude and latitude are known.


real function to_radian(degree)
  implicit none
  real, intent(in) :: degree
  real :: radian, pi
  pi=4*atan(1.0)
  radian=degree*pi/180
  to_radian=radian
  return
end function to_radian


real function haversine(deglat1,deglon1,deglat2,deglon2)
  real,intent(in) :: deglat1,deglon1,deglat2,deglon2
  real :: a,c,dist,dlat,dlon,lat1,lat2
  real,parameter :: radius = 6372.8

  dlat = to_radian(deglat2-deglat1)
         dlon = to_radian(deglon2-deglon1)
         lat1 = to_radian(deglat1)
         lat2 = to_radian(deglat2)
         a = (sin(dlat/2))**2 + cos(lat1)*cos(lat2)*(sin(dlon/2))**2
         c = 2*atan2(sqrt(a),sqrt(1-a))
```

```
          dist = radius*c
          haversine=dist
          return
end function haversine


! linear equation of state to determine density of sea water from Johnson et al. (2007)


real function rho(Temp,Sal)
implicit none

real, intent(in) :: Temp, Sal
real, parameter :: rho0= 1027.5e0, alpha= 2.e-4, beta= 8.e-4
real, parameter :: T0= 5.e0, S0= 35.e0

rho= rho0*(1.e0 - alpha*(Temp-T0) + beta*(Sal-S0))

return
end function rho
```